Second Series *November 15, 1932* *Vol. 42, No. 4*

THE

PHYSICAL REVIEW

Remarks on the Scattering of X-Rays by Gases and Crystals

By G. E. M. JAUNCEY
Washington University, St. Louis, Missouri

(Received September 9, 1932)

§§1 and 2: Woo's most recent formulas for the separation of the diffusely scattered radiation from polyatomic gases and simple crystals into coherent and incoherent radiation are discussed. It is shown that Woo's formulas for the total scattered radiation reduces to the author's respective classical formulas when $\alpha(=h/mc\lambda)$ is made zero. This removes the objection made by the author in a previous note. It is shown that the incoherent scattered radiation depends upon the root mean square of the E's while the coherent radiation depends upon the arithmetic mean of the E's, thus giving a mathematical distinction between the incoherent and coherent radiation even in the classical theory. §3: Evidence is presented in favor of the true atom form factor f of an atom in a crystal (sylvine) being a function of the temperature of the crystal. The average electron distribution about the center of an atom in a crystal must be a function of the violence of the thermal agitation of the atom. At 0°K the electron distribution in an atom of sylvine is more diffuse than in an atom of argon. As the temperature rises above 0°K the electron distribution becomes less diffuse and finally becomes like that of argon at about room temperature. §4: It is shown that the $S_0=(S+F^2/Z)_c$ relation can be replaced by a relation between experimental quantities alone—otherwise, an empirical relation. §5: A digression on the philosophy of physics in which it is noted that the empirical relation of §4 contains no vestige of the Thomson or any other theory of x-rays. This supports the view that physical laws express relations between pointer readings. §6: The classical theory for the diffuse scattering of x-rays by a crystal consisting of atoms of several kinds is worked out and a formula obtained. By the use of Woo's method, the formulas for the coherent and incoherent radiation are also obtained. The restrictions upon these formulas are discussed.

§1. POLYATOMIC GASES

THE following papers on the scattering of x-rays by gases and crystals have appeared in the Physical Review during recent months: Paper I by Jauncey,[1] Paper II by Woo,[2] Paper III by Jauncey[3] and Paper IV by Woo.[4] In this section the author wishes to comment on Paper IV by Woo. In Paper I, Jauncey discusses the classical theory of the scattering of x-rays from polyatomic gases whose molecules consist of n atoms of one kind and arrives at the formula[5]

[1] G. E. M. Jauncey, Phys. Rev. **38**, 194 (1931).
[2] Y. H. Woo, Phys. Rev. **39**, 555 (1932).
[3] G. E. M. Jauncey, Phys. Rev. **39**, 561 (1932).
[4] Y. H. Woo, Phys. Rev. **41**, 21 (1932).
[5] For definition of S *see*, G. E. M. Jauncey and P. S. Williams, Phys. Rev. **41**, 127 (1932).

$$S_{\text{class}} = 1 + (Z+1)f'^2/Z^2 + (f^2/nZ)\sum_{r=1}^{n}{}' \sum_{s=1}^{n}{}'(\sin kl_{rs})/kl_{rs} \tag{1}$$

where

$$k = (4\pi \sin \tfrac{1}{2}\phi)/\lambda \tag{2}$$

and

$$f'^2 = f^2 - \left(Z \sum_{r=1}^{Z} E_r^2 - f^2\right)/(Z-1). \tag{3}$$

In Eqs. (1) and (3) f is the true atom form factor for each atom in the molecule of the gas and l_{rs} is the distance between the rth and sth atoms of a molecule. The quantities E_r are defined in a paper by Jauncey[6] on the diffuse scattering of x-rays by solids. In Paper II Woo takes account of the Compton effect and separates the scattered radiation into coherent and incoherent parts. The result of Woo's separation is to replace Eq. (1) above by

$$S = S_{\text{incoh.}}/(1 + \alpha \text{ vers } \phi)^3 + S_{\text{coh.}} \tag{4}$$

where α is the Compton quantity $h/mc\lambda$. In Paper II Woo gives

$$S_{\text{incoh.}} = 1 - f'^2/Z^2 \tag{5}$$

and

$$S_{\text{coh.}} = (f'^2/nZ)\sum_{r=1}^{n}{}' \sum_{s=1}^{n}{}'(\sin kl_{rs})/kl_{rs} \tag{6}$$

for polyatomic gases whose molecules consist of n atoms of one kind. In Paper III the author objected to Woo's formula for $S_{\text{coh.}}$ because the author believes that a formula which takes account of the separation into coherent and incoherent scattered radiation must reduce to the classical formula when α is put equal to zero. In other words, the right side of Eq. (1) must equal $S_{\text{incoh.}} + S_{\text{coh.}}$, or, as we may write it,

$$S_{\text{class.}} = S_{\text{incoh.}} + S_{\text{coh.}}. \tag{7}$$

This is not the case when Woo's formulas as given in Eqs. (5) and (6) are used.

Before considering Woo's Paper IV, the author wishes to introduce a new symbol f''. The true atom form factor f is defined by[6]

$$f = \sum_{r=1}^{Z} E_r \tag{8}$$

or, in other words, f/Z is the arithmetic mean of the E's. The new quantity f'' is to be defined by

$$f''^2 = Z\sum_{r=1}^{Z} E_r^2 \tag{9}$$

[6] G. E. M. Jauncey, Phys. Rev. **37**, 1193 (1931).

or, in other words, f''/Z is the root mean square of the E's. Eq. (3) now becomes

$$(Z-1)f'^2 = Zf^2 - f''^2 \tag{10}$$

and Eq. (1) may be written in the form

$$S_{\text{class.}} = 1 - f''^2/Z^2 + (f^2/Z)\left\{1 + (1/n)\sum_{r=1}^{n}{}' \sum_{s=1}^{n}{}'(\sin kl_{rs})/kl_{rs}\right\}. \tag{11}$$

From the point of view of the classical theory the author has no preference as between Eq. (1) and Eq. (11). The only difference is one of symbols.

In Paper IV Woo replies to the objections raised by the author in Paper III and arrives at Eq. (4) together with the defining equations

$$S_{\text{incoh.}} = 1 - f''^2/Z^2 \tag{12}$$

and

$$S_{\text{coh.}} = (f^2/Z)\left\{1 + (1/n)\sum_{r=1}^{n}{}' \sum_{s=1}^{n}{}'(\sin kl_{rs})/kl_{rs}\right\} \tag{13}$$

which replace Eqs. (5) and (6). It is seen that these formulas for $S_{\text{incoh.}}$ and $S_{\text{coh.}}$ satisfy Eq. (7) and so the author's objections are removed. Eq. (13) takes the special forms

$$S_{\text{coh.}} = (f^2/Z)\{1 + (\sin kl)/kl\} \tag{14}$$

for a diatomic gas and

$$S_{\text{coh.}} = (f^2/Z)\{1 + (3\sin kl)/kl\} \tag{15}$$

for a gas each of whose molecules consist of similar atoms with their centers at the corners of a regular tetrahedron. The quantity l is the distance between two atoms in the same molecule. If there are thermal vibrations of the atoms in the molecules of a gas, then, comparing with the author's Paper I, it is seen that $(\sin kl)/kl$ in Eqs. (14) and (15) is replaced by

$$\{(\sin kl_0)/kl_0\}\exp(-ky^2/4)$$

where y is the most probable change in the separation of any pair of atoms in a molecule from the mean separation l_0.

§2. Simple Crystals

The classical theory of the diffuse scattering of x-rays by simple cubic crystals consisting of atoms of one kind has been worked out by Jauncey and Harvey.[7] This theory leads to the formula

$$S_{\text{class.}} = 1 - f''^2/Z^2 + (f^2 - F^2)/Z \tag{16}$$

in virtue of Eq. (10). The quantity F is the atom form factor as referred to a lattice point, but not to the center of the atom. In Paper IV Woo separates

[7] G. E. M. Jauncey and G. G. Harvey, Phys. Rev. **37**, 1203 (1931).

the diffusely scattered radiation from a crystal into two parts according to Eq. (4), where $S_{\text{incoh.}}$ is given by Eq. (12) and

$$S_{\text{coh.}} = (f^2 - F^2)/Z. \tag{17}$$

It is seen that the right sides of Eqs. (12), (16), and (17) satisfy Eq. (7).

From Eqs. (12), (13), (16), it is seen that through f the coherent portion of the scattered radiation depends upon the arithmetic mean of the E's and that through f'' the incoherent portion depends upon the root mean square of the E's. This seems to give a mathematical distinction between the coherent and incoherent radiation even in the classical theory because the distinction between f'' and f remains even if $\alpha(=h/mc\lambda)$ is zero.

§3. Temperature and the True Atom Form Factor

In his formulas for the scattering of x-rays by crystals, the author has preferred to write F for the atom form factor as referred to a lattice point, but not to the atom center, instead of in the manner fe^{-M}, where f is the true atom form factor (which is due to the electron distribution relative to the center of the atom) and e^{-M} is the Debye[8] or Waller[9] temperature factor. In the derivation of the classical formulas for the scattering of x-rays by a solid and by a crystal, Jauncey[6,7] notes two different orders of velocity—the velocity of an electron in an atom relative to the center of the atom and the velocity of thermal agitation of the center of an atom about the lattice point with which the atom is associated. The atom may be likened to a planet with an electron atmosphere. The electrons of the atmosphere will pass through all their configurations many times while the atom as a whole is performing one vibration about its lattice point. The effective atom form factor F of an atom in a crystal is made up of two factors—f the true atom form factor and H the temperature factor. The second factor H is due to the changing configurations of the centers of the atoms relative to their respective lattice points, caused by the thermal motions of the atoms in the crystal. The author has made no special assumptions[6] concerning the form of H. Since values of $F(=fH)$ are determined experimentally by measurements of the integrated reflection from crystals, it is only necessary for Eqs. (16) and (17) to include F but not to include the form of H. The form of H is not as yet accurately known. According to James and Brindley,[10] H is fairly well given for sylvine by Waller's formula[9] at low temperatures but is not given by this formula at high temperatures.

In the Debye-Waller formula

$$F = fe^{-M} \tag{18}$$

it is postulated that the true atom form factor f is not affected by the heat motions of the atoms, or, in other words, that the electron distribution in an atom is independent of the violence of the thermal agitation of the atom

[8] P. Debye, Ann. d. Physik **43,** 49 (1914).
[9] I. Waller, Zeits. f. Physik **17,** 398 (1923).
[10] R. W. James and G. W. Brindley, Proc. Roy. Soc. **A121,** 155 (1928).

amongst the surrounding atoms. If we think of an atom in a crystal as being held to a lattice point by a quasi-elastic force, the atom will be acted upon by no force when at a lattice point and may be considered when at this point as being undistorted. However, if the atom is displaced from its lattice point, some amount of distortion in the electron distribution of the atom will occur. The f value for the atom will be the result of an average electron distribution for the electron configurations of the atom about its own center taken over many (comparatively slow) thermal vibrations of the atom about its lattice point. As the temperature rises the average electron distribution will become more and more distorted, if we measure the distortion as a departure from the electron distribution when the atoms are all at rest at their lattice points. There is no actual attractive force on a given atom towards its lattice point, but this apparent force is due to the forces of the neighboring atoms upon the given atom. As the thermal vibrations of the atoms become more violent, the atoms approach each other more closely and the electron atmospheres of the atoms become more distorted. It seems therefore that the average electron distribution about the center of an atom in a lattice should be a function of the temperature. Accordingly, the true atom form factor f should be a function of the temperature. The situation is somewhat the same as the case in the kinetic theory of gases where the quantity b in van der Waal's equation has been found to be a function of the temperature.[11] As the temperature rises and the impacts between molecules become more violent, the molecules penetrate each other more and more and so the distortion of the molecules due to impacts increases with the temperature.

Jauncey and Harvey[12] have shown that the relation

$$S_{\text{gas}} = (S + F^2/Z)_{\text{cryst.}} \tag{19}$$

holds very well for argon and sylvine at room temperature. On the other hand Jauncey and Williams[5] have found that the $(S+F^2/Z)$ values for sodium fluoride at room temperatures are consistently lower than the S values for neon. Now from Eqs. (4), (12), and (17) it follows that for a crystal

$$S + F^2/Z = (1 - f''^2/Z^2)/(1 + \alpha \operatorname{vers} \phi)^3 + f^2/Z \tag{20}$$

so that, if f and f'' are not functions of the temperature, $(S+F^2/Z)$ should be independent of the temperature. Jauncey and Harvey[13] have measured the S values for sylvine at temperatures of 90°K and 300°K and, using James and Brindley's F values[10] for sylvine at these two temperatures, have found that the $(S+F^2/Z)$ values at 90°K are distinctly less than those at 300°K. According to Eq. (20) the implication of this is that either or both f and f'' are functions of the temperature. If for simplicity we for the present assume $f''=f$ (as is the case if all the E's are equal[14]), then, since $(S+F^2/Z)$ is less at

[11] See K. F. Herzfeld, Handb. d. Physik. XXII, p. 399.
[12] G. E. M. Jauncey and G. G. Harvey, Phys. Rev. **38,** 1071 (1931).
[13] G. E. M. Jauncey and G. G. Harvey, Phys. Rev. **38,** 1925 (1931).
[14] G. E. M. Jauncey, Phys. Rev. **38,** 1 (1931).

90°K than at 300°K, f is less at 90°K than at 300°K. This means that the average electron distribution in an atom of sylvine departs more and more from the electron distribution in an argon atom as the temperature falls below room temperature. It is just a matter of good fortune that at room temperature the average electron distribution in an atom of sylvine is the same as that in an atom of argon. In the case of sodium fluoride it is probable that room temperature is too low a temperature for the electron distribution in an atom of this crystal to be the same as that for neon. It therefore appears that at temperatures approaching absolute zero, the f values for a crystal (such as KCl or NaF) are less than those for the corresponding gas (argon or neon). Consequently, the electron distribution in an atom of a crystal at absolute zero is more diffuse than in the atom of the corresponding gas. As the temperature rises above absolute zero, the atoms of the crystal vibrate amongst one another with increasing violence with the result that the average electron distribution about the center of each atom becomes less diffuse and finally at high temperatures becomes like the average electron distribution about the center of an atom of the corresponding gas.

It should be remembered that the atoms in crystals like NaF and KCl are ionized. It might be expected that on this account the electron distributions in the atoms of the respective crystals at absolute zero would differ from the electron distributions in the atoms of the corresponding gases.

§4. An Empirical Relation

In a recent report Wollan[15] quotes the author as stating that the relation

$$S_{\text{gas}} = (S + F^2/Z)_{\text{cryst}}. \tag{21}$$

represents a relation which could have been established empirically without the aid of theory. As Dr. Wollan learned of this in private conversation with the author it seems worth while to discuss the statement in greater detail.

For simplicity we shall assume that the scattering occurs without change of wave-length as is pretty nearly the case for argon and sylvine. Crowther's formula[16] for the intensity of x-rays scattered in a direction ϕ from a slab of material whose thickness is t is

$$I_\phi = (AIt/R^2 \cos \tfrac{1}{2}\phi) \cdot s \tag{22}$$

where I is the intensity per unit area of the rays transmitted through the slab when held in the Crowther position, A is the area of the ionization chamber window, R is the distance of the window from the slab, and s is the linear spatial scattering coefficient per unit solid angle in the direction ϕ. The quantity s in Eq. (22) is thus measured and defined in terms of experimental quantities and may therefore itself be considered an experimental quantity. Having found s by means of Eq. (22) we divide by ρ the density of the scattering material and obtain s/ρ which we shall call the mass spatial scattering

[15] E. O. Wollan, Rev. Mod. Phys. **4**, 205 (1932).
[16] J. A. Crowther, Proc. Roy. Soc. **A86**, 478 (1912).

coefficient per unit solid angle in the direction ϕ. The quantity s/ρ has been determined for argon by Wollan[17] and for sylvine by Harvey.[18] Referring to the paper by Jauncey and Williams,[5] we see that the relation between S the scattering factor per electron and s/ρ the mass spatial scattering coefficient is

$$S = \frac{s/\rho}{(NZ/W)\cdot(e^4/m^2c^4)\cdot(1+\cos^2\phi)/2} \tag{23}$$

where N is Avogadro's number, Z is the number of electrons in an atom of the scatterer, W is its atomic weight, and e, m and c have their usual significance.

We shall now introduce the quantities r the linear reflection coefficient and r/ρ the mass reflection coefficient of a crystal for x-rays. The mass reflection coefficient is given in terms of experimental quantities by

$$r/\rho = (i_\phi \omega \cos \tfrac{1}{2}\phi)/\rho I t \tag{24}$$

where ω is the angular speed at which the crystal is turned through the Bragg reflection position, i_ϕ is the total energy of the reflected x-rays entering the ionization chamber, I is the energy per unit time per unit area penetrating the crystal, and t is the thickness of the slab of crystal.[19] According to the classical theory of reflection of x-rays from a mosaic crystal[19]

$$r/\rho = \tfrac{1}{2}\cdot\frac{\rho N^2}{W^2}\cdot\lambda^3F^2\cdot\frac{e^4}{m^2c^4}\cdot\frac{1+\cos^2\phi}{\sin\phi\cos\tfrac{1}{2}\phi}. \tag{25}$$

From Eq. (25) we may obtain an expression for F^2/Z. Upon substituting this expression for F^2/Z, and also the right side of Eq. (23) for S_{gas} and for $S_{\text{cryst.}}$ in Eq. (21), we note that the expression $(NZ/W)\cdot(e^4/m^2c^4)\cdot(1+\cos^2\phi)/2$ factors out, leaving us with

$$(s/\rho)_{\text{gas}} = (s/\rho)_{\text{cryst.}} + \frac{W\sin\phi\cos\tfrac{1}{2}\phi}{\lambda^3\rho N}\cdot(r/\rho)_{\text{cryst.}}. \tag{26}$$

Now in a simple cubic crystal the principal grating space d is given by

$$d^3 = W/\rho N. \tag{27}$$

This equation together with Bragg's law

$$n\lambda = 2d\sin\tfrac{1}{2}\phi \tag{28}$$

gives

$$\lambda^3\rho N/W = (8\sin^3\tfrac{1}{2}\phi)/n^3 \tag{29}$$

so that Eq. (26) reduces to

$$(s/\rho)_{\text{gas}} = (s/\rho)_{\text{cryst.}} + (n^3/4)\cdot\cot^2\tfrac{1}{2}\phi\cdot(r/\rho)_{\text{cryst.}}. \tag{30}$$

[17] E. O. Wollan, Phys. Rev. **37**, 862 (1931).
[18] G. G. Harvey, Phys. Rev. **38**, 593 (1931).
[19] See A. H. Compton, *X-Rays and Electrons*, pp. 125–127.

This relation contains only experimental quantities. It contains no such quantities as Avogadro's number, the atomic weight and number of the scatterer, the charge and mass of the electron, or the wave-length of the x-rays. In this present paper we have derived Eq. (30) by means of an extension of Thomson's classical theory of the scattering of x-rays. We have made use of such theoretical concepts as the charge and mass of the electron and the wave-length of x-rays, yet in the final equation all quantities connected with these concepts have cancelled out and we are left with a relation between experimental magnitudes such as angles, densities, thickness, distances, electrometer deflections, and speed of rotation of the crystal. Without any knowledge of the theory of the scattering or reflection of x-rays the relation expressed by Eq. (30) could have been established by means of experimental measurements on the diffuse scattering of x-rays from (say) argon and sylvine together with measurements on the reflecting power of the crystal for x-rays. The quantity n of Eq. (30) may be considered as a pure number obtained experimentally by counting. Hence the relation expressed by Eq. (30) may be called an empirical relation. Of course it is understood that the experimenter would use x-rays of the same hardness (perhaps Barkla's characteristic rays from a metal like copper or molybdenum) for the crystal as for the gas.

§5. Digression on Philosophy

For convenience we shall for the moment speak of Eq. (21) as a theoretical relation because the numerical values of each of the S's and of the F are obtained by dividing an experimental quantity by quantities which are introduced by the Thomson theory as for instance in Eq. (23). We have shown how the theoretical relation Eq. (21) may be replaced by the empirical relation Eq. (30) which contains no vestige of the Thomson theory. In his physical philosophy, the author inclines to the operational viewpoint of Bridgman.[20] Further, the author supports the view that physical laws express relations between pointer readings made on gross (macroscopic) instruments. Eq. (30) is such a relation. The literature of physics abounds in theoretical relations of the type of Eq. (21). Just as it has been possible to replace the theoretical Eq. (21) by the empirical Eq. (30), so the author believes it is possible to replace other theoretical relations of physics by empirical relations among gross physical magnitudes. The author believes that one purpose of theoretical physics is to facillitate the discovery of empirical relations among gross physical magnitudes. Concepts such as the charge and mass of an electron and the wave-length of x-rays are very useful but the author doubts that they represent reality in the world.[21]

§6. Complicated Crystals

The author has discussed the classical theory of the diffuse scattering of x-rays by solids[6] in a paper to be referred to as Paper V. In a second paper

[20] P. Bridgman, *Logic of Modern Physics.*

[21] G. E. M. Jauncey, *Modern Physics*, pp. 538–540.

the author together with Harvey has applied the theory to the diffuse scattering by simple cubic crystals consisting of atoms of one kind.[7] We shall refer to this second paper as Paper VI.

Following the argument of Paper V we arrive at Eq. (13) of that paper. Up to this point in Paper V the electrons are not aggregated into atoms. If, instead of aggregating the electrons into atoms of one kind as was done in Paper I, we aggregate them into atoms of two kinds, which we shall distinguish by the subscripts 1 and 2, we obtain, in place of Eq. (22) of Paper V,

$$S = 1 + \frac{\nu_1(Z_1 - 1)f_1'^2/Z_1 + \nu_2(Z_2 - 1)f_2'^2/Z_2}{\nu_1 Z_1 + \nu_2 Z_2} + \{1/n(\nu_1 Z_1 + \nu_2 Z_2)\} \sum'' \sum'' \int\int p_r p_s \cos k(z_r - z_s) dz_r dz_s \tag{31}$$

where ν_1 and ν_2 are the respective numbers of the atoms of kinds 1 and 2 in a molecule of the solid and n is the number of molecules in the scattering speck. Now, distinguishing between the rapidity of the orbital motions of the electrons in the atoms and the comparative slowness of the heat motions of the atoms about their equilibrium centers as is done on pages 1200 and 1201 of Paper V, we obtain, in place of Eq. (31) of Paper V,

$$S = 1 + \frac{\nu_1(Z_1 - 1)f_1'^2/Z_1 + \nu_2(Z_2 - 1)f_2'/Z_2}{\nu_1 Z_1 + \nu_2 Z_2} + \{1/n(\nu_1 Z_1 + \nu_2 Z_2)\} \cdot \{F_1^2 X_{11} + F_1 F_2 X_{12} + F_2^2 X_{22}\} \tag{32}$$

where the X's are double summations of cosines. The problem is now to determine the X's for a crystal.

Following the argument of Paper VI, Eq. (4) of that paper is replaced by

$$I = \{Z_1 \sum\sum\sum \cos k w_{pqr} + Z_2 \sum\sum\sum \cos k w_{pqr}\}^2 + \{Z_1 \sum\sum\sum \sin k w_{pqr} + Z_2 \sum\sum\sum \sin k w_{pqr}\}^2 \tag{33}$$

where the first triple summation in each set of braces $\{\ \}$ refers to atoms of kind 1 and the second triple summation to atoms of kind 2. Let us consider one of the single summations, say, $\Sigma \cos k w_{pqr}$ where the summation is with respect to p, so that we may write it as $\Sigma \cos k w_p$. The quantity w_p is the perpendicular from a point on a lattice line of the crystal upon the reference plane.[6,7] The lattice points on the line are either such that consecutive points are at equal distances from each other or can be separated into sets of points such that in each set consecutive points are at equal distances from each other. One of these alternatives is true even when the axes of the crystal are not rectangular and when the consecutive atoms along a lattice line are not equally spaced. Hence either $\Sigma \cos k w_p$ has a value given by Eq. (7) of Paper VI or can be broken up into a small number of summations each of which has a value given by this equation. Proceeding to the summations with respect to

q and r we arrive at a result similar to Eq. (11) of Paper VI. Now, except for particular values of $k\{=(4\pi \sin \tfrac{1}{2}\phi)/\lambda\}$, the right side of Eq. (11) of Paper VI is of the order unity. As in Paper VI, we divide by the total number of atoms in the speck of scattering matter and find S to be of the order of 10^{-17} if we are dealing with a speck of crystal of linear dimensions, say, 0.1 mm. The order 10^{-17} may be called zero, so that $S=0$ for a speck of crystal consisting of point atoms located exactly and permanently at the lattice points of the crystal. Now, referred to Eq. (32), S must become zero for point atoms located at lattice points—that is, for $f_1' = F_1 = Z_1$ and $f_2' = F_2 = Z_2$. Hence, substituting these values in the right side of Eq. (32) and rearranging, we obtain

$$(n\nu_1 + X_{11})Z_1^2 + X_{12}Z_1Z_2 + (n\nu_2 + X_{22})Z_2^2 = 0. \tag{34}$$

Since X_{11}, X_{12}, and X_{22} are constants determined only by the geometrical make-up of the crystal and do not depend on Z_1 and Z_2 and since also Eq. (34) holds for any values of Z_1 and Z_2, this equation is an identity. Hence

$$X_{11} = -n\nu_1, \; X_{12} = 0, \text{ and } X_{22} = -n\nu_2. \tag{35}$$

Substituting in Eq. (32) and eliminating f' by means of Eq. (10), we obtain

$$S_{\text{class.}} = \left\{1 - \frac{\nu_1 f_1''^2/Z_1 + \nu_2 f_2''^2/Z_2}{\nu_1 Z_1 + \nu_2 Z_2}\right\} + \left\{\frac{\nu_1(f_1^2 - F_1^2) + \nu_2(f_2^2 - F_2^2)}{\nu_1 Z_1 + \nu_2 Z_2}\right\}. \tag{36}$$

The extension of this formula to the scattering by crystals consisting of more than two kinds of atoms is obvious. Woo's method of taking account of the Compton effect gives Eq. (4) together with

$$S_{\text{incoh.}} = 1 - \left(\sum_r \nu_r f_r''^2/Z_r\right) \Big/ \sum_r \nu_r Z_r \tag{37}$$

and

$$S_{\text{coh.}} = \left(\sum_r \nu_r (f_r^2 - F_r^2)\right) \Big/ \sum_r \nu_r Z_r \tag{38}$$

where the subscript r refers to the rth type of atom in a molecule of the crystal.

In conclusion it should be noted that the validity of Eq. (36) and also of Eqs. (37) and (38) for the diffuse scattering from a complicated crystal rests upon the validity of the same simplifying assumptions as were made in Paper V in the derivation of Eq. (16) of the present paper for a simple cubic crystal consisting of atoms of one kind. The first simplifying assumption is that expressed by Eq. (14) of Paper V in which it is assumed that the probability function for each electron is symmetrical about a reference plane (see Paper V) through the nucleus. This may not be the case in certain types of crystals. This assumption of symmetry is back of Eq. (26) of Paper V. Then, again, the assumption of symmetry in the thermal vibrations of the atoms of the crystal about their respective lattice points is back of Eq. (29)

of Paper V. In section 3 of the present paper we have seen that the electron distribution about the center of an atom of a crystal is probably a function of the temperature. At absolute zero the probability of an electron in an atom of sylvine being in a volume element dv is not only a function of the distance r of dv from the nucleus but also of the direction of the line joining dv and the nucleus with respect to the axes of the crystal. This will affect the f values for the atoms of the crystal. Above absolute zero it seems from the evidence given in §3 that the function of the direction approaches a constant as the temperature increases, so that at high temperatures the electron distribution about the nucleus of an atom of sylvine is a function of the distance r alone as is the case in an atom of argon.

Mass Ratio of the Boron Isotopes from the Spectrum of BO

By F. A. JENKINS* AND ANDREW MCKELLAR
Department of Physics, University of California

(Received September 20, 1932)

Wave number data. New measurements are made of the rotational structure of the α bands of BO, and the wave numbers of the lines in the $^2\Pi_{1/2}$, $^2\Sigma$ component up to about $J=20$ are tabulated for the (0, 0), (0, 1), (0, 2), (1, 0), (1, 1), (1, 2), (2, 0), (3, 0), and (4, 0) bands of both the $B^{11}O$ and $B^{10}O$ systems. The $^2\Pi_{1/2}$, $^2\Sigma$ component of (5, 0) is also measured for $B^{11}O$ and the $^2\Pi_{3/2}$, $^2\Sigma$ component of (1, 0) for $B^{11}O$ and $B^{10}O$.

Vibrational isotope effect. Values of ΔG_v are computed by least-squares methods, and from the ratio $\Delta G_e^i/\Delta G_e$, the isotopic mass coefficient $\rho=(\mu/\mu^i)^{1/2}$ is found to be 1.02908 ± 0.00003, from the data on the $^2\Sigma$ state, and 1.02913 ± 0.00004, from that on $^2\Pi_{1/2}$. The latter figure is less trustworthy than the former, because of the presence of perturbations in the upper state. The mass-spectrograph measurements of Aston give $\rho=1.02908\pm0.00003$. The relation $\rho=x_e^i/x_e$ is verified to within the probable error, one part in 500. Improved values are obtained for the vibrational constants of the $^2\Sigma$ state, while for the $^2\Pi_{1/2}$ state, the equations $\Delta G_v=1260.415-21.870(v'+\frac{1}{2})$ and $\Delta G_v^i=1297.130-23.228(v'+\frac{1}{2})$ are considered to give the constants least influenced by perturbation effects.

Rotational isotope effect. From the rotational term-differences, the constants B_v and α are computed, also by least squares. The equations $B_v''=1.7803-0.01648(v''+\frac{1}{2})$, $B_v''^i=1.8850-0.01772(v_.''+\frac{1}{2})$, $B_{v'i_{-1/2}}=1.4277-0.0196(v'+\frac{1}{2})$, and $B_{v,-1/2}'^i=1.5115-0.0211\ (v'+\frac{1}{2})$ give values of $\rho^2=B_e^i/B_e$ and $\rho^3=\alpha_e^i/\alpha_e$ which yield values of ρ equal to those obtained from the vibrational constants to within the probable error, one part in 4000 for the B_e's and one in 100 for the α_e's. A perturbation is found in the rotational levels of $^2\Pi_{1/2}{}^{(4)}$, which reaches its maximum at $J'=13\frac{1}{2}$. It is caused by the crossing of these levels by those of $^2\Sigma^{(17)}$, and affects only one component of the Λ-doublets, as expected. The Λ-doubling is investigated, and its constants computed.

Electronic isotope effect The spin coupling constant, A, is evaluated by the 1, 0 band, and found to be the same for $B^{11}O$ and $B^{10}O$, having the value 122.36 ± 0.03 cm^{-1}. The origins of the two isotopic band systems, $^2\Pi_{1/2}$, $^2\Sigma$, are found to be $\nu_{2e}=23{,}958.85\pm0.05$, $\nu_{2e}{}^i=23{,}959.18\pm0.06$, giving an electronic shift of 0.33 ± 0.08 cm^{-1}, the $B^{10}O$ origin being displaced toward the violet.

INTRODUCTION

MANY verifications of the theory of the isotope effect in band spectra[1] have established the fundamental correctness of the theory. They have also led to the discovery of new isotopes of low abundance. The frequencies of the band lines of a suspected isotopic molecule can be predicted with great certainty. The possibility of reversing the usual procedure, and of computing accurately the relative masses of isotopic atoms from the observed frequen-

* Fellow of the John Simon Guggenheim Memorial Foundation, at present in the Physical Institute, Utrecht.

[1] F. W. Loomis, Bull. Nat. Res. Council **57**, 250 (1926). R. Mecke, Geiger and Scheel's Handbuch der Physik **21**, 565–573 (1929).

cies was first explicitly mentioned by Giauque,[2] although of course it was implied in Mulliken's original work.[3] Thus far the only case in which data of sufficient accuracy and completeness were available has been the atmospheric bands of oxygen, from which the mass ratio $O^{18}:O^{16}$ has now been found by Babcock and Birge[4] with an apparent accuracy of one part in 100,000. Since the oxygen isotopes have not yet been observed with the mass-spectrograph,[4a] the band-spectrum method is the only one at present available for determining the atomic weights of O^{18} and O^{17}.

It therefore appears highly desirable to apply this method to an element for which the isotopic masses have already been found by Aston's precision mass-spectrograph. This would allow us to decide whether the theory of the isotope effect is sufficiently correct in its finer details to be reliable in such an exacting application. For this purpose the most accurate results are obtained in the case of a light element where the proportional difference in mass of the isotopes is large. Boron and lithium are especially suitable, and in the present work it will be shown that the spectrum of BO gives satisfactory agreement with Aston's values for the mass-ratio $B^{11}:B^{10}$. Work on the $Li^7:Li^6$ ratio from the Li_2 bands is now in progress.

The BO spectrum excited in active nitrogen was used by Mulliken in his first and most accurate test of the isotope effect.[5] Of the three band systems in this spectrum, the α system is the most favorable for precise work, because it occurs at longer wave-lengths where an advantageous ratio of wave-length interval to frequency interval exists. The rotational structure of these bands was first shown by one of us[6] to be that of a $^2\Pi$, $^2\Sigma$ transition, in which the $^2\Pi$ level is inverted and constitutes a good example of the case *a* type of spin coupling. The complete experimental material was not given in this article, because further measurements, particularly of the bands of the less abundant isotopic molecule $B^{10}O$, were anticipated. In the meantime Scheib[7] has published extensive measurements of four bands of the α system as developed in the arc. Because of the higher temperature, many more rotational lines of each band are observed than in active nitrogen. All of Scheib's measurements concern the bands of the more abundant isotope, $B^{11}O$, since none of the $B^{10}O$ bands were identified in his work. Furthermore, the data given by Scheib for the (0,1), (0,2), (0,3) and (0,4) bands, while they suffice for the determination of the molecular constants of the lower, $^2\Sigma$ state, do not

[2] W. F. Giauque, Nature **124,** 127 (1929).

[3] R. S. Mulliken, Phys. Rev. **25,** 119 (1925).

[4] H. D. Babcock and R. T. Birge, Phys. Rev. **37,** 233A (1931). See also the preliminary account and discussion given by Birge in Trans. Farad. Soc. **25,** 718 (1929). In the work of Mecke and Wurm, Zeits. f. Physik **61,** 37 (1930), the data were insufficient, and the methods not sufficiently rigorous, to yield a result of much significance.

[4a] F. W. Aston, Nature **130,** 21, July 2 (1932). Here is recorded the observation of the oxygen isotopes O^{17} and O^{18} by the mass-spectrograph and their abundance is estimated but no accurate mass determinations are made.

[5] R. S. Mulliken, Phys. Rev. **25,** 259 (1925).

[6] F. A. Jenkins, Proc. Nat. Acad. Sci. **13,** 496 (1927).

[7] W. Scheib, Zeits. f. Physik **60,** 74 (1930).

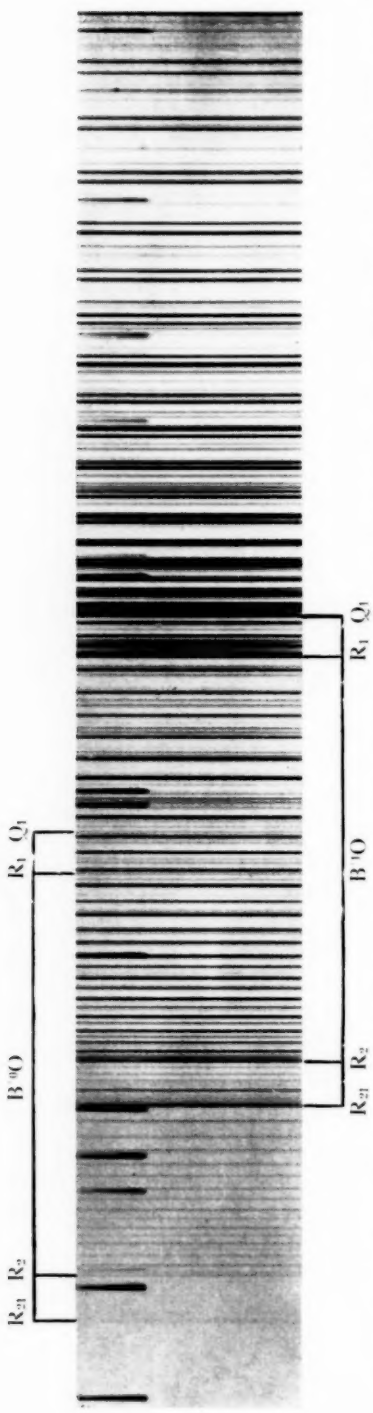

Fig. 1. The 2, 0 band of the a system of BO. First order of the 21-foot grating. The origin of the fainter, $B^{10}O$, band lies 8.876A further to the violet (i.e., to the left) in this case, and its rotational structure is seen to be almost an exact replica of that in the $B^{11}O$ band, but on a slightly larger scale.

yield all the constants of the $^2\Pi$ state, because these bands involve only $v' = 0$. Hence the present article, besides giving the first measurements on the $B^{10}O$ system, also supplements Scheib's data for the upper state of the $B^{11}O$ system.

Experimental Data

The spectrograms used in our analyses have already been briefly described in connection with the preliminary work mentioned above.[6] For a source, BCl_3 vapor was mixed with a stream of flowing active nitrogen containing traces of oxygen. The spectrum was photographed in the first and second orders of the Harvard 21-foot grating of 120,000 lines, which is mounted on the Paschen system. Double exposures of the iron arc spectrum were used to insure correct placing of the standards.

These plates have been completely remeasured with a Société Génevoise comparator. Independent measurements of the same band gave results differing on the average by less than 0.01 cm^{-1}. For the purpose in hand, it was not necessary or desirable to measure all the lines of each band, since an analysis of the $^2\Pi_{1/2}$, $^2\Sigma$ component only will give the required data. Also this sub-band is much freer from blends than the other, particularly for the fainter

Table I. *1, 0 band.*

K''	R_{21} λ4014.962	R_2 λ4017.087	R_2^i λ4012.781	Q_2	Q_2^i	P_2	P_2^i
0					24,911.64		
1	24,894.06	14,886.66	24,913.36	24,882.42			
2	896.66	886.66	913.36	879.51	905.90		
3	898.36	885.72	912.46	875.88	901.98		
4	899.48	884.14	910.75	871.47	897.30	24,861.83	
5	899.84	881.83	908.27	866.33	891.88	853.80	
6	899.84	878.71	905.04	860.44	885.72	845.16	24,869.41
7	898.36	874.92	900.94	853.80	878.71	835.81	859.47
8	896.66	870.35	896.15	846.38	870.77	825.60	848.77
9	894.06	865.02	890.50	838.24	862.14	814.71	837.00
10	890.75	858.94	884.14	829.34	852.67	803.07	824.87
11	886.66	852.10	876.79	819.70	842.50	790.66	811.64
12	881.83	844.50	868.78	809.31	831.51	777.47	797.93
13	876.26	836.15	859.92	798.16	819.70	763.54	783.06
14	870.25	827.05	850.27	786.30	807.10	748.84	767.42
15		817.19	839.83	773.61	793.75	733.52	750.99
16		806.57	828.61	760.15	779.34	717.32	733.52
17		795.24	816.55	745.98	764.48	700.31	715.99
18		783.06	803.54	731.15	748.84	682.77	
19		770.16	790.09	715.45	732.18	664.33	
20		756.58	775.56	698.99	714.75	645.16	
21		742.08		681.85	696.36	625.26	
22		726.99		663.91		604.59	
23		710.75		645.16		583.07	
24		694.28		625.71		560.91	
25		676.82		605.54		537.97	
26		658.43		584.54		514.25	
27		639.47		562.82		489.74	
28		619.77		540.24		464.59	
29		599.14		517.01			
30				492.68			
31				467.79			
32				442.10			

TABLE I. (*Continued*). *1, 0 band*

K''	R_1 λ4035.467	R_1^i λ4031.039	Q_1 λ4037.415	Q_1^i λ4033.112	P_1	P_1^i	P_{12}
0	24,764.96						
1	768.27		24,761.35	24,787.78			
2	770.94		761.19	787.78	24,754.45	24,780.54	
3	772.50	24,799.63	760.15	786.62	750.53	776.54	
4	773.31	800.52	758.23	784.55	745.98	771.52	
5	773.31	800.52	755.55	781.74	740.50	765.77	24,728.19
6	772.50	799.63	752.07	778.02	734.22	759.14	719.38
7	770.94	798.16	747.75	773.31	727.27	751.49	709.54
8	768.63	795.24	742.65	767.97	719.38	743.31	698.96
9	765.43	792.05	736.72	761.63	710.75	734.22	687.60
10	761.36	787.78	730.01	754.45	701.31	724.15	675.38
11	756.58	782.63	722.45	746.48	691.03	713.10	662.34
12	750.99	776.54	714.10	737.58	679.95	701.31	648.55
13	744.54	769.82	704.96	727.87	668.04	688.93	633.97
14	737.30	762.00	695.02	717.32	655.39	675.38	618.57
15	729.27	753.55	684.23	705.88	641.90	661.02	602.44
16	720.40	744.03	672.67	693.55	627.61	645.85	585.34
17	710.75	733.52	660.29	680.41	612.53	629.88	567.50
18	700.31	722.45	647.14	666.36	596.59	612.92	548.89
19	688.93	710.75	633.12	651.53	579.87	595.21	529.45
20	676.82	697.61	618.34	635.76	562.37	576.48	509.24
21	663.91	684.23	602.74	619.18	544.03	557.10	488.23
22	650.18	669.28	586.32	601.74	524.86	536.83	466.44
23	635.76		569.06	583.48	504.97	515.70	443.79
24	620.32		551.07		484.24		
25	604.32		532.23		462.68		
26	587.13		512.62		440.37		
27	569.49		492.18		417.24		
28	551.07		470.90		393.25		
29			448.90				
30			426.06				
31			402.37				
32			377.92				

TABLE I. (*Continued*). *1,1 band.*

K''	R_{21} λ4339.369	R_2 λ4341.931	R_2^i λ4346.957	Q_2	Q_2^i	P_2
0				23,024.05	22,997.43	
1	23,031.71	23,024.78	22,998.16	020.45	993.48	
2	034.49	024.78	998.16	017.55	990.50	
3	036.50	024.05	997.43	014.12	986.73	23,007.27
4	037.86	022.57	995.80	009.91	982.18	000.20
5	038.37	020.45	993.48	004.92	977.23	22,992.34
6	038.37	017.55	990.50	22,999.23	971.08	983.96
7	037.46	013.96	986.73	992.83	964.29	974.80
8	035.93	009.61	982.18	985.65	956.78	964.89
9	033.66	004.56	976.81	977.82	948.48	954.27
10	030.67	22,998.82	970.70	969.25	939.31	942.95
11	026.96	992.34	963.83	959.97	929.60	930.89
12	022.57	985.13	956.24	949.99	919.04	918.17
13	017.55	977.23	947.92	939.31		
14	011.50	968.62	938.77	927.84		
15	004.92	959.25	928.88	915.70		
16	22,997.43	949.16	918.17			
17	989.42	938.33				
18	980.64	926.81				
19	971.08	914.55				
20	960.89					
21	949.99					
22	938.33					

TABLE I. (*Continued*). *1, 2 band.*

K''	R_{21} λ4715.525	R_2 λ4718.660	R_2^i λ4736.250	Q_2	Q_2^i	P_2
0				21,185.85	21,107.19	
1	21,193.24	21,186.55	21,107.87	182.20	103.85	
2	196.20	186.55	107.87	179.47		21,175.35
3	198.39	185.85	107.19	175.96	096.63	168.95
4	199.40	184.56	105.75	171.87	092.28	162.29
5	200.64	182.51	103.85	167.02	087.28	154.61
6	200.64	179.86	100.84	161.52	081.28	146.37
7	199.99	176.51	097.30	155.33	074.94	137.33
8	198.82	172.46	092.97	148.49	067.59	127.71
9	196.84	167.73	088.05	140.95		117.40
10	194.11	162.29	082.38	132.70		106.38
11	190.81	156.18	075.88	123.80		094.70
12	186.55	149.38		114.21		082.38
13	182.20	141.91		103.85		068.97
14	176.51	133.72		092.97		
15	170.42	124.87		081.28		
16	163.61	115.26				
17	156.18	105.04				
18		094.07				
19		082.38				

TABLE I. (*Continued*). *0,0 band.*

K''	R_{21}	R_2 λ4227.480	R_2^i	Q_2	Q_2^i	P_2
0				23,646.02	23,637.42	
1		23,648.13		643.86	634.99	
2		648.13		641.02	632.03	
3		647.40	23,638.71	637.42	628.20	
4		646.02	637.42	633.19	623.77	
5	*not*	643.86	634.99	628.20	618.43	23,615.57
6	*observed*	641.02	632.03	622.50	612.45	606.98
7		637.42	628.20	616.09	605.66	
8		633.19	623.77	609.00	598.13	587.84
9		628.20	618.43	601.12	589.93	577.27
10		622.50	612.45	592.60	580.81	565.87
11		616.09	605.66	583.31	571.02	553.85
12		609.00	598.13	573.35	560.47	540.93
13		601.12	589.93	562.67		527.62
14		592.60	580.81	551.23	537.20	
15		583.31	571.02	539.14	524.27	
16		573.35	560.47	526.33		
17		562.67				
18		551.23	537.20			
19		539.14	524.27			
20		526.33				

TABLE I. (*Continued*). *0,1 band.*

K''	R_{21} λ4585.702	R_2 λ4588.759	R_2^i λ4601.883	Q_2	Q_2^i	P_2
0	21,789.96			21,783.90		
1	793.32	21,786.30	21,724.17	781.94	21,719.77	
2	796.15	786.30	724.33	779.22	716.84	21,775.06
3	798.41	785.73	723.64	775.75		768.70
4	799.89	784.45	722.40	771.59	708.64	761.73
5	800.83	782.50	720.35	766.76	703.80	754.11
6	800.83	779.84	717.50	761.27	697.84	745.83
7	800.42	776.54	714.06	755.08	691.33	736.86
8	799.17	772.52	709.86	748.26	684.09	727.23
9	797.31	767.83	704.90	740.74	676.22	716.84
10	794.76	762.51	699.28	732.52		705.83
11	791.48	756.44	692.89	723.64		694.20
12	787.56	749.71	685.78	714.06		681.78
13		742.31	678.04	703.80		
14		734.21		692.89		
15		725.45		681.29		
16		715.94				
17		705.83				
18		694.99				
19		683.45				

TABLE I. (*Continued*). *0,2 band.*

K''	R_{21} λ5007.846	R_2 λ5011.650	R_2^i λ5040.468	Q_2	Q_2^i	P_2
0						
1		19,947.96	19,833.91	19,943.72	19,829.65	
2	19,958.11	947.96	833.91	940.82		19,936.67
3	960.39	947.55	833.35	937.49		
4	961.93	946.48	832.34	933.46		923.60
5	962.84	944.61	830.45	928.90		916.22
6	963.12	942.16	827.85	923.60		908.17
7	962.84	938.94	824.61	917.66	802.01	899.35
8	961.93	935.34		911.05	794.98	889.94
9	960.39	930.97		903.81	787.37	879.99
10	958.11	925.93	810.87	895.96	779.07	869.29
11	955.26	920.24	804.89	887.44		857.97
12	951.69	913.91	798.19	878.25		845.90
13		906.92	790.86	868.43	749.96	833.35
14		899.35	782.81	857.97		
15		891.05	774.06	846.84		
16		882.09	764.69	835.09		
17		872.48	754.55			
18		862.18				
19		851.33				

TABLE I. (*Continued*). *2,0 band.*

K''	R_{21} λ3828.047	R_2 λ3829.857	R_2^i λ3820.962	Q_2	Q_2^i	P_2
0				26,101.49		
1		26,103.26	26,164.03	099.18	26,159.69	
2	26,112.75	103.26	164.03	096.22	156.58	
3	114.48	102.18	162.84	092.45	152.56	26,085.55
4	115.61	100.38	161.06	087.91	147.78	078.34
5	115.61	097.91	158.36	082.61	142.09	070.30
6	115.13	094.56	154.79	076.51	135.68	061.47
7	113.73	090.45	150.43	069.60	128.39	051.82
8	111.40	085.55	145.23	061.96	120.26	041.42
9	108.57	079.88	139.25	053.45	111.40	030.19
10	104.81	073.38	132.38	044.23	101.49	018.25
11	100.38	066.13	124.64	034.16	090.86	005.47
12		058.10	116.14	023.43	079.41	25,991.96
13		049.22	106.77	011.75	067.10	977.63
14		039.58	096.51	25,999.35	053.95	
15		029.14	085.55	986.19	039.94	
16		017.91	073.38		025.08	
17		005.91	060.65		009.26	
18		25,993.03	047.15		25,992.42	
19		979.45	032.79			
20			017.53			
21			001.43			

TABLE I. (*Continued*). *3,0 band.*

K''	R_{21} λ3660.631	R_2 λ3662.205	R_2^i λ3649.691	Q_2	Q_2^i	P_2
0						
1	27,304.88	27,298.22	27,391.80	27,294.37	27,387.41	
2	307.45	298.22	391.80	291.30	384.25	
3	309.14	297.12	390.50	287.44	380.23	27,280.77
4	309.95	295.14	388.37	282.77	375.31	273.25
5	309.95	292.38	385.56	277.29	369.60	265.18
6	309.14	288.85	381.78	271.00	362.97	255.95
7	307.45	284.46	377.79	263.88	355.33	246.46
8	304.52	279.21	371.59	255.95	346.98	235.70
9	301.52	273.25	365.16	247.14	337.64	224.22
10	297.12	266.28	357.87	237.54	327.44	211.91
11	292.38	258.70	349.67	227.13	316.36	198.88
12		250.13	340.61	215.89	304.52	184.89
13		240.76	330.65	203.79	291.44	
14		230.63	319.96	190.90	277.84	
15		219.57	308.20	177.03	263.42	
16		207.74			247.76	
17		195.06			231.57	
18		181.60	267.95		214.43	
19			252.58		196.40	
20			236.45			
21			219.57			
22			201.64			
23			183.44			

TABLE I. (*Continued*).

	4,0 band				*5,0 band*	
K''	R_2 λ3511.222	$R_2{}^i$ λ3495.848	Q_2	$Q_2{}^i$	R_2	Q_2
0						
1	28,472.01	28,597.22				29,621.18
2	472.01	97.22	28,465.22	28,590.06	29,624.75	617.95
3	470.71	95.65	461.25	85.58	623.49	613.87
4	468.66	93.40	456.45	80.41	621.18	608.93
5	465.71	90.41	450.80	74.50	617.95	603.11
6	461.90	86.15	444.31	67.61	613.87	596.43
7	457.20	81.38	436.91	59.80	608.93	588.87
8	451.70	75.39	428.70	51.01	603.11	580.29
9	445.31	68.60	419.62	41.45	596.43	570.89
10	438.05	60.86	409.61	30.76	588.87	560.61
11	430.00	52.21	398.80	19.33	580.29	549.41
12	421.08	42.77	387.16	06.98	570.89	537.36
13	411.75	32.20	374.61	28,493.69	560.61	524.31
14	400.10	20.83	361.18		549.41	
15	388.60	08.58			537.36	
16	376.20				524.31	
17	362.98					

isotopic system. This will be evident from the enlargement, Fig. 1. All the four branches of the $^2\Pi_{1/2}$, $^2\Sigma$ sub-band, which are designated in order R_{21}, R_2, Q_2, and P_2, could be accurately measured in most cases for the stronger system, $B^{11}O$, but the R_{21} branch (and sometimes the P_2) of $B^{10}O$ was too faint to measure. To get the constants of the lower state, the two progressions $v'=0$ and $v'=1$ were measured from $v''=0$ to 2, while for the upper state four additional bands of the strong $v''=0$ progression, (2,0), (3,0), (4,0) and (5,0), were investigated. Of these ten bands, only 0,1 and 0,2 had been measured by Scheib. Our results are systematically lower by 0.21 cm^{-1} in the former band, and by 0.16 cm^{-1} in the latter. The possibility of a constant error of this magnitude in our measurements was eliminated by checking against the lines of the 0,9 β-band of NO and the boron doublet, λλ2496.778, 2497.733 (in the second order), which were present in the band source.

In Table I will be found the wave numbers in vacuum of all of the measured lines assigned to the various branches in these bands, with the wavelength in I.A. of the observed heads at the top of the appropriate columns. The column headings for the less intense system, that of $B^{10}O$, carry the superscript i. For 1,0 the low-frequency sub-band $^2\Pi_{1\ 1/2}$, $^2\Sigma$ was also measured and analyzed in order to find the constants of the $^2\Pi_{1\ 1/2}$ state and the electronic coupling coefficient, A. The 0, 0 band was unsatisfactory for this purpose because it is fainter, and confused with the 3,2 band.

VIBRATIONAL ISOTOPE EFFECT

The vibrational terms of the two isotopic molecules may be represented[8] by the following equation:

$$\begin{aligned} B^{11}O\ G &= \omega_e(v+\tfrac{1}{2}) - x_e\omega_e(v+\tfrac{1}{2})^2 + y_e\omega_e(v+\tfrac{1}{2})^3 + \cdots \\ B^{10}O\ G^i &= \omega_e{}^i(v+\tfrac{1}{2}) - x_e{}^i\omega_e{}^i(v+\tfrac{1}{2})^2 + y_e{}^i\omega_e{}^i(v+\tfrac{1}{2})^3 + \cdots \\ &= \rho\omega_e(v+\tfrac{1}{2}) - \rho^2 x_e\omega_e(v+\tfrac{1}{2})^2 + \rho^3 y_e\omega_e(v+\tfrac{1}{2})^3 + \cdots, \end{aligned} \qquad (1)$$

[8] R. S. Mulliken, Phys. Rev. **25**, 125 (1925).

in which ρ^2 is the ratio of the reduced masses μ/μ^i. We shall use the superscript i to distinguish quantities pertaining to the less abundant molecule $B^{10}O$. The problem of finding the relative masses thus becomes one of evaluating as accurately as possible the constant ρ from the relation

$$\omega_e{}^i/\omega_e = \rho. \tag{2}$$

Other values of this constant, though much less accurate, can be found from the higher power term; since

$$x_e{}^i/x_e = \rho, \quad y_e{}^i/y_e = \rho^3. \tag{3}$$

From the spectrum we can evaluate the term-differences

$$\Delta G_v = \omega_e - 2x_e\omega_e(v + \tfrac{1}{2}) + 3y_e\omega_e[(v + \tfrac{1}{2})^2 + 1/12] + \cdots \tag{4}$$

by finding the separation of the origins of two adjacent bands in a progression. This separation is best determined by a study of the combination differences of the type

$$\begin{aligned} R_2{}^{(0,0)}(K) - R_2{}^{(0,1)}(K) &= Q_2{}^{(0,0)}(K) - Q_2{}^{(0,1)}(K) = P_2{}^{(0,0)}(K) - P_2{}^{(0,1)}(K) \\ &= \Delta G_{1/2}'' - (B_0'' - B_1'')(K + \tfrac{1}{2})^2 + \cdots \\ &= \Delta G_{1/2}'' - \alpha''(K + \tfrac{1}{2})^2 + \cdots \end{aligned} \tag{5a}$$

$$\begin{aligned} R_2{}^{(1,0)}(K) - R_2{}^{(0,0)}(K) &= Q_2{}^{(1,0)}(K + 1) - Q_2{}^{(0,0)}(K + 1) \\ &= P_2{}^{(1,0)}(K + 2) - P_2{}^{(0,0)}(K + 2) \\ &= \Delta G'_{1/2} - (B'_{0,-1/2} - B'_{1,-1/2})(K + \tfrac{1}{2})^2 + \cdots \\ &= \Delta G'_{1/2} - \alpha'(K + \tfrac{1}{2})^2 + \cdots \end{aligned} \tag{5b}$$

in which the higher power terms can be shown to be negligible for all practical purposes. $B_{v,-1/2}$ represents the effective B_v for the component $^2\Pi_{1/2}$ of the upper state. These term-differences, which we shall refer to as ΔT, are fitted by least squares to a parabola having its vertex at $K = -\frac{1}{2}$. The constant term in this solution yields the best value of the vibrational term-difference ΔG, which is required. Fig. 2c shows by diagrams the relation of pairs of lines, connected by arrows, whose wave-number difference gives a single value of ΔT (and of ΔT^i) for the lower state. This will be clear from the term diagram in Fig. 2b.

The first step in the computation is obviously to prove from the experimental data that the vertex of the $\Delta T{:}K$ parabola actually does occur at $K = -\frac{1}{2}$ to within the error of the measurements. Fig. 2d shows the data from the R_2 branches of the 1,0 and 1,1 bands and their least squares solution in the form of Eq. (5a). By carrying through the solution, admitting a linear term in $(K+\frac{1}{2})$, a value of the constant term was obtained which differed from the first value by less than its probable error. This justifies the assumption that the vertex occurs at $K = -\frac{1}{2}$, an assumption made in obtaining all of the results discussed below. To show the extent to which Eq. (5a) is capable of representing the data, we give in Table II the results of the solution for $Q_2{}^{(0,0)}(K) - Q_2{}^{(0,1)}(K)$. This is a typical example from the

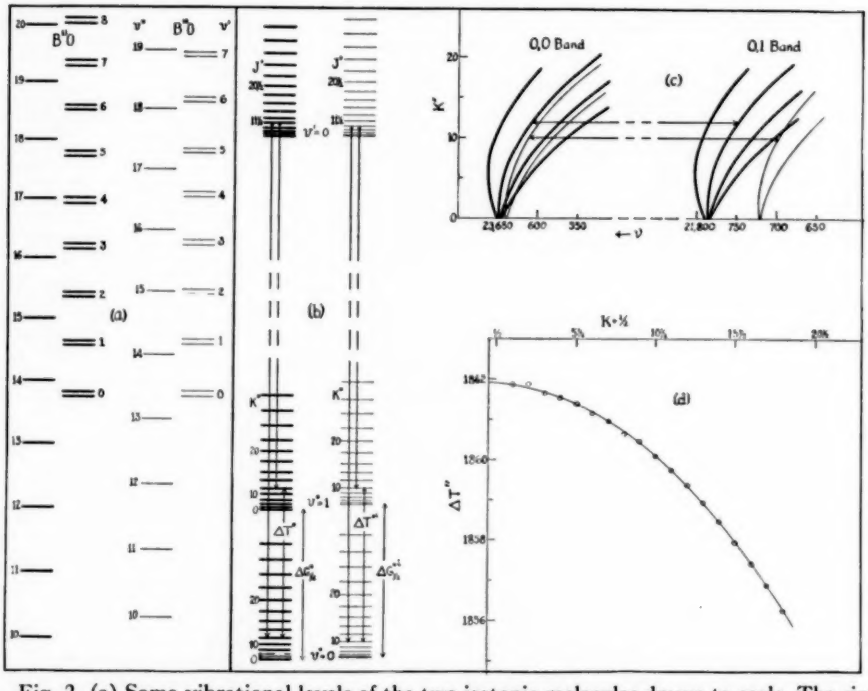

Fig. 2. (a) Some vibrational levels of the two isotopic molecules drawn to scale. The single levels on the left belong to the lower, $^2\Sigma$ state, and the double levels are $^2\Pi$. For $B^{11}O$, the $v''=17$ level of $^2\Sigma$ lies very close to $v'=4$ of $^2\Pi_{1/2}$, the upper component. This explains the observed perturbation in the $v'=4$ rotational levels (cf. Fig. 3 and text, p. 478). (b) Alternate rotational levels associated with $v''=0$ and 1 of $^2\Sigma$ and with $v'=0$ of $^2\Pi_{1/2}$. The difference in frequency of the two lines whose transitions are indicated by the long vertical arrows, $R_2^{(0,0)}$ (12) and $R_2^{(0,1)}$ (12), gives the term-difference $\Delta T''$ (12) in the lower state. As explained in the text, the various values of $\Delta T''$ and $\Delta T''^i$ are extrapolated to $\Delta T''(-\frac{1}{2})$, giving accurate values of the vibrational term-differences $\Delta G''$ and $\Delta G''^i$. (c) Fortrat diagrams of the $^2\Pi_{1/2}$, $^2\Sigma$ components of the 0, 0 and 0, 1 bands. Heavy curves represent branches of the $B^{11}O$ bands, and light curves those measured for $B^{10}O$. The arrows indicate the differences $\Delta T''$ (12) and $\Delta T''^i$ (10). (d) A typical $\Delta T : K+\frac{1}{2}$ parabola, derived from the R_2 branches of the 1, 0 and 1, 1 bands. Circles are observed values, while the curve is the least squares solution, which intersects the axis, $K+\frac{1}{2}=0$, at the value of $\Delta G_{1/2}''$.

TABLE II. $\Delta T''=\Delta G_{1/2}''-(B_0''-B_1'')\,(K+1/2)^2=1861.937-0.01698\,(K+1/2)^2$.

K''	$\Delta T''$ (*Obs.*)	$\Delta T''$ (*Calc.*)	$O-C$
1	1861.92	1861.899	+0.021
2	1861.80	1861.831	−0.031
3	1861.67	1861.729	−0.059
4	1861.60	1861.593	+0.007
5	1861.44	1861.423	+0.017
6	1861.23	1861.220	+0.010
7	1861.01	1860.982	+0.028
8	1860.74	1860.710	+0.030
9	1860.38	1860.404	−0.024
10	1860.08	1860.065	+0.015
11	1859.67	1859.691	−0.021
12	1859.29	1859.284	+0.006
13	1858.87	1858.842	+0.028
14	1858.34	1858.367	−0.027
15	1857.85	1857.857	−0.007

42 least squares solutions carried out in evaluating the various values of $\Delta G_v''$ and $\Delta G_v'$.

TABLE III. *Vibrational constants of the* $^2\Sigma$ *state.*

$B^{11}O$	*Branch*	*Bands*	$\Delta G_v''$	α''	*Wt.*
	R_2	0,0–0,1	1861.86 ±0.01	0.0164	19
	Q_2	0,0–0,1	1861.94 ±0.01	0.0170	15
	P_2	0,0–0,1	1861.92 ±0.04	0.0171	6
		Av.	1861.896 ±0.018		
	R_2	0,1–0,2	1838.37 ±0.01	0.0164	18
	Q_2	0,1–0,2	1838.37 ±0.01	0.0164	14
	P_2	0,1–0,2	1838.38 ±0.03	0.0162	8
		Av.	1838.375 ±0.002	*Av.* 0.01656 ±0.00013	
$B^{10}O$					
	R_2^i	0,0–0,1	1915.28 ±0.02	0.0189	11
	Q_2^i	0,0–0,1	1915.29 ±0.01	0.0173	6
			1915.286 ±0.003		
	R_2^i	0,1–0,2	1890.41 ±0.02	0.0179	11
	Q_2^i	0,1–0,2	1890.10 ±0.02	0.0138	3
			1890.343 ±0.078	0.01774 ±0.00082	
	$\omega_e = 1885.417 \pm 0.037$		$\omega_e^i = 1940.229 \pm 0.078$		$\rho = 1.02907 \pm 0.00004$
	$x_e = 0.006238$		$x_e^i = 0.006428$		$\rho = 1.030$

$B^{11}O$	*Branch*	*Bands*	$\Delta G_v''$	α''	*Wt.*
	R_2	1,0–1,1	1861.90 ±0.01	0.0164	18
	Q_2	1,0–1,1	1861.94 ±0.01	0.0169	14
	P_2	1,0–1,1	1861.86 ±0.02	0.0160	9
			1861.903 ±0.015		
	R_2	1,1–1,2	1838.34 ±0.01	0.0164	19
	Q_2	1,1–1,2	1838.36 ±0.01	0.0164	14
	P_2	1,1–1,2	1838.33 ±0.03	0.0167	10
			1838.348 ±0.005	0.01641 ±0.00007	
$B^{10}O$					
	R_2^i	1,0–1,1	1915.27 ±0.02	0.0177	15
	Q_2^i	1,0–1,1	1915.40 ±0.06	0.0189	9
			1915.318 ±0.044		
	R_2^i	1,1–1,2	1890.36 ±0.03	0.0179	11
	Q_2^i	1,1–1,2	1890.29 ±0.04	0.0154	6
			1890.336 ±0.025	0.01770 ±0.00040	
	$\omega_e = 1885.458 \pm 0.031$		$\omega_e^i = 1940.300 \pm 0.092$		$\rho = 1.02909 \pm 0.00005$
	$x_e = 0.006246 \pm 0.000006$		$x_e^i = 0.006438 \pm 0.000013$		$\rho = 1.031 \pm 0.002$

Lower state

The $^2\Sigma$ state is the easiest and most satisfactory to deal with because it does not involve complicated interactions of electronic and rotational mo-

tions. That the spin doubling is negligible, even for large rotation, is shown by an examination of Scheib's results.[9] Further advantages of the $^2\Sigma$ state over the $^2\Pi$ for the precise determination of ρ lie in the greater magnitude of ω_e, as well as in the fact that this is the normal state, and therefore should be free from perturbations.

Table III contains the results of the various solutions for $\Delta G_v''$, with the probable error of each computed from the residuals by the accepted least squares formulas.[10] It will be noticed that the faint R_{21} branch has not been used at all, nor the P_2 branch in the case of $B^{10}O$. The mean values have been taken separately for the progressions $v'=0$ and $v'=1$, so that two independent evaluations of the vibrational constants are obtained. Computation of the probable errors of the mean $\Delta G_v''$ values based on their internal consistency[10] (on the probable errors of the individual determinations of ΔG_v) showed that these are considerably smaller than the probable errors found from external consistency (determined from the deviation of the individual determinations from their mean). Therefore, following the recommendation of Birge,[10] we have adopted the probable errors from external consistency even though these are based on such a small number of items. The items are then logically weighted according to the number of observations, or values of ΔT, used in the evaluation of each, rather than inversely as the squares of their probable errors. In this way the most consistent set of values of a given vibrational term-difference is obtained, as well as a conservative estimate of the probable error of the mean.

Following each set of results in Table III are given the ω_e and x_e calculated by Eq. (4) The data, involving as they do only $v''=0$, 1, and 2, are not sufficient to determine the term $y_e\omega_e(v+\frac{1}{2})^3$ or higher powers. But these terms are usually negligibly small for the ground states of stable molecules, and in fact Mulliken's data on band heads shows no departure from a linear dependence of ΔG_v on v up to $v''=8$. Hence we obtain the constants on the assumption that these terms are zero. Our best values of ρ, from the ratio $\omega_e{}^i/\omega_e$, are listed in Table III. The values from $x_e{}^i/x_e$ are much less accurate but agree to well within the probable error.

Upper state

In the determination of the vibrational constants for the $^2\Pi$ state, there are several complications not present in the $^2\Sigma$ state. In the first place, since the spin lies coupled to the figure axis by the field of the orbit, the electronic level is two-fold with a separation of about 122 cm^{-1}. Assuming no interaction of the spin with the molecular rotation, we could work exclusively with the one component, $^2\Pi_{1/2}$, $^2\Sigma$, as a separate band system. This procedure is largely justified, as will be shown below in the discussion of the rotational energy function. However, there are unknown additive constants,[11] such as

[9] Cf. R. S. Mulliken and A. Christy, Phys. Rev. **38,** 87 (1931). We have also reexamined the data and find no evidence of an appreciable spin doubling.

[10] R. T. Birge, Phys. Rev. **40,** 207 (1932).

[11] R. S. Mulliken, Rev. Mod. Phys. **2,** 114 (1930).

$\overline{G^2}$ and C_Σ, in the energy function which, though small, cannot be corrected for in obtaining the true ΔG values. Finally, the most serious difficulty is the possibility of perturbations, which may affect the vibrational, as well as the rotational terms. These are known in the analogous band system of CN,[12] and are also found here, though to a lesser degree. Because of these draw-

TABLE IV. *Vibrational constants of the* $^2\Pi$ *state.*

	Branch	*Bands*	$\Delta G_v'$	α'	*Wt.*
$B^{11}O$	R_2	1,0–0,0	1238.58	0.0196	18
	Q_2	1,0–0,0	1238.53	0.0193	14
	P_2	1,0–0,0	1238.49	0.0181	7
			Av. 1238.545 ±0.016		
	R_2	2,0–1,0	1216.65	0.0196	18
	Q_2	2,0–1,0	1216.70	0.0200	15
	P_2	2,0–1,0	1216.67	0.0204	9
			1216.675 ±0.010		
	R_2	3,0–2,0	1195.08	0.0193	18
	Q_2	3,0–2,0	1195.10	0.0196	13
	P_2	3,0–2,0	1195.11	0.0195	8
			1195.095		
	R_2	4,0–3,0	1173.87	0.0194	11
	Q_2	4,0–3,0	1173.92	0.0200	13
			1173.896		
	R_2	5,0–4,0	1152.88	0.0195	10
	Q_2	5,0–4,0	1152.73	0.0193	11
			1152.799	0.01959	
$B^{10}O$	R_2^i	1,0–0,0	1273.93	0.0213	15
	Q_2^i	1,0–0,0	1273.87	0.0214	13
			1273.902 ±0.021		
	R_2^i	2,0–1,0	1250.66	0.0209	18
	Q_2^i	2,0–1,0	1250.69	0.0211	14
			1250.674 ±0.008		
	R_2^i	3,0–2,0	1227.83	0.0210	17
	Q_2^i	3,0–2,0	1227.81	0.0206	14
			1227.823		
	R_2^i	4,0–3,0	1205.426	0.0214	14
	Q_2^i	4,0–3,0	1205.329	0.0210	11
			1205.383	0.02111	

With only $\Delta G'_{1/2}$ *and* $\Delta G'_{1\,1/2}$:		
$\omega_e = 1260.415 \pm 0.033$	$\omega_e^i = 1297.130 \pm 0.048$	$\rho = 1.02913 \pm 0.00004$
$x_e = 0.008676$	$x_e^i = 0.008954$	$\rho = 1.032$

[12] F. A. Jenkins, Y. K. Roots and R. S. Mulliken, Phys. Rev. **39**, 16 (1932).

backs the resulting values of ρ are of little importance in bettering those already obtained. However, the analysis has been done since it gives fairly reliable values of the vibrational constants, and affords a check on the ρ already found from the lower state.

Our measurements include bands of the $v''=0$ progression up to $v'=5$ for $B^{11}O$, and $v'=4$ for $B^{10}O$. All of the values were computed from the ΔT parabolas of the type of Eq. (5b), using least squares in exactly the same way as for the lower state. The results are shown in Table IV. The probable errors of the individual ΔG_v's have not been calculated because internal consistency is of little value in getting the probable error of the mean, as explained above. But the residuals were always examined, and where a trend was noted, the worst value or values were discarded, and a new solution made. In the solutions for $\Delta G'_{3\,1/2}$ and $\Delta G'_{4\,1/2}$ from the R_2 branch, the residuals

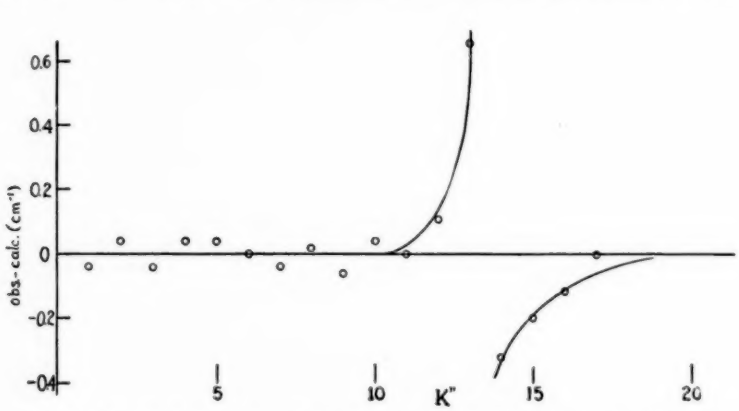

Fig. 3. Residuals of the ΔT parabola $R_2^{(4,0)}-R_2^{(3,0)}$ from the solution adopted. The large discontinuity in the curve at $K=13$ represents a perturbation in the rotational terms of the upper state.

grew suddenly large above $K=11$, showing the presence of a large perturbation in the R_2 branch of the 4,0 band. The Q_2 branch is perfectly regular. The perturbation reaches its maximum (0.66 cm^{-1}) at $J'=13\frac{1}{2}$ of the $^2\Pi_{1/2}$ state. Fig. 3 is a plot of the residuals from the final, adopted solution for $\Delta G'_{3\,1/2}$ (R_2 branch), and shows the usual form characteristic of a large perturbation.

This perturbation is obviously analogous to one of those occurring in the $v'=6$ levels of the $^2\Pi$ state in CN.[12] It results from the near equality of energy levels with the same J in the $^2\Pi$ and the lower $^2\Sigma$ states. When we computed the terms in these two states from the data already established, it was found that by far the closest approach of any two terms is $^2\Sigma^{(17)}$ to $^2\Pi_{1/2}{}^{(4)}$. The levels are drawn to scale in Fig. 2a, and one sees that the lowest $^2\Pi_{1/2}$ terms are far removed from the $^2\Sigma$ terms, and hence not likely to be seriously perturbed. But for the vibrational states near $v'=4$, we expect irregularities in the ΔG values, such as were found in CN. Actually, anomalies are present, the ΔG curve departing greatly from a straight line, and showing a large

"positive" curvature (positive y_e).[13] It does not seem of value to attempt an analytical representation of all the observed vibrational terms of the upper state.

For the determination of ρ, the states $v'=0$, 1, and 2 only have been used, to avoid as far as possible the effect of the perturbations. The resulting values, shown in Table IV, agree surprisingly well with those from the normal state, considering the difficulties and approximations in their evaluation.

Rotational Isotope Effect

Although the rotational effect is capable of yielding values of ρ which are only about one-tenth as accurate as those from the vibrational effect, we have studied it to obtain the best possible values of the rotational constants for both "main" ($B^{11}O$) and "isotopic" ($B^{10}O$) systems. This is essential if conclusions are to be drawn about the electronic effect, as will be done below. The principal constant, B_v, which occurs in the expressions for the rotational energy, differs for the two isotopic molecules according to the following equations.[8]

$$\mathbf{B^{11}O}: B_v = B_e - \alpha_e(v+\tfrac{1}{2}) + \gamma_e(v+\tfrac{1}{2})^2 + \cdots \tag{6a}$$

$$\begin{aligned}\mathbf{B^{10}O}: B_v{}^i &= B_e{}^i - \alpha_e{}^i(v+\tfrac{1}{2}) + \gamma_e{}^i(v+\tfrac{1}{2})^2 + \cdots \\ &= \rho^2 B_e - \rho^3\alpha_e(v+\tfrac{1}{2}) + \rho^4\gamma_e(v+\tfrac{1}{2})^2 + \cdots .\end{aligned} \tag{6b}$$

Here the only value of ρ which is at all accurate is found from

$$B_e{}^i/B_e = \rho^2,$$

the constants α_e and γ_e being too small to permit much precision.

Lower state

For the main system, values of B_v'' could be calculated directly by least squares from the combination differences

$$\Delta_2F_2''(K) = R_2(K-1) - P_2(K+1) = 4B_v''(K+\tfrac{1}{2}) + 8D_v''(K+\tfrac{1}{2})^3 + \cdots \tag{7}$$

after eliminating the cubic term as usual[14] by preliminary calculation of D_v from the theoretical relation with B_e and ω_e. We have used $D_e''=-6.29\times10^{-6}$ $\beta''=0$ $D_e''{}^i=\rho^4D_e''=7.05\times10^{-6}$. For the isotopic system, however, where the P_2 branch was not available, we must use the quantities

$$\begin{aligned}\Delta_1F''(K) &= R_2(K-\tfrac{1}{2}) - Q_2(K+\tfrac{1}{2}) - \Delta\nu_{dc}\cdots \\ &= 2B_v''(K+\tfrac{1}{2}) + 4D_v''(K+\tfrac{1}{2})^3 - \Delta\nu_{dc}\cdots\end{aligned} \tag{8}$$

The term $\Delta\nu_{dc}$ represents the Λ-doubling in the upper state from which the two lines come. It can easily be corrected for, as we shall show later, and we have proved by tests on the main system that the resulting B_v's agree exactly

[13] Although it is commonly said that a negative curvature is the normal one (Birge and Sponer), it appears that in the few cases where extensive and accurate measures of band origins are available (NOβ, SiN) a positive curvature for the upper state is most common. However, perhaps perturbing effects are also at work in these cases.

[14] Reference 1, p. 174.

with those from Eq. (7). The chief results of these calculations are collected in Table V. No values are quoted for $v''=2$, since the data from the isotopic system for this state are too fragmentary to be of value here.

The data of Table V were derived from the analysis of the rotational term-differences alone, and thus furnish a valuable independent check on the results from the vibrational analyses contained in Tables III and IV. It is

TABLE V. *Rotational constants of the* $^2\Sigma$ *state.*

$B^{11}O$ Bands	B_v''		B_v''	$B^{10}O$ Bands	$B_v''^i$		$B_v''^i$
0,0	1.7715	0,1	1.7569	0,0	1.8738	0,1	1.8600
1,0	1.7720	1,1	1.7545	1,0	1.8763	1,1	1.8581
2,0	1.7725		1.7557 ± 0.0008	2,0	1.8768		1.8587 ± 0.0009
3,0	1.7719			3,0	1.8753		
Av.	1.7720 ± 0.0001				1.8758 ± 0.0006		
$B_e''=1.78015\pm0.0004$				$B_e''^i=1.88465\pm0.0008$			
$\alpha_e''=0.0163\pm0.0008$				$\alpha_e''^i=0.0171\pm0.0011$			
$\rho^2=B_e''^i/B_e''=1.0587\pm0.0005$				$\rho=1.0289\pm0.00025$			
$\rho^3=\alpha_e''^i/\alpha_e''=1.05$				$\rho=1.02$			

possible to improve somewhat the accuracy of the value of ρ from rotational constants, by assuming the more accurate values of α_e obtained in connection with the vibrational analysis. Thus, if we fix $\alpha_e''=0.01648\pm0.00008$, $\alpha_e''=0.01772\pm0.00042$ and us the B_v'' values of Table V, we find:

$$B_e = 1.7803 \pm 0.0004$$

$$B_e^i = 1.8850 \pm 0.0005$$

$$\rho^2 = 1.0588 \pm 0.0004 \qquad \rho = 1.0290 \pm 0.0002$$

$$\rho^3 = \alpha_e''^i/\alpha_e'' = 1.075 \pm 0.024 \qquad \rho = 1.024 \pm 0.008$$

Upper state

As stated above, the initial state of these bands is an inverted $^2\Pi$. Because of the large multiplet separation, it is obviously very near to case *a* type of spin coupling, at least for small rotation. The form of the rotational energy function is in general complicated in such a state, because of the spin uncoupling which occurs as the rotation increases. In the present instance, however, the departure toward case *b* should be inappreciable at small rotational quantum numbers. This was found to be true, by investigating graphically the combination differences

$$\begin{aligned}\Delta_2F_2'(K) &= R_2(K) - P_2(K) = 4B'_{v,-1/2}(K+\tfrac{1}{2}) + 8D'_{v,-1/2}(K+\tfrac{1}{2})^3 + \cdots \\ \Delta_2F_1'(K) &= R_1(K) - P_1(K) = 4B'_{v,+1/2}(K+\tfrac{1}{2}) + 8D'_{v,+1/2}(K+\tfrac{1}{2})^3 + \cdots\end{aligned} \tag{7}$$

using the very complete data for the 1,0 band. The quantities $B_v'_{,-1/2}$ and $B_v'_{,+1/2}$, although not equal, were found to be practically constant below $J\sim30$. Hence, if lines of low J are used, the spin uncoupling need not be considered. Probably this $^2\Pi$ state departs more toward case *c*, where the two

components can be considered as separate electronic levels (each with its own constants) than toward case *b*. Fortunately, this makes it possible to apply the usual least squares methods for the evaluation of B_v, and in doing so we have confined ourselves to lines having rotational quantum numbers below 15.

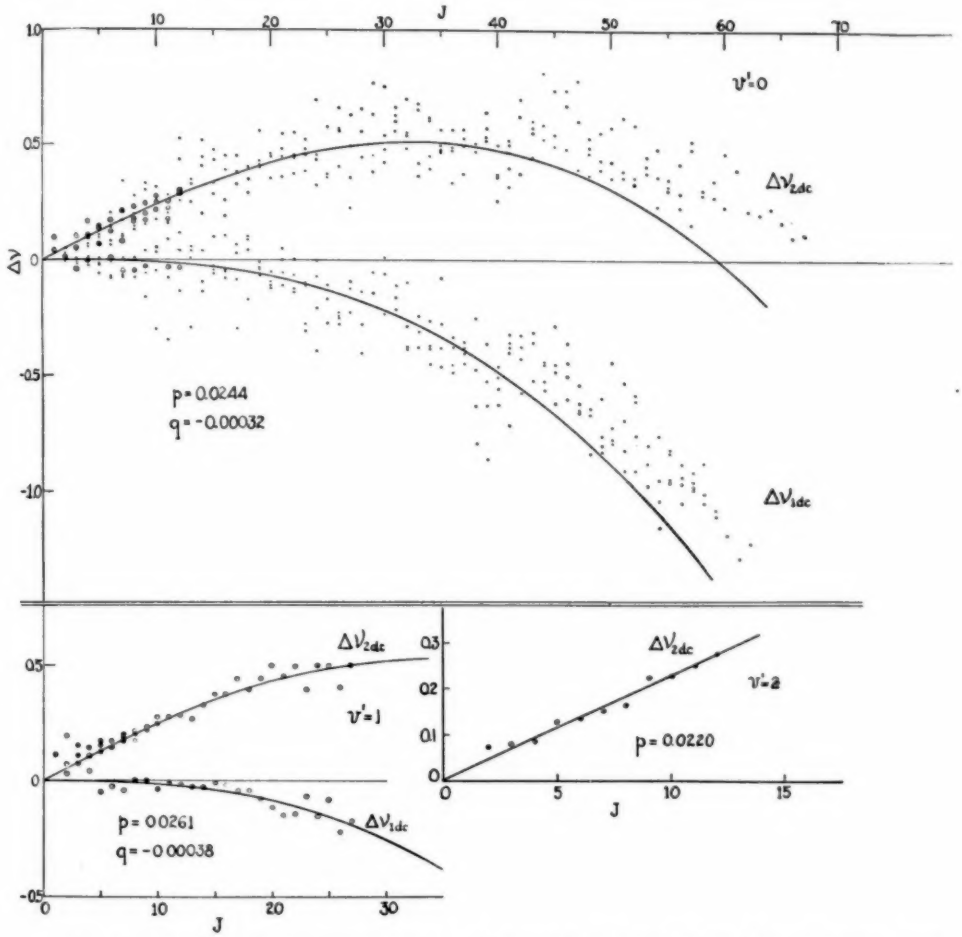

Fig. 4. Λ-doubling in the upper states $v'=0$, 1 and 2. Values indicated by circles are from our data, and the small dots are from the measurements of Scheib.[7] The curves are the theoretical ones, drawn according to the constants indicated.

Another factor which must be considered is the Λ-doubling, which splits all the $^2\Pi$ rotational states into two. Particularly, this must be corrected for in the $B^{10}O$ combination differences, where only R_2 and Q_2 branches are available. For the main system, the Λ-doubling could be evaluated directly as the combination defect:

$$2\Delta\nu_{dc}(J+\tfrac{1}{2}) = [R(J) - Q(J)] - [Q(J+1) - P(J+1)]. \qquad (8)$$

Fig. 4 shows graphically the course of $\Delta\nu_{2dc}$ (in $^2\Pi_{1/2}$) and $\Delta\nu_{1dc}$ (in $^2\Pi_{1\ 1/2}$)

for the lowest three vibrational levels. Below about $J=15$, they may be well represented by the equation[15] of Van Vleck for inverted case a states:

$$\begin{aligned}\Delta\nu_{2dc} &= p(J+\tfrac{1}{2})\\ \Delta\nu_{1dc} &= -(p/Y^2+2q/Y)(J-\tfrac{1}{2})(J+\tfrac{1}{2})(J+1\tfrac{1}{2}).\end{aligned} \tag{9}$$

Y stands for A/B_v, A being the spin coupling constant, while p and q are small constants. Their values, as found graphically, are given in Table VI.

TABLE VI. *Constants of the Λ-doubling.*

$B^{11}O$	v'	p	q	$B^{10}O$	p (calc.)
	0	0.0244	−0.00032		0.0257
	1	0.0261	−0.00038		0.0277
	2	0.0220			0.0233
	3	0.0244			0.0258
	4	0.0188			0.0199

For $v'=0$ and 1, we have used the more general expression given by Mulliken and Christy,[9] for states intermediate between cases a and b. The curves in Fig. 4 for these states are the theoretical ones, based on these equations. For $B^{10}O$, not enough branches are observed to permit the direct determination of $\Delta\nu_{dc}$. However, an examination of the theoretical expression,[9] for these constants shows that the magnitude of p depends on B_v and of q on B_v^2. In connection with Eqs. (9), this requires that $\Delta\nu_{2dc}$ be greater for $B^{10}O$ than for $B^{11}O$ by the factor ρ^2, and $\Delta\nu_{1dc}$ greater by ρ^6. Thus we obtain the values in the last column of Table VI. The determination of $B_{v,\Sigma}$ was then made by correcting the combination difference, so that

$$\begin{aligned}R_2(K)\underset{\bullet}{-}Q_2(K)-\Delta\nu_{2dc}(K+\tfrac{1}{2}) &= \Delta_1F_2'(K+\tfrac{1}{2})\\ &= 2B_{v,-1/2}(J+\tfrac{1}{2})+4D_v(J+\tfrac{1}{2})^3\\ R_1(K)-Q_1(K)-\Delta\nu_{1dc}(K+\tfrac{1}{2}) &= \Delta_1F_1'(K+\tfrac{1}{2})\\ &= 2B_{v,+1/2}(J+\tfrac{1}{2})+4D_v(J+\tfrac{1}{2})^3.\end{aligned}$$

The cubic term was first eliminated, with

$$\begin{aligned}D_v &= -7.09\times10^{-6}+5.08\times10^{-8}(v'+\tfrac{1}{2})\\ D_v{}^i &= -7.92\times10^{-6}+5.86\times10^{-8}(v'+\tfrac{1}{2}).\end{aligned}$$

The resulting values of $B_{v,\Sigma}$ are collected in Table VII. As before, a considerably better ρ is obtained if we use the more accurate α_e's from the ΔT parabolas. Adopting these, and solving by least squares the values of $B_{v,-1/2}$ from $v'=0$ to 3, we find

$$\begin{aligned}B_{e,-1/2} &= 1.4277\pm0.0005 & B^i{}_{e,-1/2} &= 1.5115\pm0.0006\\ \rho^2 &= 1.0587\pm0.0006 & \rho &= 1.0289\pm0.0003\\ \alpha_e &= 0.0196 & \alpha_e{}^i &= 0.0211\\ \rho^3 &= 1.078\pm0.008 & \rho &= 1.025\pm0.003.\end{aligned}$$

[15] R. S. Mulliken, Rev. Mod. Phys. **2**, 109 (1930).

TABLE VII. *Rotational constants of the* $^2\Pi$ *state.*

$B^{11}O$	B_v	*From bands*			$B^{10}O$	B_v^i
$B_{0,-1/2}$	1.4172	0,0	0,1	0,2	$B^i_{0,-1/2}$	1.4991
$B_{1,-1/2}$	1.3969	1,0	1,1	1,2	$B^i_{1,-1/2}$	1.4793
$B_{1,+1/2}$	1.3679		1,0		$B^i_{1,+1/2}$	1.4488
$B_{2,-1/2}$	1.3789		2,0		$B^i_{2,-1/2}$	1.4605
$B_{3,-1/2}$	1.3609		3,0		$B^i_{3,-1/2}$	1.4382
$B_{4,-1/2}$	1.3450		4,0		$B^i_{4,-1/2}$	1.4243
$B_{5,-1/2}$	1.3346		5,0			

With only data for $v'=0, 1, 2,$ *and* 3

$B_{e,-1/2}=1.4266$ $\qquad$ $B^i_{e,-1/2}=1.5092$

$\rho=1.0286$

$\alpha_e=0.0188$ $\qquad$ $\alpha_e^i=0.0203$

$\rho=1.03$

In computing ρ, the values of $B_{e,-1/2}$ have been used rather than the "true" B_e, which the theory of case a states shows to be the mean of $B_{v,-1/2}$ and $B_{v,+1/2}$. This was done because it appeared that the difference between $B_{1,-1/2}$ and $B_{1,+1/2}$ was less than the theoretical value, $2B_1^2/A$ by from 5 to 10 percent and it was therefore uncertain how well the state approximates the theoretical case a.

ELECTRONIC ISOTOPE EFFECT

It is important to note that the above results, because they are derived from analyses of the vibrational and rotational term-*differences*, involve no assumption as to the presence or absence of differences in the electronic terms of the two molecules. It is only when one is concerned with the frequency differences between corresponding bands of the two molecules, the "isotope shift," that the electronic effect enters. Since we have now fixed the relative position of all the terms of each type of molecule, within a given electronic state, it remains to find the separations of the terms of the $^2\Pi$ state from those of $^2\Sigma$. This requires the determination of the origin of one band, and we have chosen to do it for 1,0. The lines of the R_2 and Q_2 branches are given by the differences:

$$\begin{aligned} R_2(J) &= [T_{2e}' + G_1' + F_2'(J+1)] - [T_e'' + G_0'' + F''(J)] \\ Q_2(J) &= [T_{2e}' + G_1' + F_2'(J)] - [T_e'' + G_0'' + F''(J)]. \end{aligned} \tag{11}$$

Hence, the band origin may be expressed:

$$\begin{aligned} \nu_2^{(1,0)} = (T_{2e}' - T_e'' + G_1' - G_0'') &= R_2(J) - F_2'(J+1) + F''(J) \\ &= Q_2(J) - F_2'(J) + F''(J). \end{aligned} \tag{12}$$

In the lower state, we have

$$F''(J) = B_0''(K+\tfrac{1}{2})^2 = B_0''(J+1)^2. \tag{13}$$

In the upper state, we can use the expansion of the Hill and Van Vleck equation for large negative values of $Y=A/B_v$. Neglecting the small, unknown constants, this reduces to

$$F'(J) = B_{v,-1/2}(J + \tfrac{1}{2})^2 + B_v/Y \pm \tfrac{1}{2}p(J + \tfrac{1}{2}) + \cdots. \quad (14)$$

The positive sign applies to R_2, and the negative to Q_2. Y has the value -88.51, as shown ahead. From the first eight lines of these two branches, sixteen values of the origins were computed for both main and isotope bands. The results are

$$\nu_2^{(1,0)} = 24{,}885.09 \pm 0.01 \text{ cm}^{-1} \quad \nu_2^{(1,0)i} = 24{,}911.73 \pm 0.01 \text{ cm}^{-1}.$$

The two system-origins are then readily obtained from the relation

$$\nu_{2e} = \nu_2^{(1,0)} - [\omega_e'(1\tfrac{1}{2}) - 2x_e'\omega_e'(1\tfrac{1}{2})^2] + [\omega_e''(\tfrac{1}{2}) - 2x_e''\omega_e''(\tfrac{1}{2})^2]. \quad (15)$$

We find

$$\mathbf{B^{11}O}: \nu_{2e} = 23{,}958.85 \pm 0.05 \quad \mathbf{B^{10}O}: \nu_{2e}^i = 23{,}959.18 \pm 0.06.$$

Thus there remains a discrepancy of 0.33 ± 0.08 cm^{-1} which in all probability represents an electronic isotope effect. It agrees in sign and order of magnitude with the value 0.47 cm^{-1} obtained by one of us[6] in 1927 from measurements on the main and isotope Q_2 head of the 0,0 bands, a less accurate method. Although it is commonly supposed that electronic isotope effects are smaller than the above, recent work both experimental and theoretical on the atomic spectrum of lithium[16] have yielded shifts even greater than this. Our result appears to be the first evidence of any sort of an electronic isotope effect in molecular spectra.

In the above, we have treated the $^2\Pi_{1/2}$ component as a separate band system. This is justified if the value of the coupling coefficient, A, is the same for $B^{11}O$ and $B^{10}O$ in different vibrational levels of the $^2\Pi$ state. The data are insufficient for testing this point except in the case of the 1,0 band. Here the values of A have been calculated separately for main and isotope systems. The term-formula for $^2\Pi_{1\ 1/2}$, corresponding to Eq. (14) is

$$F_1'(J) = B_{v,+1/2}(J + \tfrac{1}{2})^2 - B(2 - 1/Y), \quad (16)$$

omitting the Λ-doubling, which is negligible for small J. The separation of pairs of terms of the same J in the two components may thus be expressed as follows:

$$\begin{aligned} T_2(J) - T_1(J) &= (T_{2e} - T_{1e}) + (B_{1,-1/2} - B_{1,+1/2})(J + \tfrac{1}{2})^2 \\ &\quad + 2B_1(1 + 1/Y) \pm \tfrac{1}{2}p(J + \tfrac{1}{2})^2 \quad (17) \\ &= -A - [2B_1/\alpha](J + \tfrac{1}{2})^2 + 2B_1(1 + 1/Y) \pm \tfrac{1}{2}p(J + \tfrac{1}{2})^2. \end{aligned}$$

This separation was evaluated from the combination differences

$$R_2(J - 1) - Q_1(J) \text{ and } Q_2(J) - P_1(J + 1),$$

the positive sign in the final term of Eq. (17) being applicable in the former, and the negative in the latter case. The A computed in this way was constant below about $J = 10$, and the mean values adopted are

[16] D. S. Hughes and C. Eckart, Phys. Rev. **36**, 694 (1930); D. S. Hughes, Phys. Rev. **38**, 857 (1931).

$$A = -122.36 \pm 0.03\ \text{cm}^{-1} \qquad A^i = -122.36 \pm 0.05\ \text{cm}^{-1}.$$

Hence $Y = A/B_v = -88.51$, from the mean value of B_1. It is not surprising to find the spin coupling coefficients equal for the two isotopic molecules, since they should be practically uninfluenced by the nuclear masses.

Discussion of Results

The different determinations of the coefficient ρ are summarized in Table VIII. It will be seen that the accuracy in this quantity obtainable from the four important constants decreases in the order of their size; thus in the order ω_e, B_e, x_e and α_e. For these the probable error is roughly one part in 20,000, 4000, 500 and 100, respectively. The agreement between the several values is always of the order of magnitude of their probable errors, and more often closer than the computed errors would indicate. This shows that the latter represent conservative estimates. We note a slight tendency of the x_e to give too high a value of ρ, while α_e gives values too low. Considering the probable errors, however, it seems that little significance can be attached to these trends.

Table VIII. *Results from analysis of vibrational structure.*

Constants used	*Bands used*			ρ	*Probable error*
ω_e''	0,0	0,1	0,2	1.02907	±0.00004
ω_e''	1,0	1,1	1,2	1.02909	±0.00005
x_e''	0,0	0,1	0,2	1.030	—
x_e''	1,0	1,1	1,2	1.031	±0.002
α_e''	0,0	0,1	0,2	1.023	±0.018
α_e''	1,0	1,1	1,2	1.026	±0.009
ω_e'	0,0	1,0	2,0	1.02913	±0.00004
x_e'	0,0	1,0	2,0	1.032	—
α_e'	0,0	1,0	2,0		
	3,0	4,0		1.025	±0.003
Results from analysis of rotational structure.					
B_e''	0,0	1,0	2,0	1.0289	±0.00025
	3,0	1,1	0,1	1.0290*	±0.0002
α_e''	0,0	1,0	2,0	1.02	—
	3,0	1,1	0,1		
B_e'	0,0	1,0	2,0	1.0286	—
	3,0	1,1	0,1	1.0289*	±0.0003
α_e'	0,0	to	5,0	1.03	—
	0,1	1,1			

* These values obtained if the more accurate α_e from the vibrational analysis is used.

Aston[17] has measured the masses of the boron isotopes with the precision mass-spectrograph, and found the following results:

B^{10}: 10.0135 Limit of error 0.0015

B^{11}: 11,0110 " " " 0.0016.

[17] F. W. Aston, Proc. Roy. Soc. **115A**, 509 (1927).

The masses are based on $O^{16} = 16$. From these we find

$$(\mu/\mu^i)^{1/2} = \rho = 1.02908. \quad \textit{Limit of error } 0.00009$$
$$= 1.02908 \pm 0.00003$$

assuming the probable error to be one-third of the assigned limit of error. This agrees strikingly well with the best results in Table VIII. Thus the mean of the two determinations from ω_e'' is exactly the above value, with the same probable error. The value from ω_e' is untrustworthy for reasons given above, while those from the B_e's should be given negligible weight, because of the magnitude of their probable errors. Hence the agreement with Aston's result is complete, and constitutes the first independent check on the accuracy of his relative masses.

Since it is ρ, the square root of the ratio of the reduced masses, which is obtained from the band spectrum, one must assume one of the absolute masses to evaluate their ratio. This is because the ratio of the vibration frequencies is dependent not only on the ratio of the masses of the molecules, but also on their absolute values. If we let m_{11} and m_{10} be the respective atomic weights, we have

$$m_{11}/m_{10} = 16\rho^2/[m_{10}(1 - \rho^2) + 16] = [m_{11}(\rho^2 - 1) + 16\rho^2]/16$$

Assuming Aston's value, $m_{10} = 10.0135$, our mean value of ρ gives for the mass ratio

$$m_{11}/m_{10} = 1.09961 \pm 0.00006$$

and from Aston's two masses, directly

$$m_{11}/m_{10} = 1.09962. \quad \text{Limit of error } 0.00032$$
$$= 1.09962 \pm 0.00011.$$

We have therefore verified the value of the slope of the packing fraction curve of Aston, assuming the absolute value of the packing fraction, at atomic weight 10.

In closing, we wish to acknowledge the kind assistance of Professor R. T. Birge on the methods of treating the data. Most of the above methods have already been applied by him in his very accurate computation of the masses of the oxygen isotopes.

The Emission of Positive Ions from Heated Metals

By LEROY L. BARNES
Department of Physics, Cornell University

(Received September 27, 1932)

The positive ion emission from iron, nickel, copper, rhodium, columbium, platinum, uranium and thorium has been studied. In addition to the emission of singly charged atoms of the alkalies, reported by others, it is found that iron, nickel, copper, rhodium and columbium emit singly charged atoms of their own metals. The results from rhodium and columbium are in agreement with those already reported by H. B.Wahlin.

INTRODUCTION

FOR many years it has been known that positive electricity will leak away from a metal when the metal is heated to a visible red. This leakage has been found, in some cases at least, to be due to two types of ion emission (1) to positive ions of impurities[1,2,3] in the metal (2) to positive ions of the metal[4,5] itself. Mass-spectrographic studies indicate that the first type of emission, from a given sample of metal, can be reduced to zero by sufficient heating and aging of the sample. In this paper we shall be primarily interested in the second type of positive ion emission.

That a well-aged tungsten filament emitted positive ions when heated to a high temperature, was first discovered by Jenkins[6] and independently by L. P. Smith.[7]

By means of a Dempster type mass-spectrograph, Smith[4] made an analysis of the positive ion emission from both tungsten and molybdenum. In addition to the ions of the alkalies, which were emitted at relatively low temperatures, he found that, when the temperatures of the respective metals were sufficiently high to produce fairly rapid vaporization, ions corresponding to singly charged atoms of the metals were emitted.

While Smith's work was in progress, H. B. Wahlin[8] was making similar investigations and reported that tungsten, molybdenum, tantalum and rhodium each emitted singly charged atoms of its own metal. Later Wahlin[5] reported similar results for chromium, columbium and ruthenium.

The author has made a mass-spectrographic examination of the positive ion emission from iron, nickel, copper, rhodium, columbium, platinum,

[1] O. W. Richardson, *Emission of Electricity from Hot Bodies.*
[2] J. J. Thomson, *Conduction of Electricity through Gases.*
[3] Barton, Harnwell and Kunsman, Phys. Rev. **27,** 739 (1926).
[4] L. P. Smith, Phys. Rev. **35,** 381 (1930).
[5] H. B. Wahlin, Phys. Rev. **37,** 467 (1931).
[6] Jenkins, Phil. Mag. **47,** 1025 (1924).
[7] Smith, Phys. Rev. **33,** 279 (1929).
[8] Wahlin, Phys. Rev. **34,** 164 (1929).

uranium and thorium. The mass-spectrograph used was essentially the same as that used by Smith.[4] The positive ion currents from the mass-spectrograph were measured by means of an FP-54 Pliotron and a high sensitivity galvanometer, the maximum current sensitivity being of the order of 10^{-16} amperes.

Experimental Work and Results

In addition to the sodium and potassium emission observed by others,[1,2,3,4,5] the author has found that when platinum is first heated to a dull red, a relatively weak emission of rubidium and caesium ions is obtained. The purpose of the investigation, however, was to find out, in the case of each metal tried, whether or not positively charged atoms of the metal itself would be emitted when the metal was heated.

Iron and Nickel

Filaments of iron and nickel, when heated to temperatures just below their respective melting points, were found to emit singly charged atoms of these metals, but the filaments lasted only a few seconds because of the high temperature required to get the emission. This made it impossible to obtain data on the positive ion currents. In order to obtain an emission which would last long enough to make possible a more accurate recording of the location of the ions on the mass scale, a source of the following type was tried.

A wire of the metal to be investigated, was rolled out into a uniform strip from two to three thousandths of an inch thick. One end of the strip was then made pointed so that it could enter a small wire die. A piece of nickel wire about 0.02 inch in diameter was placed in contact with the strip and the two were drawn through the die. This left the strip in the shape of a trough and

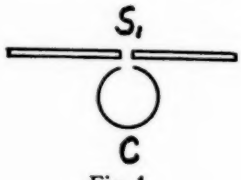

Fig. 1.

with continued drawing of the trough alone, through successively smaller dies, it took on the shape of a cylindrical shell with a slit down the side. The ends of this cylindrical shell were then spot welded to the filament leads of the mass-spectrograph and it was placed in front of the slit S_1 as shown in Fig. 1. Fig. 1 is an end view of the slit S_1 (the first slit of the mass-spectrograph) and the cylindrical shell C. The shell was heated by means of an electric current.

Because of radiation the outside of such a source is cooler than the inside. Thus the shell may be cool enough on the outside to support its own weight, while on the inside it is hot enough to vaporize quite rapidly and give a measurable emission of positive ions.

From one nickel source of this type an emission of positive ions of nickel was maintained for more than an hour before the cylinder melted. Data taken

with this source are shown by the first curve in Fig. 2. The currents were very small, of the order of 10^{-16} to 10^{-15} amperes, and in this case not very steady, as is shown by the roughness of the curve. The mass scale was checked by the potassium peak from the same source, and as is shown the two peaks fall quite close to atomic weights 58 and 60, the mass numbers of the two isotopes of nickel.

A large number of iron sources, of the type described above, were tried but the emission of positive ions of iron was never maintained for more than three or four minutes before the cylinder melted. This did not allow sufficient

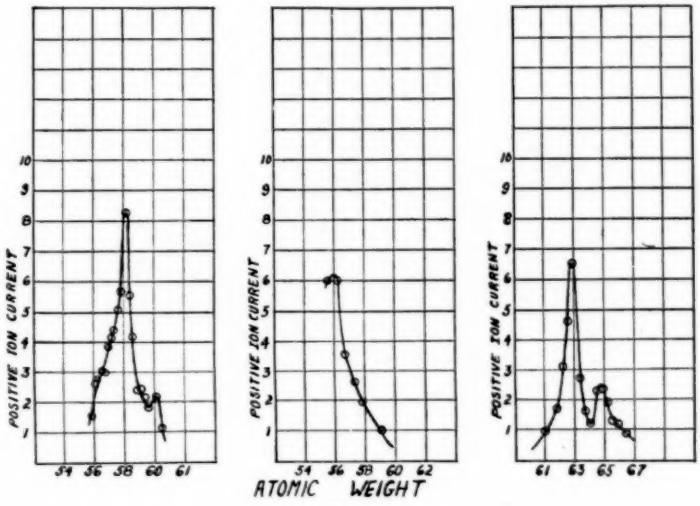

Fig. 2.

time for data to be taken on a complete peak. The second curve of Fig. 2 shows that part of the curve due to iron ions which it was possible to obtain before the cylinder melted.

It may be of interest to note that the melting point of iron is nearly 100° higher than that of nickel and that the rate of vaporization[9] of iron, just below its melting point, is a little higher than for nickel just below its melting point. The above results show, however, that nickel gives the stronger ion emission. The ionization potentials for iron and nickel[10] are 7.83 volts and 7.63 volts respectively. One might raise the question whether or not the difference in the emission in the two cases could be due to this small difference in ionization potentials.

Copper

The author has previously reported[11] that positive ions of copper were obtained when the copper was supported and heated by a tungsten filament. In that case, due precaution was not taken to avoid the possibility of obtain-

[9] Jones, Langmuir and MacKay, Phys. Rev. **30,** 201 (1927).
[10] Ruark and Urey, *Atoms, Molecules and Quanta.*
[11] L. L. Barnes, Phys. Rev. **37,** 218 (1931).

ing copper ions produced by thermal ionization of the copper vapor striking the hot tungsten filament. The production of copper ions by this method has been described by Kingdon.[12]

To make certain that no mistake had been made in saying that the copper ions were emitted by the copper itself, a thin strip of copper was bent into the shape of a trough and placed over the straight tungsten filament and then closed on the under side of the filament. This source was placed at right angles to the slit of the mass-spectrograph so that no part of the tungsten was exposed to the slit. With such an arrangement all ions entering the slit must come from the copper surface. With this source the third curve in Fig. 2 was obtained, showing the two isotopes of copper at atomic weights 63 and 65.

Wahlin[13] has recently reported that he has obtained positive ions of copper at a temperature just below and at the melting point of the metal.

Rhodium

The two peaks shown in Fig. 3 were obtained from a rhodium filament at a temperature of about 1800°C. The smaller peak falling at atomic weight 103 corresponds to singly charged atoms of rhodium and the larger peak at 137 to singly charged atoms of barium. A recent communication from the company from which the rhodium was purchased, states that they have detected,

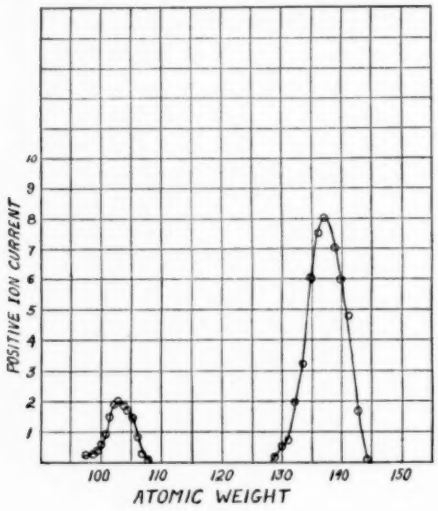

Fig. 3.

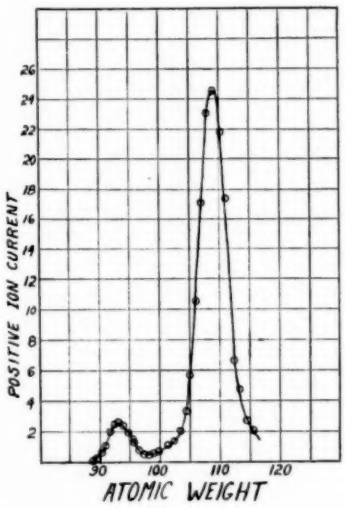

Fig. 4.

by spectroscopic analysis, a trace of barium in all of the samples of rhodium which they have tested. The fact that the barium ion current is larger than the rhodium ion current may be explained by the fact that the ionization potential for barium is so much lower than that for rhodium. One would expect that with both metals at the same temperature, a much greater percentage of the vaporized barium would be ionized than of the vaporized rhodium.

[12] Kingdon, Phys. Rev. **23**, 778 (1924).
[13] Wahlin, Phys. Rev. **38**, 1074 (1931).

The peak due to rhodium ions is a confirmation of results already reported by Wahlin.[5]

Columbium or Niobium

Fig. 4 shows two peaks due to positive ions from a columbium filament at a temperature of about 1800°C. The smaller peak at atomic weight 93 corresponds to singly charged atoms of columbium (also reported by Wahlin).[5] The larger peak at 109 is just 16 mass units greater than that due to columbium ions. It has been demonstrated by Wahlin[14] that uranium oxide ions and thorium oxide ions may be obtained from heated tungsten filaments containing these oxides. It would not be surprising if the columbium used here contained some of its own oxide, near the surface at least, and, in view of Wahlin's results, that some of the evaporating oxide comes off as CbO^+ (mass 109).

Platinum

Several attempts to obtain positive ions of platinum have resulted in nothing more than a rush of current at the time that the filament burned out. This rush of current accompanying the burning out of the filament came only if the accelerating potential, for the ions in the mass-spectrograph, happened to be set at approximately the correct value for platinum ions to be recorded. To be sure that it was not due to an electrical disturbance accompanying the burning out of the filament, a platinum filament was burned out with the accelerating potential set well off the value for platinum ions and no rush of ion current was observed. Both filaments and cylindrical shells, of the type used in the case of iron and nickel, were tried in an attempt to get an emission of platinum ions which could be recorded, but none was obtained.

Both Smith and Wahlin were unsuccessful in obtaining platinum ions by this method. Murawkin[15] reports that from a heated platinum foil alone he obtained no platinum ions but with an electrolytic layer of copper on a platinum foil he obtained a surprisingly large emission of platinum ions. The positive ion currents which he has recorded for platinum ions are some 10,000 times larger than the smallest current detectable in the author's experiments. If the ions which he obtains in this way are positive ions of platinum, it is, indeed, an interesting fact in view of its analogy to the enhanced electron emission from tungsten when covered with a layer of thorium.

Uranium and Thorium

Strips of uranium and thorium, very kindly provided by Professor Wahlin, were heated in the mass-spectrograph and a careful search for positive ions of these metals was made but none were found. This is in agreement with Wahlin's report.[5]

The author wishes to express his appreciation to Dr. L. P. Smith who was responsible for his first acquaintance with this field of research, and to Professors R. C. Gibbs and C. C. Murdock for their helpful suggestions and criticisms during the course of the work reported here.

[14] Wahlin, Phys. Rev. **39**, 183 (1932).
[15] Murawkin, Ann. d. Physik **8**, 385 (1931).

The Temperature Variation of the Positive Ion Emission from Molybdenum

By LEROY L. BARNES
Department of Physics, Cornell University

(Received September 27, 1932)

The temperature variation of the positive ion emission from aged molybdenum filaments was studied with two different types of tube. The values for the positive ion work function and for the reflection coefficient for molybdenum ions are found to be in better agreement with the theory of positive ion emission presented by L. P. Smith than were his experimental results on molybdenum ions.

INTRODUCTION

L. P. SMITH[1] has made a study of the temperature variation of the positive ion emission from tungsten and molybdenum. Following, in a general way, the work of Bridgman[2] he has developed an expression for the rate of evaporation of positive ions as a function of the temperature. From this work the particular expression for molybdenum is,

$$\log_{10} I + 0.453 \log_{10} T + 2.70 \times 10^{-4} T = -\Phi_{+0} e/2.303kT + \frac{1}{2.303k}\int_0^T \frac{dT}{T^2}\int_0^T C_{\gamma\rho} dT + \frac{S}{2.303k} + \log_{10}(1-r) + 12.76 \quad (1)$$

where I is the positive ion current per cm^2 of the emitting surface at the temperature T degrees absolute, Φ_{+0} is the positive ion work function at $T=0$, e the electronic charge, k the Boltzmann constant, r the reflection coefficient for the positive ions, $C_{p\rho}$ the heat capacity associated with the surface heat of charging produced by the evaporation of one ion, and S_ρ the entropy associated with the surface heat of charging at $T=0$. By a separate calculation it was shown that no serious error should be introduced by neglecting the terms containing $C_{p\rho}$ and S_ρ. Thus Eq. (1) becomes

$$\log_{10} + 0.453 \log_{10} T + 2.70 \times 10^{-4} T = -\Phi_{+0} e/2.303kT + \log_{10}(1-r) + 12.76. \quad (2)$$

Plotting values of the left side of this equation against corresponding values of $1/T$ gave a straight line, the slope of which gave, for molybdenum, $\Phi_{+0} = 6.09$ volts, and the constant term obtained from the intercept was 6.90.

At this point two difficulties were encountered. First, it was pointed out that if one computes the value for r from the equation $\log_{10}(1-r)+12.76 = 6.90$ it is found to be so large that only one ion out of about 100,000 striking a surface would be condensed. Secondly, the value obtained for Φ_{+0} was found

[1] L. P. Smith, Phys. Rev. **35**, 381 (1930).
[2] Bridgman, Phys. Rev. **27**, 173 (1926).

to be too small to close the following energy cycle. Starting with an inclosure in which molybdenum is in equilibrium with its radiation at a given temperature T, we remove an electron and a positive ion from the metal thus requiring an amount of work $\Phi_{-T}+\Phi_{+T}$, where Φ_{-T} and Φ_{+T} are the respective work functions at the temperature T. Then allow the electron and positive ion to combine to form a neutral atom, yielding an amount of energy corresponding to its ionization potential V. The cycle is believed to be completed when the atom has been allowed to condense back on the metal, yielding a amount of energy equal to the heat of condensation U_T. If this is a reversible cycle we should have,

$$\Phi_{+T} + \Phi_{-T} = V + U_T. \tag{3}$$

Putting in the accepted values for the different terms along with the above value for Φ_{+0} we have

$$V + U_0 = 7.35 + 6.33 = 13.68$$

$$\Phi_{+0} + \Phi_{-0} = 6.09 + 4.42 = 10.51$$

and we see that the cycle fails to close by 3.17 volts.

The results from tungsten gave rise to the same difficulties and Smith was thus led to conclude that "unlike the evaporation of electrons and neutral atoms, the evaporation of ions is not strictly represented by an equation based upon thermodynamical arguments under equilibrium conditions." He suggests the possibility that tungsten and molybdenum may slowly recrystallize in an irreversible manner, when raised to high temperatures, thus yielding the necessary energy to close the above cycle.

Considering the previous success of the type of thermodynamical argument used here by Smith, in explaining similar phenomena, and knowing the very marked differences in experimental results obtained by different observers investigating the thermionic properties of metals, the author was led to make a further study of the temperature variation of the positive ion emission from molybdenum. Molybdenum was chosen rather than tungsten because Smith had found that its emission decayed much less with time than did the emission from tungsten.

Experimental Work and Results

The first tube used was of the type shown in Fig. 1, a type used by many observers in the study of the thermionic properties of metals. The molybdenum filament was held in place along the axis of the three nickel cylinders by means of a weak molybdenum spring. The two end cylinders were kept at the same potential as the center cylinder but only the positive ion current to the center cylinder was measured.

A temperature scale for the central portion of the filament was obtained by the method described by Smith,[1] from Worthing's[3] data on the total radiation, in watts per cm^2, from molybdenum.

[3] Worthing, Phys. Rev. **28**, 190 (1926).

The tube was baked at a temperature of about 470°C before and after the first outgassing of the metal parts. The metal parts were first heated with an induction furnace and then the cylinders were brought to a higher temperature by electron bombardment. Then with the three cylinders made negative with respect to the filament, the filament was aged at a temperature of 2000°K for 20 hours before any readings were taken. During the time the aging was going on the filament was flashed occasionally, for a few seconds, at a temperature of about 2600°K. Even after this aging process was completed it was found that the filament had to be taken over the temperature range to be used several times before the rate of decay of the emission became small.

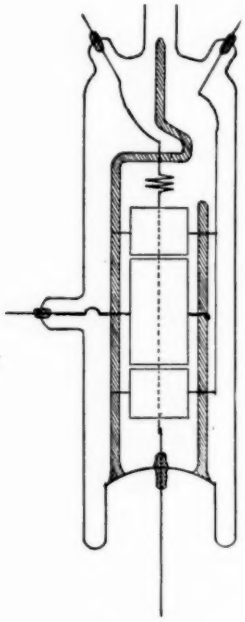

Fig. 1.

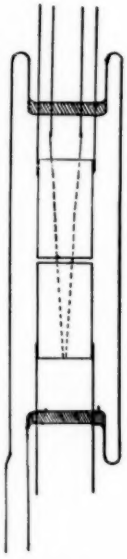

Fig. 2.

A sample of the data taken with this tube is shown in Fig. 3. From the slope of this line the value of Φ_{+0} is 8.15 volts and from the intercept the constant term is 11.96.

Since these values are so much higher than those obtained by Smith it was decided that a more exact duplicate of his experiments might lead to an explanation of the difference in the results. For this purpose a tube of the type he used was built. A diagram of this tube is shown in Fig. 2. The two cylinders were kept at the same potential but only the current to the lower cylinder was measured. The hairpin filament used in this tube had been shaped by heating it, while under tension, in a vacuum. Smith's filaments were shaped by heating them, under tension, in hydrogen. (This difference in procedure does not seem to lead to any serious difference in results as will be shown later.)

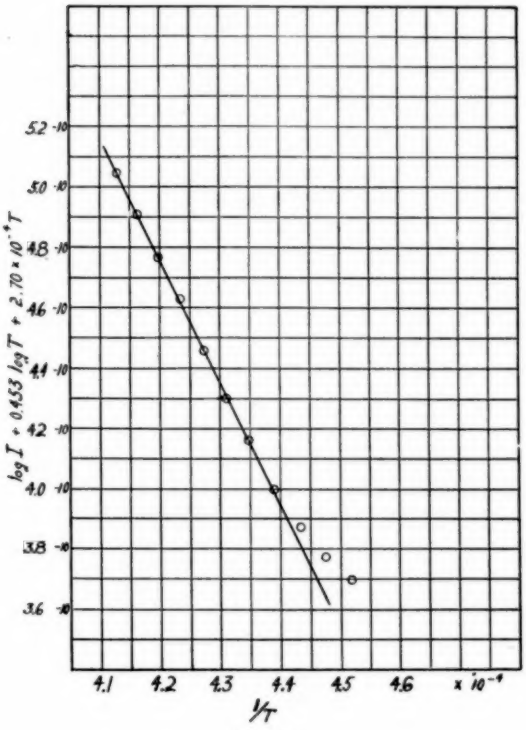
5.2 -10
5.0 -10
4.8 -10
4.6 -10
4.4 -10
4.2 -10
4.0 -10
3.8 -10
3.6 -10
log I + 0.453 log T + 2.70 × 10⁻⁴ T
4.1
4.2
4.3
4.4
4.5
4.6
× 10⁻⁴
1/T

Fig. 3.

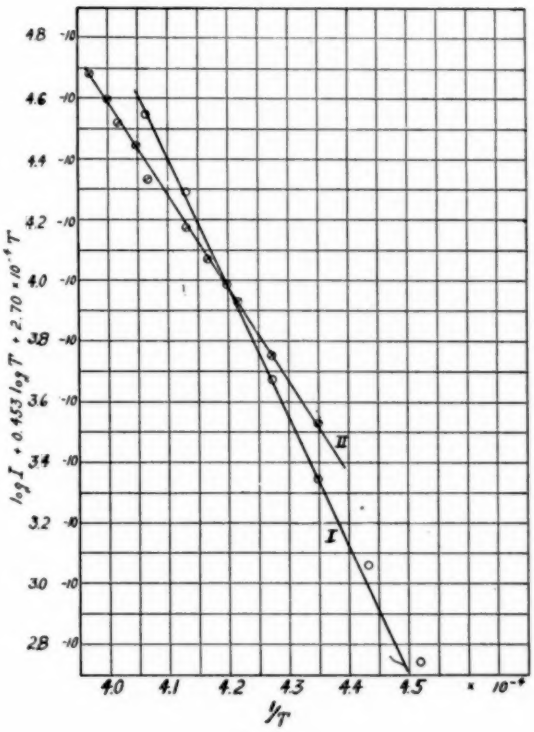
4.8 -10
4.6 -10
4.4 -10
4.2 -10
4.0 -10
3.8 -10
3.6 -10
3.4 -10
3.2 -10
3.0 -10
2.8 -10
log I + 0.453 log T + 2.70 × 10⁻⁴ T
II
I
4.0
4.1
4.2
4.3
4.4
4.5
× 10⁻⁴
1/T

Fig. 4.

Curve I of Fig. 4 is a plot of representative data obtained from this tube. From this curve $\Phi_{+0}=8.5$ volts and the constant term is 11.8. Curve II of Fig. 4 is a plot of the data for molybdenum given in Smith's paper. Quite obviously the slopes are different, and the results obtained by the author are in fair agreement with those obtained from the other type of tube.

After all of the data to be discussed later had been taken, hydrogen was admitted to the tube to a pressure of 6 mm Hg and the filament glowed for 15 minutes at a temperature of about 1800°K. The hydrogen was then pumped out and the filament kept at a temperature of 1900°K for one hour. Then after taking the filament slowly over the temperature range to be used, the

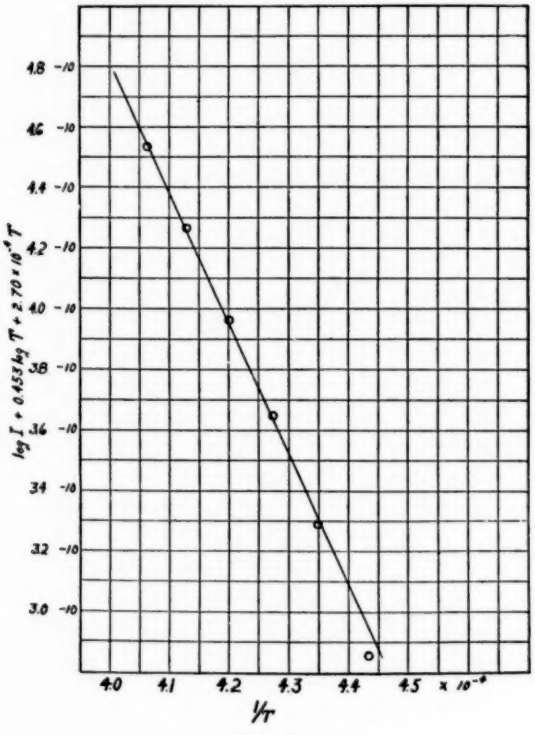

Fig. 5.

data shown by the curve of Fig. 5 were taken. From this curve $\Phi_{+0}=8.65$ volts and the constant term is 12.2. Whether or not the small increase in these values, over the previous values obtained, is to be attributed to the use of the hydrogen is a matter to be decided by more detailed experiment, but these results obviously do not serve to explain the difference between the results obtained by Smith and those obtained by the author.

In Table I the values of the constant term and of Φ_{+0} are given for four separate runs taken with each tube.

The variations in the values of Φ_{+0} and of the constant term which appear here, do not seem to follow any definite order as regards aging of the filaments, and, within the limits of error of the experiments, no variation of

TABLE I. *Values of the constant and of* Φ_+.

Straight filament		Hairpin filament	
Φ_{+0} (volts)	Constant term	Φ_{+0} (volts)	Constant term
8.12	11.8	8.15	11.0
8.23	11.9	8.20	11.3
8.06	11.7	8.00	11.0
8.15	12.0	8.50	11.8
8.14	11.8	8.20	11.3 Average

these values with the applied voltage, over the range of 100 to 400 volts, could be detected.

It should be noted that the lower points on the curves of Figs. 3 and 4, fall above the straight line which fits the other points reasonably well. This was true of all of the curves obtained with the exception of the one taken after the hydrogen was used. A study of the positive ion emission in this lower temperature range, with higher current sensitivity than that used here might prove to be interesting.

The average of the work function values, given in Table I, comes within about one volt of closing the energy cycle, and the average of the constant term values gives a value for r of about 0.9. This would mean that one ion out of about 10 striking a surface would be condensed. This result seems more reasonable than that obtained by Smith but in comparison with the values of reflection coefficients for neutral atoms and electrons it seems large.

At this point due respect should be paid the suggestion that a gradual irreversible recrystallization of the metal might account for the necessary energy to close the cycle (3). E. A. Hazlewood[4] has found that such a recrystallization does take place for tungsten and molybdenum at high temperatures. The results, however, are of such a qualitative nature that no quantitative comparison with the positive ion emission data can be made.

The experimental results presented in this paper indicate that the theory of positive ion emission developed by Smith may be better than his experimental results led him to believe, and that the amount of energy called for from the recrystallization process may not be as great as he supposed.

[4] E. A. Hazlewood, *Crystal Growth in Molybdenum and Tungsten Filaments at High Temperatures*. A thesis, Cornell University Library.

Rotational Analysis of Ultraviolet Bands of Silicon Monoxide

By PAUL G. SAPER
Ryerson Physical Laboratory, University of Chicago

(Received September 6, 1932)

From measurements on silicon arc spectrograms a rotational analysis has been made of the (0,1), (0,2), (0,3), (0,4) and (1,4) bands of the ultraviolet band system of silicon monoxide (SiO). The bands were found to be due to a $^1\Pi \rightarrow {}^1\Sigma$ transition as was expected by analogy with the fourth positive bands of CO. Among the constants obtained from the analysis are

$B_0' = 0.6270$	$r_e' = 1.62 \times 10^{-8}$ cm	$\alpha' = 0.00657$
$B_0'' = 0.7238$	$r_e'' = 1.51 \times 10^{-8}$ cm	$\alpha'' = 0.00494$

A number of perturbations of the Q branch lines were observed. Some conclusions were reached as to the nature of the perturbing levels. From measurements of band heads of this system made by Jevons and the results of the present analysis the following equation was obtained for the band origins:

$$\nu_0 = 42835.3 + 851.51(v'+1/2) - 6.143(v'+1/2)^2 + 0.0437(v'+1/2)^3 - 1242.03(v''+1/2) + 6.047(v''+1/2)^2 - 0.00329(v''+1/2)^3.$$

INTRODUCTION

THE ultraviolet band system of silicon monoxide (SiO) has heads, as listed by Jevons,[1] extending from 2176.6A to 2925.3A. The bands are shaded toward longer wave-lengths. According to Cameron,[2] these bands might be the analog of the fourth positive bands of CO. If so, they must be of the type $^1\Pi \rightarrow {}^1\Sigma$.

The writer has now made a rotational analysis of the (0,1), (0,2), (0,3), (0,4) and (1,4) bands. The analysis confirms the idea that they are $^1\Pi \rightarrow {}^1\Sigma$. Each band was found to consist of one P, one Q and one R branch.

SPECTROGRAMS

Using as a source a carbon arc with SiO_2 placed in the lower (positive) carbon, the writer photographed these bands in the first and second orders of a twenty-one foot concave grating. The iron arc was used as a comparison spectrum. Measurements of the (0,1) and some other bands were made from the spectrograms thus obtained in the second order, and the (0,1) band was partly analyzed. Then measurements were made of the (0,1), (0,2), (0,3), (0,4) and (1,4) bands from plates of silicon arc spectrograms, which Professor R. S. Mulliken received through the kindness of Professor W. F. C. Ferguson of New York University. The exposures were made by Professor Ferguson with the new, very large Hilger quartz spectrograph at the Bureau of Standards. The iron arc served as a comparison spectrum on these plates. The

[1] W. Jevons, Proc. Roy. Soc. London **106**, 174 (1924).
[2] W. H. B. Cameron, Phil. Mag. (7) **3**, 110 (1927).

iron arc wave-lengths which were used were from those measured by K. Burns and F. M. Walters, Jr.[3] The quartz spectrograph plates just mentioned showed a dispersion, at 2500A, of about 0.874A/mm, as compared with about 1.24A/mm for the grating second order plates, and also showed a greater resolution than the grating plates. From measurements on these quartz spectrograph plates the five bands mentioned above were analyzed.

Rotational Analysis

As the bands were excited at high temperature the series were long, and there was some overlapping of series lines from one band to another. Many of the observed lines were blends, and there were a number of atomic lines in the spectrum. The (0,1) band was analyzed first. The Q branch lines could be distinguished from the other series lines because of their greater intensity. The R branch lines near the origin were considerably stronger than the P branch lines in this region. Members of the P, Q and R series with common values of the rotational quantum number of the lower energy state were selected from these series with the aid of the relation

$$R(J) - Q(J) \cong Q(J+1) - P(J+1). \tag{1}$$

According to the quantum theory of band spectra, there is Λ-type doubling in a $^1\Pi$ state; each rotational level of this electronic state is double (c and d sets of sub-levels[4]). The Q lines are due to transitions from a different set of sub-levels of the $^1\Pi$ state than those from which the P and R lines originate. As a result there is a "combination defect" equal to $[R(J)-Q(J)]-[Q(J+1)-P(J+1)]$. In the case of these SiO bands this defect was found to be relatively small compared to the quantities $[R(J)-Q(J)]$ or $[Q(J+1)-P(J+1)]$ themselves.

In order to assign correctly the absolute J'' values the following relations were used:

$$\Delta_2 T'(J) = R(J) - P(J) = 4B'(J+\tfrac{1}{2}) + 8D'(J+\tfrac{1}{2})^3 + \cdots \tag{2}$$

$$\Delta_2 T''(J) = R(J-1) - P(J+1) = 4B''(J+\tfrac{1}{2}) + 8D''(J+\tfrac{1}{2})^3 + \cdots . \tag{3}$$

These relations were also used to calculate the constants B' and B''. The values of $[R(J)-P(J)]$ were plotted against successive integers. For relatively small values of J'' these points lay very approximately on a straight line and then with increasing J'' they began to deviate slightly from the line. A straight line was drawn through the points up to where they began to deviate. The slope of this line gave a good approximation to the value of $4B'$. Similarly, by plotting the values of $[R(J-1)-P(J+1)]$ against successive integers a good approximation to $4B''$ was obtained. Then D' and D'' were calculated with the aid of the theoretical relation

$$D_e = -4B_e^3/\omega_e^2, \tag{4}$$

[3] K. Burns and F. M. Walters, Jr., Publications of the Allegheny Observatory of the University of Pittsburgh, Vol. VIII, No. 4.

[4] R. S. Mulliken, Rev. Mod. Phys. **3**, 89 (1931).

neglecting the difference between D_e and D_v. The values of ω_e' and ω_e'' were obtained from the vibrational analysis of SiO made by Jevons,[1] from measurements on the heads of the bands. It was found that when the quantity $[R(J)-P(J)-8D'(J+1/2)^3]$ was plotted against successive integers, the points now all lay very approximately on a straight line, showing that there was no need of considering terms of higher power than the third to represent $\Delta_2T'(J)$. A similar statement holds for $\Delta_2T''(J)$. Thus by successive approximations and least squares the values of B' and B'' were obtained for the five bands analyzed. The values of B_0' as thus obtained from the analysis of the (0,1), (0,2), (0,3) and (0,4) bands agreed to within one-tenth of one percent or less. The values of B_1'', B_2'', B_3'' and B_4'' showed a very approximately linear variation according to the formula

$$B_v = B_0 - \alpha v. \tag{5}$$

The wave numbers of the P, Q and R lines, together with the rotational quantum numbers assigned to them, are listed in Table I. There are a number of perturbations of the Q branch lines. Their significance will be considered in a later section.

TABLE I.

The first six numbers give the wave number of the line considered. The seventh number, in bold-face type, expresses the estimated relative intensity of the line. Blends of two or more lines are indicated by an asterisk (*). The letter A indicates that a heavy atomic line is superposed on a band line.

(0,1) band				(0,2) band		
P	Q	R	J''	P	Q	R
	41392.74		14		40174.56	
	89.74		15		71.98*	
	86.66		16		68.94	
	83.04		17		66.16	
	79.36*		18		62.96	
	75.76*		19		59.79*	
	71.96*		20		56.26	
	67.98*		21	40126.44	52.6A*	
	63.96		22	21.54	48.86	
	59.76*		23	15.84	44.96	
	55.46*		24	10.44	40.56	
	50.76*		25	04.64	36.06*	40167.53
	45.86*		26	40099.15	31.38*	64.62
	40.98*		27	92.93	26.76*	61.64
41300.46*	35.76*	41371.96*	28	86.74	22.16*	58.06
41293.86*	30.56*	67.98*	29	80.33	17.08*	54.14
87.13	24.86*	63.54	30	73.85	11.88*	50.34
80.33	19.06*	58.78*	31	67.24	06.08*	46.04
73.22	13.06*	54.14	32	60.69*	00.48*	41.54
65.73	06.86*	49.04	33	53.34	40094.48*	36.06*
57.93	00.46*	43.96	34	46.19*	88.89*	31.88*
50.03	41293.86*	38.36	35	38.89*	82.58	26.76*
42.13	88.06	33.74	36	31.28*	76.88	22.16*
34.83	80.76	28.14	37	24.28*	70.06	17.08*
26.13	73.66	22.24	38	15.58*	63.16	11.88*
17.53	66.26	15.84	39	07.56*	56.46	06.08*
08.83	58.66	09.64	40	39999.26*	49.16	00.48*
00.13	51.16	03.24	41	90.78*	42.06	40094.48*
41191.03	43.26	41296.54	42	82.16*	34.56	87.99*
81.53	35.26	89.74	43	72.86*	26.96	81.84

TABLE I. (*Continued*).

(0, 1) band				(0, 2) band		
P	*Q*	*R*	*J''*	*P*	*Q*	*R*
72.03	27.06	82.84	44	64.64	19.26	75.04
62.43	18.66	75.74	45	55.16	11.36	68.34
52.63	09.96	68.44	46	45.64	03.16	61.39*
42.63	01.26	60.64	47	36.14	39994.66	53.94
32.43	41192.28*	52.64	48	26.24	86.16	46.19*
22.03	82.86	44.64	49	16.34	77.56	38.89*
11.53	73.68*	36.54	50	06.34	68.66	31.28*
00.66*	63.98*	27.94	51	39896.04	59.56	24.28*
41089.56*	54.18*	19.64	52	85.84	50.36	15.58*
78.36*	44.08*	10.84	53	75.2A*	40.86	07.56*
66.76*	34.06	01.54	54	63.94	31.16	39999.26*
54.96*	23.66	41192.28*	55	53.04	21.26	90.78*
43.23	13.06	84.04	56	41.84	11.36	82.16*
31.53	02.36	73.68*	57	30.28*	01.06	72.86*
20.04	41091.26	63.98*	58	19.52	39890.65	63.34
06.94	80.06	54.18*	59	07.34	80.1A*	54.04
40994.24	41068.76	41144.08*	60	39795.14	39869.35	39944.24
81.44	56.66	33.34	61	82.64	58.15	34.44
68.64	45.86	22.54	62		47.65	24.54
55.54	33.46	11.74	63		36.05	14.14
42.04	21.26	00.66*	64		24.25	03.94
28.35	08.86	41089.56*	65		12.64	39893.24
14.7A*	40996.16	78.36*	66		00.85	82.94
00.25	83.26	66.76*	67		39788.75	71.94
40886.74	70.16	54.96*	68			61.96*
72.24	57.16	42.84	69			49.34
57.54	43.66	30.44	70			37.63
42.57*	29.96	18.06	71			26.04
27.84	16.36	05.36	72			
12.63	02.16	40991.7A*	73			
40797.13	40887.96	79.26	74			
81.73	73.46	66.05	75			
65.83	58.55	52.55	76			
49.63	42.57*	38.65	77			
33.55*	29.65	24.95	78			
16.83	13.95	10.64	79			
00.45*	40798.15	40896.34	80			
40683.35*	82.35	81.64	81			
66.15*	66.44	66.83	82			
48.75*	50.04	51.53	83			
30.95*	33.55*	37.53	84			
13.15*		21.03	85			
		05.63	86			
		40789.53	87			
		73.33	88			
		57.13	89			
		40.33	90			
		23.53	91			

TABLE I. (*Continued*).

(0,3) band				(1,4) band		
P	*Q*	*R*	*J''*	*P*	*Q*	*R*
	38980.56*		7			
	79.54*		8			
	78.54*		9			
	77.04*		10			
	75.99*		11			
	74.08*		12			

TABLE I. (*Continued*).

(0, 3) band				(1, 4) band		
P	*Q*	*R*	*J''*	*P*	*Q*	*R*
	71.59*		13		38617.22	
	69.44*		14		15.11	
	67.04*		15		12.53	
	64.54*		16		10.04*	
	61.48*		17		07.36*	
	58.76*		18		03.94*	
	55.79*		19		00.96*	38625.34
	52.29*		20		38597.63	23.23
	48.79*	38974.08*	21		93.95	21.22
	45.29*	72.19*	22		90.24	18.64
	41.56*	69.44*	23	38558.33	86.44	16.01
	37.56	67.04*	24	52.83	82.53	13.23
	33.36	64.54*	25	47.26*	78.43	10.04*
	29.19*	62.44	26	41.51	73.93	07.36*
38890.88*	24.56	59.44	27	35.72	69.23	03.94*
85.06*	19.99*	56.39*	28	30.04*	64.54	00.36*
78.97*	15.24	52.29*	29	23.82	59.86	38596.62
72.56*	10.39*	48.79*	30	17.42	54.74	92.82
66.16*	05.06	45.29*	31	11.14*	49.43	88.83
59.56*	38899.86	40.94	32	04.41	43.82	84.73
52.86*	94.38	36.25	33	38497.84	38.66*	80.42
46.14	88.56	31.75	34	90.64*	32.76*	75.43
38.94	83.85	28.04	35	83.64*	26.83	70.72
31.64	77.56	23.14	36	76.14*	20.72	66.03
25.15*	71.16	18.79*	37	68.53	14.59*	61.24*
17.06*	64.66	13.09*	38	60.93	07.94*	55.83
09.44	58.16	07.78*	39	53.44	01.26*	50.56*
01.36*	51.46	02.39*	40	45.13	38494.64*	45.24
38793.54	44.76	38896.69*	41	37.04	87.54*	39.06*
85.34	37.56	90.88*	42	29.04	80.34*	33.26*
76.94	30.56	85.06*	43	19.84	73.03*	27.82
68.14	23.26*	78.97*	44	11.63	66.13	21.42
59.44	15.69*	72.56*	45	03.14*	58.69*	14.59*
50.54	07.96*	66.16*	46	38393.93	50.53	07.94*
41.44	38799.99*	59.56*	47	84.43	42.86	01.26*
32.04	92.06*	52.86*	48	75.04*	33.53	38494.64*
22.75	83.86	45.44	49	65.38*	25.34	87.54*
13.14	75.36	38.34	50	55.53	17.84	80.34*
03.44	66.86	31.14	51	45.93	08.94	73.03*
38693.24	58.16	23.26*	52	36.74*	00.86*	65.64
83.15	49.16	15.69*	53	26.14*	38391.23	57.92
72.95	40.06	07.96*	54	15.64*	81.86*	48.54
38662.44	38730.76	38799.99*	55	38304.63*	38371.76	38440.13
51.74	21.26	92.06*	56	38293.64*	62.26	31.73
40.85*	11.66	83.04	57	82.66*	52.26	22.94
	01.86	74.44	58		42.25	14.03
	38691.86	65.74	59		32.06	05.23
	81.46	56.64	60		21.76	38396.34
	70.96	47.64	61		10.96	86.44
		38.24	62		00.25	77.04
		28.55	63		38289.46	67.63
		19.05	64			57.13
		08.65	65			47.13
		38699.15	66			36.74*
		88.65	67			26.14*
		78.22	68			15.64*
		67.35	69			04.63*
		56.64	70			38293.64*
		45.64	71			82.66*

TABLE I. (*Continued*).

J''	(0,4) band P	Q	R	J''	(0,4) band P	Q	R
11		37782.53		43	37592.03	45.74	00.44*
12		80.83		44	83.93	38.94	37694.75*
13		78.73		45	75.72	31.74	89.14*
14		76.62		46	67.23	24.74	82.94*
15		74.34		47	58.73	17.24	76.62
16		71.83*		48	49.64*	09.64	70.23
17		69.14*		49	40.93	01.94	63.64
18		66.36*		50	31.93	37594.36	57.03
19		63.53		51	22.63	86.05	50.13
20		60.66*		52	13.13	77.75	43.44*
21		57.26*		53	03.53	69.45	36.63
22		53.73		54	37493.83	60.85	28.83
23		50.13		55	83.73	52.04	21.03
24		46.53		56	73.83*	43.14	14.12
25		42.54		57	37463.43	37534.24	37605.63
26		38.44	37771.83*	58		25.04	37597.63
27	37700.44*	34.23	69.14*	59		15.54	89.43
28	37694.75*	30.14*	66.36*	60		05.94	81.43
29	89.14*	25.43	63.01	61		37496.04	72.44
30	82.94*	20.83	59.44*	62		86.65	63.63
31	77.23	15.94*	55.83	63		76.43	54.63
32	70.82	11.04*	52.02	64		66.14	45.63
33	64.52	05.94*	48.13	65		56.09*	36.03
34	57.93	00.44*	43.93	66		45.16*	27.23
35	51.22	37694.75*	39.43	67		34.16*	17.74*
36	44.33*	89.94	35.63	68		23.46*	07.73
37	38.13	84.14	31.04	69			37497.73
38	30.43	77.94	26.33	70			87.43
39	23.13	71.84	21.33	71			77.32
40	15.63	65.63	16.44*	72			66.94
41	07.93	59.14	11.04*	73			56.09*
42	00.22	52.54	05.94*				

In Tables IIA and IIB, there are listed agreements in the combination differences.

TABLE IIA. *Agreements in the combination differences.*

Note (1): $R(J)-Q(J+1)$ should not necessarily be exactly the same for the (0,4) and (1,4) bands, since the Λ-type doublet widths are not necessarily the same, for given J values, for $v'=0$ and $v'=1$.

Note (2): In some of the bands, additional combination differences are available, but are omitted from the table because of the absence of comparison data from other bands.

J	$R(J)-Q(J)=T'(J+1)-T'(J)+\Delta\nu_{de}'(J)$ (0,1)	(0,2)	(0,3)	(0,4)	$R(J)-Q(J+1)=T''(J+1)-T''(J)+\Delta\nu_{de}''(J+1)$ (0,4)	(1,4)
25		31.5	31.2			
26		33.3	33.3	33.4	37.6	38.1
27		34.9	34.9	34.9	39.0	39.4
28	36.2	35.9	36.4	36.2	40.9	40.5
29	37.4	37.1	37.0	37.6	42.2	41.9
30	38.7	38.5	38.4	38.6	43.5	43.4
31	39.7	40.0	40.2	39.9	44.8	45.0
32	41.1	41.1	41.1	41.0	46.1	46.1
33	42.2	41.6	41.9	42.2	47.7	47.7
34	43.5	43.0	43.2	43.5	49.2	48.6
35	44.5	44.2	44.2	44.7	49.5	50.0
36	45.7	45.3	45.6	45.7	51.5	51.5

TABLE IIA. (*Continued*)

J	$R(J)-Q(J)=T'(J+1)-T'(J)+\Delta\nu_{de}'(J)$				$R(J)-Q(J+1)=T''(J+1)-T''(J)+\Delta\nu_{de}'(J+1)$	
	(0,1)	(0,2)	(0,3)	(0,4)	(0,4)	(1,4)
37	47.4	47.0	47.6	46.9	53.1	53.3
38	48.6	48.7	48.4	48.4	54.5	54.6
39	49.6	49.6	49.6	49.5	55.7	55.9
40	51.0	51.3	50.9	50.8	57.3	57.7
41	52.1	52.4	51.9	51.9	58.5	58.7
42	53.3	53.4	53.3	53.4	60.2	60.2
43	54.5	54.9	54.5	54.7	61.5	61.7
44	55.8	55.8	55.7	55.8	63.0	62.8
45	57.1	57.0	56.9	57.4	64.4	64.0
46	58.5	58.2	58.2	58.2	65.7	65.1
47	59.4	59.3	59.6	59.4	67.0	67.7
48	60.4	60.0	60.8	60.6	68.3	69.3
49	61.8	61.3	61.6	61.7	69.3	69.7
50	62.9	62.6	63.0	62.7	71.0	71.4
51	64.0	64.7	64.3	64.1	72.4	72.2
52	65.5	65.2	65.1	65.7	74.0	74.4
53	66.8	66.7	66.5	67.2	75.8	76.1
54	67.5	68.1	67.9	68.0	76.8	76.8
55	68.6	69.5	69.2	69.0	77.9	77.9
56	71.0	70.8	70.8	71.0	79.9	79.5
57	71.3	71.8	71.4	71.4	80.6	80.7
58	72.7	72.7	72.6	72.6	82.1	82.0
59	74.1	73.9	73.9	73.9	83.5	83.5
60	75.3	74.9	75.2	75.5	85.4	85.4
61	76.7	76.3	76.7	76.4	85.8	86.2
62	76.7	76.9		77.0	87.2	87.6
63	78.3	78.1		78.2		
64	79.4	79.7		79.5		
65	80.7	80.6		80.0		
66	82.2	82.1		82.1		
67	83.5	83.2		83.6		
68	84.8			84.3		

TABLE IIB. *Agreements in the combination differences.*

J	$R(J)-P(J)=\Delta_2T'(J)$				$R(J-1)-P(J+1)=\Delta_2T''(J)$	
	(0,1)	(0,2)	(0,3)	(0,4)	(0,4)	(1,4)
27		68.7	68.6	68.7	77.1	77.3
28	71.5	71.3	71.3	71.6	80.0	80.1
29	74.1	73.8	73.3	73.9	83.4	82.9
30	76.4	76.5	76.2	76.5	85.8	85.5
31	78.4	78.8	79.1	78.6	88.6	88.4
32	80.9	80.9	81.4	81.2	91.3	91.0
33	83.3	82.7	83.4	83.6	94.1	94.1
34	86.0	85.7	85.6	86.0	96.9	96.8
35	88.3	87.9	89.1	88.2	99.6	99.3
36	91.6	90.9	91.5	91.3	101.3	102.2
37	93.3	92.8	93.6	92.9	105.2	105.1
38	96.1	96.3	96.0	95.9	107.9	107.8
39	98.3	98.5	98.3	98.2	110.7	110.7
40	100.8	101.2	101.0	100.8	113.4	113.5
41	103.1	103.7	103.1	103.1	116.2	116.2
42	105.5	105.8	105.5	105.7	119.0	119.2
43	108.2	109.0	108.1	108.4	122.0	121.6
44	110.8	110.4	110.8	110.8	124.7	124.7
45	113.3	113.2	113.1	113.4	127.5	127.5
46	115.8	115.7	115.6	115.7	130.4	130.1

TABLE IIB. (*Continued*).

J	$R(J)-P(J)=\Delta_2T'(J)$				$R(J-1)-P(J+1)=\Delta_2T''(J)$	
	(0,1)	(0,2)	(0,3)	(0,4)	(0,4)	(1,4)
47	118.0	117.8	118.1	117.9	133.3	132.9
48	120.2	119.9	120.8	120.6	135.7	135.9
49	122.6	122.5	122.7	122.7	138.3	139.1
50	125.0	124.9	125.2	125.1	141.0	141.6
51	127.3	128.2	127.7	127.5	143.9	143.6
52	130.1	129.7	130.0	130.3	146.6	146.9
53	132.5	132.3	132.5	133.1	149.6	150.0
54	134.8	135.3	135.0	135.0	152.9	153.3
55	137.3	137.7	137.5	137.3	155.0	154.9
56	140.8	140.3	140.3	140.3	157.6	157.5
57	142.1	142.6	142.2	142.2		
58	143.9	143.8				
59	147.2	146.7				
60	149.8	149.1				
61	151.9	151.8				

Λ-TYPE DOUBLING

The combination defects in the (0,1), (0,2), (0,3) and (0,4) bands were computed for each value of J and, where possible, averaged over the different bands. The definition of $\Delta\nu$ (in cm^{-1}) for Λ-type doubling,[5] which will be used here is

$$\Delta\nu_{de}(J) = T_d(J) - T_e(J). \tag{6}$$

For a $^1\Pi$ state,[5] according to Van Vleck, one expects theoretically

$$\begin{aligned} T_d(J) &= T_0 + B_vJ(J+1) - 2C + (C + C_1)J(J+1) + \cdots; \\ T_e(J) &= T_0 + B_vJ(J+1) - 2C + (C + C_2)J(J+1) + \cdots. \end{aligned} \tag{7}$$

$$\begin{aligned} \Delta\nu_{de}(J) &= qJ(J+1), \text{ where } q = C_1 - C_2, \\ &= (B_d - B_e)J(J+1). \end{aligned} \tag{8}$$

The combination defect is:[5]

$$\begin{aligned} &[R(J) - Q(J)] - [Q(J+1) - P(J+1)] \\ &\quad = \Delta\nu_{dc}(J) + \Delta\nu_{dc}(J+1) \\ &\quad \leqq 2\Delta\nu_{dc}(J + \tfrac{1}{2}) \\ &\quad \leqq 2q(J + \tfrac{1}{2})(J + 3/2) \\ &\quad \leqq 2q(J+1)^2. \end{aligned} \tag{9}$$

From the numerical values of the combination defect corresponding to the various quantum numbers J, the value of q was computed by least squares. It was found that $q=B_d-B_e=-6.7\times10^{-5}$. In Fig. 1, the observed combination defects are plotted in comparison with a curve given by $-13.4\times10^{-5}(J+1)^2$.

[5] R. S. Mulliken and A. Christy, Phys. Rev. **38**, 87 (1931).

If the almost certainly correct assumption[5] is made that the $^1\Sigma$ lower electronic state of the observed bands is $^1\Sigma^+$, then the Q series lines originate from c levels.[4]

As mentioned before, there are a number of perturbations of the Q lines. This suggests the presence of other electronic energy levels near the $^1\Pi$ level. Since there are a number of perturbations of the Q lines, but not of the P and R lines, apparently the c levels are perturbed much more than the d

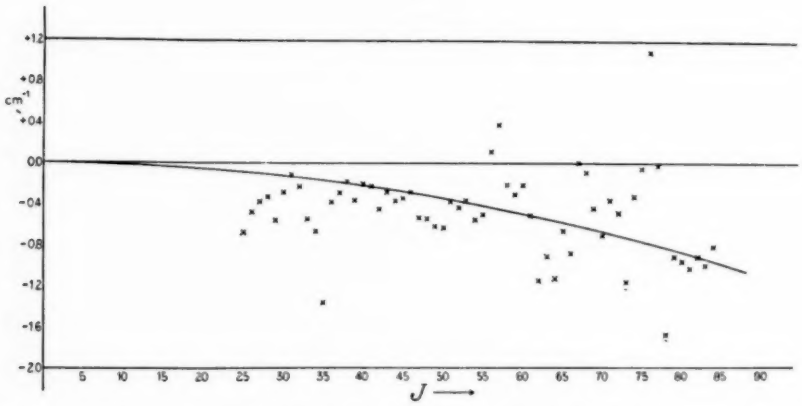

Fig. 1. The observed combination defects (cf. Eq. (9)) are shown by crosses. Each point indicated is, where possible, the average for the (0,1) (0,2), (0,3) and (0,4) bands. The curve is that given by $-13.4\times10^{-5}(J+1)^2$. Most of the small deviations between the experimental points and the curve may be due to experimental error, but most of the large ones are due to the perturbations of the Q lines.

levels and it seems likely that even for the unperturbed lines, it is the c levels rather than the d levels which are mainly responsible for the Λ-type splitting. If so (cf. Eqs. (7, 8)), $|C_2| \gg |C_1|$. Then since experimentally $(C_1 - C_2)$ is negative, C_2 would be positive. The expressions for the coefficients C_1 and C_2 are[5]

$$\begin{aligned} C_1 &= 8\Sigma(\text{all } v \text{ values of all } {}^1\Sigma^+ \text{ states}) \left| BL_v(\Pi, \Sigma^+) \right|^2 / \nu(\Pi, \Sigma^+), \\ C_2 &= 8\Sigma(\text{all } v \text{ values of all } {}^1\Sigma^- \text{ states}) \left| BL_v(\Pi, \Sigma^-) \right|^2 / \nu(\Pi, \Sigma^-). \end{aligned} \tag{10}$$

The quantites BL_v are approximate constants for any pair of electronic states, Π, Σ. $\nu(\Pi, \Sigma^+)$ is the wave number (cm^{-1}) corresponding to the energy difference between the $^1\Pi$ state and v value considered and any $^1\Sigma^+$ state and v value. If the $^1\Pi$ level is above the $^1\Sigma^+$ level it is taken as positive, if it is below the $^1\Sigma^+$ level it is taken as negative. $\nu(\Pi, \Sigma^-)$ has a similar meaning. Hence, from the argument above, that $|C_2| \gg |C_1|$ and $C_2 > 0$, it would follow that $\nu(\Pi, \Sigma^-) > 0$. This would indicate the presence relatively close to and below the given $^1\Pi$ state of one or more $^1\Sigma^-$ levels, which cause perturbations of the c levels of the $^1\Pi$ state.

Band Origins

From the relation

$$\begin{aligned}\nu = \nu_0 &+ B_v'J'(J'+1) + D_v'J'^2(J'+1)^2 \\ &- B_v''J''(J''+1) - D_v''J''^2(J''+1)^2\end{aligned} \tag{11}$$

as the equation of a band line for a $^1\Pi \rightarrow {}^1\Sigma$ transition, the value of ν_0, for a given band, was taken as the definition of the band origin. With the observed wave numbers of twelve P, twelve R and ten Q lines of relatively small rotational quantum numbers, thirty-four values of ν_0 were calculated for the band under consideration. The average of these values was taken as the origin of the band. This was done for each of the five bands analyzed. Then a parabola was fitted by least squares to the values of ν_0 for the (0,1), (0,2), (0,3) and (0,4) bands, and by this means the values of ν_0 for the (0,0) and (0,5) bands were calculated. Then with aid of the values of B_v' and B_v'' the interval $(\nu_{\text{head}} - \nu_0)$ was calculated for most of the bands (other than those here analyzed) whose heads were measured by Jevons,[1] and with the wave numbers of the heads as listed by him, values of ν_0 were obtained. From the aggregate of the values of ν_0 calculations were made for ω_e', ω_e'', $x_e'\omega_e'$ and $x_e''\omega_e''$, giving greatest weight to the ν_0 data obtained directly by the present measurements, and the following equation was obtained for the origins of this band system:

$$\begin{aligned}\nu_0 = 42835.3 &+ 851.51(v'+\tfrac{1}{2}) - 6.143(v'+\tfrac{1}{2})^2 \\ &+ 0.0437(v'+\tfrac{1}{2})^3 - 1242.03(v''+\tfrac{1}{2}) + 6.047(v''+\tfrac{1}{2})^2 \\ &- 0.00329(v''+\tfrac{1}{2})^3.\end{aligned} \tag{12}$$

Molecular Constants

In Table III there are listed the values of all the molecular constants obtained in the present work. The values of β' and β'' corresponding to the relation

$$D_v = D_e + \beta(v+\tfrac{1}{2}) = D_0 + \beta v \tag{13}$$

were calculated from the theoretical formula[6]

$$\beta = \frac{\alpha^2}{6\omega_e} + \frac{20\alpha B_e^2 - 32x_e B_e^3}{\omega_e^2}. \tag{14}$$

A check on the correctness of the analysis was afforded by a rule, due to R. T. Birge. According to this rule the quantity $2x_eB_e/\alpha_e$ is approximately equal to 1.4. For these bands substitution of the proper values showed that

$$2x_e'B_e'/\alpha' = 1.38$$

$$2x_e''B_e''/\alpha'' = 1.43.$$

An additional check is given by the approximate relation[7] that for molecules composed of two atoms of nearly equal mass, the quantity $r_e^3\omega_e$ is approximately equal to 3000×10^{-24} cm^2. For these bands

[6] E. C. Kemble, Jour. Opt. Soc. Am. **12**, 1 (1926).
[7] P. M. Morse, Phys. Rev. **34**, 57 (1929).

$$r_e'^3\omega_e' = 3620 \times 10^{-24}$$
$$r_e''^3\omega_e'' = 4276 \times 10^{-24}.$$

TABLE III. *Values of the molecular constants.*

Upper state $^1\Pi$	Lower state $^1\Sigma$
$B_e' = 0.6303$	$B_e'' = 0.7263$
$B_0' = 0.6270$	$B_0'' = 0.7238$
$B_1' = 0.6205$	$B_1'' = 0.7189$
$\alpha' = 0.00657$	$B_2'' = 0.7138$
$D_e' = -1.382 \times 10^{-6}$ (calc.)	$B_3'' = 0.7091$
$\beta' = 2.88 \times 10^{-9}$ (calc.)	$B_4'' = 0.7041$
$I_e' = 43.95 \times 10^{-40}$ g cm^2	$\alpha'' = 0.00494$
r_e' (for $Si_{28}O_{16}$) $= 1.62 \times 10^{-8}$ cm	$D_e'' = -0.993 \times 10^{-6}$ (calc.)
$q = B_d - B_e = -6.7 \times 10^{-5}$	$\beta'' = -1.55 \times 10^{-9}$ (calc.)
$\omega_e' = 851.5$	$I_e'' = 38.14 \times 10^{-40}$ g cm^2
$x_e'\omega_e' = 6.14$	r_e''(for $Si_{28}O_{16}$) $= 1.51 \times 10^{-8}$ cm
$y_e'\omega_e' = 0.0437$	$\omega_e'' = 1242.0$
	$x_e''\omega_e'' = 6.05$
	$y_e''\omega_e'' = 0.00329$

It is to be expected that for SiO the values of $r_e'^3\omega_e'$ and $r_e''^3\omega_e''$ will be greater than 3000×10^{-24}, since the masses of the two atoms are rather unequal.

The writer wishes to express his thanks to Professor R. S. Mulliken for proposing this problem and for his valuable advice and suggestions; also to Professor W. F. C. Ferguson of New York University for the spectrograms taken by him with the large quartz spectrograph, and to Dr. W. F. Meggers of the Bureau of Standards for the use of the latter.

Zeeman Effect of Perturbed Terms in the CO Angstrom Bands

By WILLIAM W. WATSON
Sloane Physics Laboratory, Yale University

(Received September 29, 1932)

The Zeeman effect of the perturbed lines in the CO angstrom bands ($^1\Sigma \rightarrow {}^1\Pi$) is described. The perturbations are multiple, occur in the $^1\Pi$ state, and contain excess, much-displaced lines. New lines extending the "resonance" curves of Rosenthal and Jenkins are found. The perturbed lines show large, irregular Zeeman patterns, whereas the neighboring band lines with these intermediate and high J values are apparently insensitive to the magnetic field. Always the greater the displacement of the perturbed line, the larger its Zeeman effect. The patterns differ at each perturbation point: they are either broad, asymmetrical doublets; very broad, uniform blocks; sharp, narrow doublets; or just a shift, increasing the amount of the perturbation. An explanation is offered, assuming the perturbing state to be case a $^3\Pi$.

INTRODUCTION

THE details of the perturbations in a number of band spectra have been examined by Rosenthal and Jenkins,[1] Dieke[2] and others. These observations are in general in good agreement with the requirements of the theory as set up by Kronig[3] and by Ittmann.[4] Briefly, perturbations should occur whenever two energy levels for the molecule having the same J value approach closely to one another, the two levels having the same symmetry characteristics, Λ values the same or differing by at most 1 unit, the same multiplicity, and about the same internuclear distance. The perturbed energy levels do not cross, but rather separate from each other, so that the curves showing the departures of the perturbed band lines from the regular course of the branches to which they belong are of the "resonance" type.

Especially violent perturbations occur in the CO angstrom bands[1] ($^1\Sigma \rightarrow {}^1\Pi$), particularly in the 0, 0 band at 4511A. Rosenthal and Jenkins were the first to give a correct quantum analysis of this band, basing their assignments on the necessity of obtaining smooth deviation curves for the perturbed lines, agreement with known $\Delta_2 F'(J)$ combination differences, and the abandonment of the notion that the Λ-doubling in the $^1\Pi$ state should remain small and regular. This work showed that the perturbations are in the lower $^1\Pi$ state and that they are multiple, coming in this 0, 0 band at $J=9$, 16, 17 and >30 in the P and R branches and at $J=12$, 29 and >35 in the Q branch. From the fact that these perturbations are multiple and from an examination of the nature of the near-lying levels of CO, it was concluded that the perturbing state is probably a $^3\Pi$ state, in violation of the Kronig rule that the

[1] J. E. Rosenthal and F. A. Jenkins, Proc. Nat. Acad. **15,** 381 and 896 (1929).
[2] G. H. Dieke, Phys. Rev. **38,** 646 (1931).
[3] R. de L. Kronig, Zeits. f. Physik **50,** 347 (1928).
[4] G. P. Ittmann, Zeits. f. Physik **71,** 616 (1931).

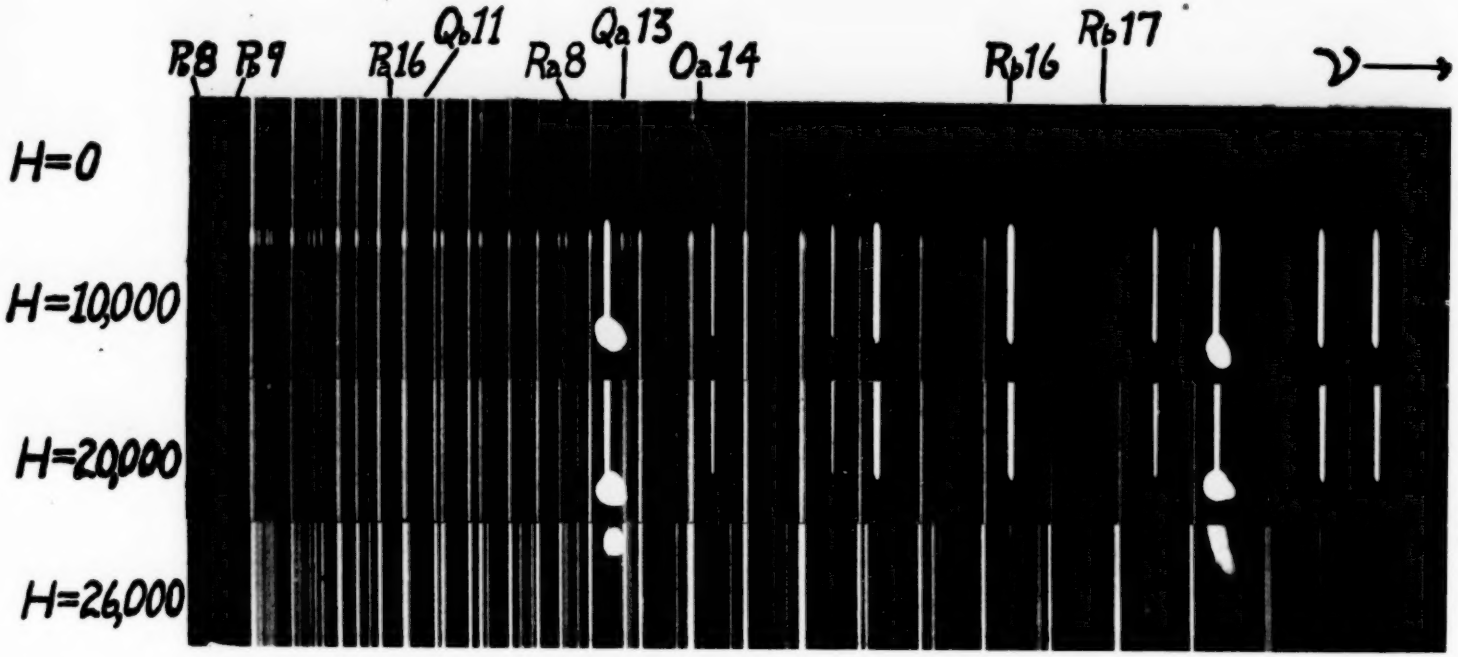

Fig. 1. The (0, 0) CO angstrom band at 4511A with magnetic field strengths up to 26,000 gauss. Several of the more violently perturbed lines are indicated, others being of too low intensity to show in the reproduction. Fe comparison lines.

perturbing terms should have the same multiplicity. We shall return to this point below.

In his work on the regular Zeeman effect in these CO bands, Crawford[5] noted the existence of large, irregular Zeeman effects for certain of the band lines which are involved in these perturbations. In the present investigation the details of these peculiar Zeeman patterns have been examined, and possible explanations are presented in connection with the facts about the perturbations and the probable nature of the interacting levels.

Experimental Procedure

Spectrograms of the 0, 0 and 0, 1 bands of the CO angstrom system were obtained in the second order of the 21-foot concave grating in a stigmatic mounting, the dispersion being approximately 2.42A per mm. The magnetic field strengths varied from 10,000 gauss to 26,700 gauss. On each plate was placed in addition to the field exposure a no-field comparison spectrum and the spectrum of the Fe arc for wave-length determinations. The source was a 15,000 volt a.c. discharge between small copper disks 3 to 4 mm apart, mounted in the gap space of a large Weiss electromagnet. These electrodes were attached to the electrode holders of a modified Back chamber, and were insulated from the pole faces with mica. CO_2 gas from a commercial cylinder was pumped slowly through the discharge chamber at a pressure of about 5 mm, in some cases directly from the cylinder, while in other cases the gas was first passed through a hot copper oxide tube and a tube filled with P_2O_5. The time of exposure was of the order of 12 hours each for the Zeeman effect spectrogram and for the no-field comparison.

This source is of course weak, but because of the increased intensity of the spectra with the grating in the stigmatic mounting, the exposure times were not excessive. Disturbing discharge in regions outside that of uniform field was effectually reduced by having copper disk electrodes but 4 mm in diameter as against a pole face diameter of 20 mm, and by taking care to see that the gas pressure never became too low. A faint background of impurity lines increasing in intensity towards the violet is present on all the spectrograms. It was found, however, that by allowing a slight leak of air into the CO_2, this unwanted spectrum was reduced in intensity to the point where it caused but little trouble in the measuring of the spectrograms. The N_2^+ bands thus introduced could be tolerated because they do not overlap the interesting perturbation points in the CO bands.[6] In Fig. 1 are to be seen Zeeman patterns of some of the perturbed lines in the (0, 0) 4511A band at the several field strengths.

Additional Lines at Perturbation Points in 0, 0 Band

A marked feature of the quantum analysis of the (0, 0) band as made by Rosenthal and Jenkins[1] is the occurrence of two lines for each of one or more

[5] F. H. Crawford, Phys. Rev. **33**, 341 (1929).

[6] These $^2\Sigma \rightarrow {}^2\Sigma$ bands of N_2^+ also display interesting Zeeman patterns for lines involved in their perturbations. These perturbations are very similar to those in the corresponding band system of the isoelectronic molecule CN, and will be the object of further study.

J values at the center of a perturbation. Furthermore, they reported the sum of the intensities of the two lines to be always about that calculated by interpolation for an unperturbed line of that J value. Also, the greater the displacement of the line the less is its intensity. According to the theory this appearance of extra lines is to be expected, for around the perturbation points the wave functions of the molecule for the two electronic states concerned become "mixed," losing their separate identity, with the result that transitions from the upper $^1\Sigma$ state to the perturbing state ($^3\Pi$?) are possible.

There are in fact more of these extra lines than are given in Table I of reference 1. The assignments of these additional lines are given in Table I,

TABLE I. *Quantum assignments of lines of intermediate J value in the (0, 0) CO angstrom band.*

J''	P		Q		R	
	a	*b*	*a*	*b*	*a*	*b*
7	22,164.60		22,191.30		22,222.99	
8	167.25	150.90*	197.10		233.45	217.08*
9	172.10	159.48	203.84		246.09	233.45
10	180.96	166.32	211.55	185.00*	d	248.11
11		171.65	220.63	200.73		261.16
12		176.87	231.85	214.38		274.08
13		182.54	246.09	227.05		287.59
14		188.97	263.48	238.77		301.79
15	179.86*	196.47		250.26	d	317.02
16	193.44	205.92		261.92	321.80	334.21
17	205.41	219.03*		274.08	341.39	355.32*
18	215.59			286.77	359.43	

where the new lines are indicated by a *. The line $P_b(8)$ lies some 12 cm^{-1} beyond the head of the band, and there is even an indication of a line P_b (7) still further to the red. The new lines are all displaced many cm^{-1} from the unperturbed points for the particular J values, and are all consequently of low intensity. The correctness of the assignments is attested however by the existence of exactly the required $\Delta_2F'(J)$ combination differences, and by the fact that they are all much affected by the magnetic field, being even broadened slightly in the no-field comparison spectrum by the field due to the residual magnetism in the magnet. Strong lines of other branches lie in the positions indicated for R_a (10) and R_a (15), making their observation impossible. The perturbations in the region of higher J values have not been examined in detail.

OBSERVED ZEEMAN PATTERNS

All of the band lines in the immediate neighborhood of the perturbations exhibit large, irregular Zeeman patterns, whereas the regular Zeeman effect for lines with these intermediate and high J values for a $^1\Sigma \rightarrow {}^1\Pi$ transition is so small as to leave the unperturbed lines totally unaffected by the magnetic field. There is a different type of Zeeman effect at each of the perturbations in the (0, 0) band, and always the perturbed lines having the greatest displacements are magnetically the most sensitive. A brief tabulation of some of the details of these patterns at three different field strengths is given in

Table II. Measurement on some of the perturbed lines is prevented either by their nearness to or fusion with other lines in the band, or by their low inten-

TABLE II. *Zeeman patterns of perturbed band lines in the (0, 0) CO angstrom band at 4511A* cm^{-1} units. + indicates a shift to the high-frequency side, − to the low-frequency side of the no-field band line.

	10,000 gauss	20,000 gauss	26,000 gauss
	a. P, R branch perturbation at $J=9$.		
$P_b(8)$	Broadened +0.80 to −0.84 Min. intens. in center + side stronger	Broad doub. −0.75 to −1.35 and (stronger) +0.62 to +1.34	Broad doublet
$P_b(9)$	Broadened +0.31 to −0.49	Broadened (stronger) −0.83 to −0.36 and weaker to +1.07	Broadened, − stronger
$R_a(7)$	No effect	Slight sym. broadening	Broadened +0.38 to −0.63
$R_a(8)$ + $R_b(9)$	Slight sym. broadening	Broadened +0.42 to −0.38	Broadened +0.43 to −0.56
$R_b(8)$	Broadened +0.72 to −0.83 Min. in center, + side stronger	Broad doub. + stronger +0.48 to +1.25. −block block fuses into $P_a(18)$	Stronger +0.38 to +1.10 − block weaker
$R_b(10)$	No effect	Broadened +0.33 to −0.26	Broadened +0.40 to −0.45
	b. Q branch perturbation at $J=12$.		
$Q_a(10)$	No effect	No effect	
$Q_a(11)$	No effect	Shift of +0.06. Sharp	Slight + shift
$Q_a(12)$	No effect	Shift of +0.13. Sharp	Shift of +0.15. Sharp
$Q_a(13)$	No effect	Shift of +0.51. Sharp	Shift of +0.67. Slight broadening
$Q_a(14)$	No effect	Shift of +0.89. Slight broadening	Shift of +1.06. Slight broadening
$Q_b(11)$	No effect	Shift of −0.32. Sharp	Shift of −0.58. Slight broadening
$Q_b(12)$	No effect	Slight—shift	Definite—shift
$Q_b(13)$	No effect	No effect	Shift of −0.12
$Q_b(14)$	No effect	No effect	Shift of −0.06
	c. P, R branch perturbation at $J=16$.		
$P_a(16)$	Broadened +0.55 to −0.56	Broad block +1.09 to −1.03	Very broad and diffuse
$R_b(15)$	No effect	Slight sym. broadening	Broadened +0.49 to −0.27.
$R_b(16)$	Broadened +0.25 to −0.26	Broadened +0.62 to −0.66	Broadened +0.79 to −0.73
$R_b(17)$	Slight broadening	Broad doub. +0.38 to +1.14 and −0.39 to—	Broad doub +0.24 to +1.28 −block weaker
$R_a(16)$	Broad block 1.13 wide	Strong −block	Stronger at −1.04
$R_a(17)$	Broadened +0.27 to −0.26	Broadened +0.36 to −0.26	Sym. broadened
$R_a(18)$	No effect	Slight broadening	Slight broadening
	d. Q branch perturbation at $J=29$.		
$Q(30)$			Sharp doub. +0.30 and (weaker) −0.20.

sity. A sufficient number of observations can be made at each perturbation, however, to enable one to say definitely the kind of pattern that is developed.

Several points about these Zeeman patterns should be emphasized. The doublets which the field produces for some of the most perturbed lines are never quite symmetrically placed with respect to the original line, the asymmetry increasing with increasing field strength. Also when a line which at low field strength is just uniformly broadened splits in stronger fields into two blocks of radiation, the two are never of the same intensity, the block on the side of increased perturbation energy being in some instances the stronger, while for other lines the reverse is true. In the Q branch around $J=12$ the displaced lines are not noticeably affected by a field of 10,000 gauss, although the perturbation is just as violent as the first two P and R branch perturbations, i.e., the two sets of interacting levels must come just as close to each other. The effect of the higher field strengths on these Q lines is merely to increase slightly the magnitude of their displacement in the perturbation, the Q_a lines being shifted to higher frequencies, the Q_b lines to lower frequencies. The most perturbed lines experience the greatest shift, and are but slightly broader than the corresponding no-field lines. A similar Zeeman effect has been observed for one of the perturbations in the (0, 1) band, but has not been worked out in detail.

The lines at the center of the P and R branch perturbation around $J=16$ mostly undergo a uniform symmetrical broadening as the field increases, but the line R_b (17) which has the largest displacement in the perturbation does become a broad doublet at the higher field strengths. And the widths of these patterns is just as large as those in the first P, R perturbation, despite the fact that the overall spread of the $2J+1$ component levels due to the field in the $^1\Pi$ state is but one half as great (varies as $1/J$), while the perturbations are of about the same degree. This would indicate that the interacting levels of the other electronic state are here more affected by the field, for instance that they are $^3\Pi_2$ levels, while for the first perturbation $^3\Pi_0$ levels are responsible. We shall mention this again in the discussion below.

Finally the character of the Q (30) line pattern at the high field strength should be mentioned. This is a narrow, sharp, but not symmetrical doublet, and the same is true of the pattern for the line Q (29) at the second Q-branch perturbation in the (0, 1) band. One would expect narrower Zeeman patterns with sharper components, other things being equal, from these perturbed lines of high J values because of the decreased width of the group of Zeeman sublevels if J is large. And for the same reason only the one or two most displaced lines at these perturbations of high rotational levels should be appreciably affected by the magnetic field. Our observations show this to be the case.

Discussion

As Rosenthal and Jenkins have shown,[1] the $a^3\Pi$ state of CO could be the state that interacts with the $^1\Pi$ levels to produce these perturbations, for extrapolation of the known vibrational levels of the a state indicates that its $v=10$ level approaches closely $^1\Pi^{(0)}$ with nearly the same ω values. Or it may be that the $d(^3\Pi?)$ level which lies below and very close to the $^1\Pi$

state is responsible for the perturbations. There is definitely no singlet level in this energy range. Also the fact that the perturbations are multiple would indicate that the perturbing terms do not belong to a singlet state. And in addition the finding of a very different type of Zeeman effect at each of the principal perturbations in the (0, 0) band seems to require different interacting levels at each of the points, in order that some variations in the arrangement of the magnetic sublevels exist. It is true that $^3\Pi$ and $^1\Pi$ levels perturbing each other constitutes a violation of the Kronig rule that the two perturbing states must have the same multiplicity. However, this rule need not be expected to hold here, for singlet-triplet transitions of fair intensity do occur in CO. And from such a $^1\Pi$, $^3\Pi$ interaction as many as six perturbations could be produced in one of the $^1\Sigma \rightarrow {}^1\Pi$ bands, since all Π terms are doubled (Λ-doubling).

It is reasonable to assume that the $^3\Pi$ state is fairly close to case *a*, for the separation[7] of the P_1 and P_3 branches near the origins of the $^3\Sigma \rightarrow a^3\Pi$ third positive CO bands is some 50 to 60 cm^{-1}. This spacing is almost entirely due to the multiplet intervals in the $^3\Pi$ level, since Dieke and Mauchly report that the triplet separation of the $^3\Sigma$ state is unnoticeable near the origin.[8] In the range of rotational energy levels in which we are interested, then, this spacing of the $^3\Pi$ levels is still probably considerably greater than the splitting produced by the magnetic field. The partial transition towards case *b* with increasing rotational energy would only tend to make the group of magnetic sublevels slightly asymmetrical with respect to the no-field level.

In case *a* states of diatomic molecules the additional energy of the component levels due to the magnetic field is given by the well-known formula[9]

$$W_{\text{mag.}} = \frac{\Lambda(\Lambda + 2\Sigma)M}{J(J+1)} \frac{eh}{4\Pi mc} |H| \tag{1}$$

where all the symbols have their usual significance. For $^1\Pi$ levels this reduces to

$$W_{\text{mag.}} = \frac{+M}{J(J+1)} \left(\frac{eh}{4\Pi mc} |H| \right) \tag{1a}$$

while for the $^3\Pi_0$, $^3\Pi_1$ and $^3\Pi_2$ levels with $\Sigma = -1, 0$ and $+1$, respectively, we have

$$^3\Pi_0 : W_{\text{mag.}} = [-M/J(J+1)](\Delta\nu_{\text{norm}}) \tag{1b}$$

$$^3\Pi_1 : W_{\text{mag.}} = [+M/J(J+1)](\Delta\nu_{\text{norm}}) \tag{1c}$$

$$^3\Pi_2 : W_{\text{mag.}} = [+3M/J(J+1)](\Delta\nu_{\text{norm}}). \tag{1d}$$

[7] R. K. Asundi, Proc. Roy. Soc. **A124,** 277 (1929).
[8] G. H. Dieke and J. W. Mauchly, Phys. Rev. **40,** 123 A(1932).
[9] Cf. for instance, R. de L. Kronig, *Band Spectra and Molecular Structure*, p. 37.

The $^3\Pi_1$ levels have exactly the same Zeeman splitting, then, as $^1\Pi$ levels of the same J value, while for $^3\Pi_0$ the splitting is of exactly the same amount but with the level $+M$ lowest and the level $-M$ highest. In $^3\Pi_2$ the overall width of the group of sublevels is three times that in the $^3\Pi_0$ and $^3\Pi_1$ levels.

As an aid in discussing the effect of the magnetic field on the perturbed levels, the possible arrangements of these levels at the intersection points is sketched in Fig. 2, only the extreme values of $M=\pm J$ being shown. If the $^3\Pi$ level lies just below the $^1\Pi$, the explanation is the same with the substitution of $-M$ for $+M$ and $+M$ for $-M$ throughout. Now the matrix elements of the perturbation energy will be different from zero only if diagonal in M as well as J; i.e., only levels of the same M will perturb each other. With a normal $^3\Pi$ the first close approach of levels with the same J will involve the $^3\Pi_0$ levels (Fig. 2a). In this case the levels with $+M$'s are thrown closer to levels of the same $+M$ value in the other group, and are thus perturbed more,

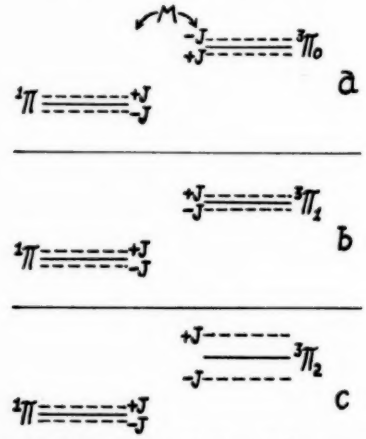

Fig. 2. Rough sketch showing the relative placing of the magnetic sublevels and widths of level patterns in case a $^1\Pi$ and $^3\Pi$ levels of the same J value. Only the no-field levels (solid lines) and the levels with extreme values of $M=\pm J$ are drawn. The other $2J-1$ sublevels will be spaced fairly uniformly between the two extreme levels in each case. The separation of the $^1\Pi$ and $^3\Pi$ levels and the scale of the splitting is quite arbitrary.

say into or beyond the normal region of $-M$ levels. The latter at the same time are forced farther apart from the $-M$ levels of the same value in the other state, and so are perturbed less than before, being thrust through or beyond the region where normally the group of $+M$ levels would be found. This effect would just tend to invert and spread out the whole pattern of magnetic sublevels in each group. The sensitiveness of the perturbation energy to slight change in the interval between the interacting levels is evidenced by the magnification of the Zeeman patterns of the lines (P_b (8) pattern spread 1.64.cm^{-1} at 10,000 gauss as compared to the regular $2\Delta\nu_{norm}/J \leqq 0.11$ cm^{-1}). The occurrence of a region of zero intensity at the center of the Zeeman pattern for a much displaced line such as P_b (8) at the higher field strengths must be attributed to this sensitiveness of the perturbation energy to the size of the interval between the perturbing levels, and to the fact that in

the $^3\Pi$ groups the level $M=0$ will probably be of not exactly the same energy as the original level owing to a slight tendency to spin uncoupling by the field.

If the crossing-over occurs between the $^1\Pi$ and $^3\Pi_1$ levels (Fig. 2b), no effect of the magnetic field on the perturbed band lines should be observed if the $^3\Pi_1$ is strictly case *a*, for the field splitting in the two sets of levels is identical. But a small asymmetry with respect to the no-field levels of the block of magnetic sublevels, due to spin-field coupling, could have the effect of increasing or decreasing slightly the energy interval between the two levels having the same J value. And because this energy interval is already small (perturbation very large), the perturbation energy is appreciably increased or decreased. The type of Zeeman effect observed at the Q-branch perturbation at $J=12$ could originate in this kind of interaction.

When the levels concerned are $^1\Pi$ and $^3\Pi_2$ (Fig. 2c), the situation is somewhat like that for the $^1\Pi$, $^3\Pi_0$ interaction. Because the splitting due to the field in the $^3\Pi_2$ level is about three times that in the $^1\Pi$ level of the same J value, the $-M$ levels are forced closer together, with resulting increased perturbation, while each $+M$ level is separated further from the corresponding $+M$ level of the other group with consequent decrease in the perturbation energy. The result should be a much-broadened, solid Zeeman pattern for the perturbed band line, with perhaps a narrow minimum of intensity in the center at the highest field strengths. This is the type of pattern observed for the lines of the P, R perturbation at $J=16$.

The narrow, sharp doublets observed in the field for the $J=29$ Q-branch perturbation could originate in the $^1\Pi$, $^3\Pi_0$ type of interaction described above, the comparative narrowness being caused by the decrease in the splitting of the levels the higher the J, and the sharp doublet character originating in an asymmetry in the $^3\Pi_0$ group of Zeeman levels, caused by the ever closer approach to case *b* as J increases.

Theory of Continuous Absorption of Oxygen at 1450A

By E. C. G. STUECKELBERG
Palmer Physical Laboratory, Princeton University

(Received September 6, 1932)

The continuous absorption of O_2 has lately been measured by Ladenburg, Van Voorhis and Boyce. Their suggested explanation in the term diagram of the molecule is compared to the corresponding matrix elements.

PART I. THEORY OF CONTINUOUS ABSORPTION IN DIATOMIC MOLECULES

CONTINUOUS absorption and emission in diatomic molecules have been explained as transitions between electronic states with discrete vibrational energy and electronic states with continuous energy.

Condon[1] gave in his paper a qualitative way of obtaining the relative intensities of the observed continua. This has been applied to the continuous emission of H_2 by Winans and Stueckelberg[2] and by Finkelnburg and Weizel.[3] Other applications have been made by Kuhn.[4]

The present paper gives a quantitative explanation of the continuous absorption of O_2 as measured by Ladenburg, Van Voorhis and Boyce.[5] The probability (number of transitions per second) of a transition from the discrete state k to the energy continuum W is:

$$\Gamma_{kW} = (\pi^2/h)\,|\,H_{kW}\,|^2(dQ_W/dW).$$

H_{kW} is the matrix element of the perturbing energy H, and dQ_W/dW is the number of states per region dW. In our case we have $H=\boldsymbol{ME}$ where $\boldsymbol{M}$ is the electric moment of the system, and $\boldsymbol{E}=\boldsymbol{E}_0\cos 2\pi\nu t$ the electric field strength of the incoming light wave. One obtains $|H_{kW}|^2=|M_{kW}|^2E_0^2/3$. The factor $\frac{1}{3}$ is due to the averaging over the angle between $\boldsymbol{E}_0$ and $\boldsymbol{M}$. Let N_k be the number of molecules in the state k per cm^3, and let n be the number of incident light quanta per cm^2 and sec. The number of quanta absorbed in the thin layer Δl per sec. is

$$\Delta l dN_k/dt = \Delta n = -\sum_k \Gamma_{kW}N_k\Delta l.$$

Between n and E_0^2 we have the relation: $cE_0^2/8\pi = nh\nu = I_\nu$. This leads to the following expression for the absorption coefficient:

$$\alpha_\nu = -\frac{\Delta n}{n\Delta l} = \frac{8\pi^3}{3}\sum_k \frac{N_k}{h}\,|\,M_{kW}\,|^2\,\frac{\nu}{c}\,\frac{dQ}{d\nu};\quad I_{\nu l} = I_{\nu 0}e^{-\alpha_\nu l}. \tag{1}$$

[1] E. U. Condon, Phys. Rev. **32**, 858 (1928).
[2] J. G. Winans and E. C. G. Stueckelberg, Proc. Nat. Acad. Amer. **14**, 867 (1928).
[3] W. Finkelnburg and W. Weizel, Zeits. f. Physik **68**, 577 (1931).
[4] H. Kuhn, Zeits. f. Physik **63**, 558 (1930).
[5] R. Ladenburg, C. C. Van Voorhis and J. C. Boyce, Phys. Rev. **40**, 1018 (1932); referred to as L.V.a.B.

The eletric moment $\boldsymbol{M}$ $(\epsilon, r\theta\rho)$ depends on the coordinates ϵ of all the electrons and on the usual coordinates $r\theta\phi$ of the two heavy nuclei. We assume, that the wave function $\Psi_k(\epsilon, r\theta\phi)$ can be decomposed into

$$\psi_k(\epsilon, r\theta\phi) = \phi_n(\epsilon, r)\Theta_{JM}(\theta\phi)\psi_{nv}(r).$$

The matrix element $\boldsymbol{M}$ $(n''J''M''v'', n'J'M'v')$ can be written, after integrating over ϵ, $\theta\phi$,[6] (if $J \gg 1$ and $\Lambda' = \Lambda'' = 0$, and if there is no external magnetic field) as:

$$|M(n''J''v'', n'J'v')| = |M_{k''W'}| = (2J)^{1/2} \int dr \cdot M_{n''n'}(r)\psi_{n''v''}\psi_{n'W'}. \quad (2)$$

$M_{n''n'}(r) = M(r)$ is the electric moment associated with an electron jump from state $n' \rightarrow n''$, if the nuclei are held fixed at the distance r. We assume for the vibrational states v'' the states of a harmonic oscillator i.e.:

$$\psi_{n''v''}(r) = e^{(-1/2)(r-r_0'')^2/a''^2} \times \text{Polynomial in } (r - r_0'') \quad (3)$$

$$\psi_{n''v''=0}(r) = \psi_0 = a^{-1/2}\pi^{-1/4}e^{(-1/2)(r-r_0'')^2/a''^2}, \quad (3b)$$

where a'' (in cm) is defined by the molecular constants ω_0'' and μ:

$$a''^2 = a^2 = (h^2/8\pi^2\mu)(1/hc\omega_0''/2);$$

$$1/\mu = 1/M_{\mathrm{I}} + 1/M_{\mathrm{II}} \quad W'' = hc\omega_0''(v'' + \tfrac{1}{2})$$

and where r_0'' is the equilibrium separation. The functions (3a) and (3b) are different from zero only in the immediate neighborhood of r_0''. We expand:

$$M(r) = M(r_0'') + (r - r_0'')M'(r_0'') + \cdots \quad (4)$$

(2) will be of a similar form:

$$M_{k''W'} = g[M(r_0'') + \beta \cdot M'(r_0'') + \cdots]. \quad (5)$$

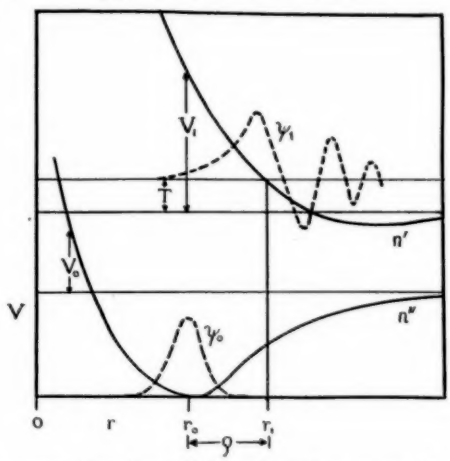

Fig. 1. Potential energy functions $V(r)$ and nuclear wave functions: $\psi_1(r)$ for a non-quantized level of the electronic state n', $\psi_0(r)$ for the lowest vibrational level of the electronic state n''.

[6] W. Weizel, Bandenspectren, Hb.d. Exp. Phys. Ergänzungsband I, p. 164.

We are left with the determination of the wave function $\psi_{n'W'}$ representing an oscillation between a finite $r=r_1$ and infinity ($r=R$, lim $R=\infty$) (see Fig. 1). r_1 is the separation at which the potential energy V_1 equals the kinetic energy at infinity T. We make use of the method by Kramers[7] in order to obtain an expression for $\psi_{n'W'}=\psi_1$. His solution is, if $p^2=8\pi^2\mu(T-V_1)/h^2$: and if $\gamma=(8\pi^2\mu)/h^2\cdot\partial/\partial r\cdot V_1(r)$; $\rho=r_1-r_0''$; $\xi=r-r_1$; $p_\infty^2=8\pi^2\mu T/h^2$:

$$\xi\gg 0\ ;\ T-V_1\gg 0:\psi_1=\psi_{1>}=R^{-1/2}\left(\frac{2p_\infty}{p}\right)^{1/2}\cos\left[\int_0^\xi p\,d\xi-\frac{\pi}{4}\right]$$

$$\xi\cong 0\ ;\ T-V_1\cong 0:\psi_1=\psi_{10}=R^{-1/2}\left(\frac{2p_\infty}{\gamma^{1/3}}\right)^{1/2}\omega(\gamma^{1/3}\xi) \tag{6}$$

$$\xi\ll 0\ ;\ T-V_1\ll 0:\psi_1=\psi_{1<}=R^{-1/2}\text{ neg. real. exp.}$$

Condon[2] has shown in a qualitative way, that the part where $T-V_1\leqq 0$, i.e., the region near r_1, is the most important in evaluating (2). We assume therefore that the part of the integrand in the neighborhood of r_1 only (i.e., the function ψ_{10}) is of importance. This is certainly true, if the slope of the potential energy curve γ of the state n' is constant over the range where ψ_0 is different from zero, and if $\gamma a^3\ll 1$.

(2) becomes:

$$M_{k''W'}\leqq g\,M(r_0)\leqq \mathrm{M}\,(r_0)\left\{\frac{4}{\pi^{1/2}}\,\frac{Jp_\infty}{\gamma^{1/3}aR}\right\}^{1/2}\int_{-\infty}^{+\infty}d\xi e^{-\xi^2/2a^2}\omega(\gamma^{1/3}\xi).$$

The function $\omega(z)$ is tabulated by Kramers[7] and can be expressed by a complex integral (Airy's Integral):[8]

$$\omega(z)=\frac{-i}{2\pi^{1/2}}\int_{(P)}dt\,e^{zt+t^3/3}\qquad\text{(for the path } P \text{ see Kramers).}^{7}$$

Then one has for g.

$$g=\left[\frac{4}{\pi^{1/2}R\gamma^{1/3}\cdot a}\,Jp_\infty\right]^{1/2}\frac{-i}{2\pi^{1/2}}\int_{(P)}dt$$
$$\int_{-\infty}^{+\infty}d\xi e^{-[(\xi+\rho-a^2\gamma^{1/3}t)^2/2a^2]}e^{(t^3/3)+(1/2)a^2\gamma^{2/3}t^2-\gamma^{1/3}\rho\cdot t}.$$

If the substitutions $\xi'=\xi+\rho-a^2\gamma^{1/3}t$; $\tau=t+b$; $b=\frac{1}{2}\gamma^{2/3}a^2$; and $x=\gamma^{1/3}\rho$ are made, the integration over $d\xi'$ can be carried out:

$$g=\left[\frac{8\pi^{1/2}Jp_\infty a}{R\gamma^{1/3}}\right]^{1/2}e^{bx+(2/3)b^3}\omega(-(x+b))=\left[\frac{4\pi^{1/2}Jp_\infty}{R\gamma a}\right]^{1/2}f^{1/2}. \tag{8}$$

We abreviate

$$f=4b\omega^2(-(x+b))e^{2b+(4/3)b^3}. \tag{9a}$$

[7] A. H. Kramers, Zeits. f. Physik 828 (1926).
[8] G. N. Watson, Theory of Functions, p. 188, Cambridge, 1922.

If the argument of $\omega(z)$ takes large negative values ($-z>2$), a good approximation is

$$2\omega(z) = (-z)^{-1/4}e^{-(2/3)(-z)^{3/2}}$$

we make a further substitution: $y=x/b^2=(\rho/a)(4/\gamma a^3)$ and have for $-(x+c)\gg 2$:

$$\begin{aligned} f &= (1+y)^{-1/2}\exp\left[-\frac{4b^3}{3}\left\{(1+y)^{3/2}-(1+(3/2)y)\right\}\right] \\ &= \left(1+4\frac{\rho}{a}\frac{1}{\gamma a^3}\right)^{-1/2} e^{-(\rho^2/a^2)-\cdots}. \end{aligned} \tag{9b}$$

If $\gamma a^3\gg 1$, this is practically the same result as one obtains if one "reflects" the function $\psi_0{}^2$ on the potential energy curve of the repulsive state $\nu/c=(\nu/c)\ (\rho)$.

If the argument of the function ω is positive, i.e., if $(x+b^2)$ is negative the expression for M_0 oscillates. This was also predicted from the qualitative picture of Condon.[2] The conditions for oscillations are

$$\begin{aligned} -(x+c^2) &= -\gamma(\tfrac{1}{4}\gamma a^3(a+\rho)) \gg 0 \quad \text{(order of 1)} \\ -\rho/a &\gg \tfrac{1}{4}\gamma a^3 + 1/(\gamma a^3)^{1/3}. \end{aligned}$$

The next step is to justify the application of ψ_{10} in (7) in the whole region ξ between $-\infty$ and $+\infty$.

The function $M(r)$ depends on r. The final result involves an average value of $M(r)$, say $M(r_i)$. If r_i coincides with r_1, we can conclude, that the region around $r=r_1$ is the most important one. Taking the expansion (4) and (5) this means $\beta=r_1-r_0=\rho$.

In the integral:

$$g\beta M'(r_0) = M'(r_0)\int_{-\infty}^{+\infty} d\xi(\rho+\xi)\psi_0(r)\psi_1(r) \tag{10}$$

we make the same substitutions and notice, that

$$\int_{-\infty}^{+\infty} dt\gamma^{1/3}te^{(t^3/3)+(1/2)\gamma^{2/3}a^2t^2-\gamma^{1/3}t\rho} = -\frac{\partial}{\partial\rho}\int_{-\infty}^{+\infty} dt e^{(t^3/3)+\cdots}.$$

This gives:

$$\beta = -(a^2/4)(1/f)(\partial/\partial\rho)f. \tag{10a}$$

As long as $y<1$, we have roughly:

$$\beta = \rho + a\left[1/(\gamma a^3)^{1/3}\right] \leqq (r_1-r_0), \text{ if } \gamma a^3 > 1.$$

The application of ψ_{10} is therefore justified. The parts of the integrand due to $\psi_{1<}$ and $\psi_{1>}$ are negligible to the same extent as the far away parts of ψ_{10}, which, even if taken into account, do not change appreciably the final result, as long as

$$\gamma a^3 \gg 1 \text{ or } a^3(\partial/\partial r)V_1 \gg h^2/(8\pi^2\mu). \tag{11}$$

The evaluation of matrix elements for which $v'' \neq 0$ can be carried out in the same way as (10) and (10a).

The number of energy levels dQ/dp_∞ in the unstable part of state n' per region dp_∞ goes to infinity as the radius R becomes infinite: $dQ=(R/\pi)dp_\infty$. Going from p to $h\nu$, we have for the number of levels per $d\nu$

$$dQ/d\nu = 4\pi\mu R/hp_\infty. \tag{12}$$

If $\omega_0'' \gg kT/hc$, practically all the molecules are in the level $v''=0$. The expression for the absorption coefficient is, making use of (1), (7), (8) and (12):

$$\alpha_\nu = \frac{128\pi^{9/8}}{3}\frac{\mu}{h^2\gamma a}\sum_J\left(\frac{\nu}{c}\right)M^2(r_1)fJN_J.$$

We have to average over the different rotational levels J. (ν/c), M^2 and f can be considered as independent of J: $\sum_J J\cdot N_J \cong (3\pi^{1/2}/2)N(kT'/hc\cdot B_0)^{1/2}$ (see Weizel[6] p. 167).

$$\alpha_\nu = 64\pi^5\cdot\frac{N\mu(kT/hc\cdot B_0)^{1/2}}{h^2\cdot\gamma a}\left(\frac{\nu}{c}\right)M^2(r_1)f\cdot\text{cm}^{-1}. \tag{13}$$

Part II. The Continuous Absorption of Oxygen

The continuous absorption of oxygen, extending from 1750A to 1300A, has been measured by L.V.a.B.[5] They explain this absorption as a transition from the normal $^3\Sigma$ state of the molecules to the upper $^3\Sigma$ state. The Frank-Condon principle applied to the potential energy curves, calculated by Morse[9] and Stueckelberg,[10] gives the right order of magnitude for ν/c. We have $\omega_0'' \gg kT/hc$ and $\Lambda'=\Lambda''=0$ for $\Sigma\rightarrow\Sigma$ transitions. Therefore a comparison between the experimental curve $\alpha_\nu=\alpha_\nu(\nu/c)$ by L.V.a.B.[5] and the theoretical expression (13) can be carried out in the following way. We plot

$$\text{const.} - \log\left[\alpha_\nu/(\nu/c)\right] = -\log f = (4b^3/3)\left[(1+y)^{3/2} - (1+(3/2)y)\right] + \tfrac{1}{2}\log\left[1+y\right]$$

as a function of y (Fig. 2). To do this we had to assume a value for $b=b_0$. As a is a known quantity ($\omega_0''=1566$ cm^{-1}; $a=5.16\times10^{-10}$ cm) this fixes the value of $\gamma=\gamma_0$.

The comparison between $-\log f$ and the experimental curve of $-\log(\alpha_\nu/(\nu/c))$ gives ν/c as a function of y. This relation is also plotted in Fig. 2. Instead of marking the individual points, an area was drawn. According to the theory $\nu/c=(\nu/c)\ (y)$ ought to be a straight line, if M and γ are constants over the region. This seems to be true within the limits of error. We obtain a value for $d(\nu/c)/dy$. The definition of y and γ leads to the relation

[9] P. M. Morse, Phys. Rev. **34**, 57 (1929).
[10] E. C. G. Stueckelberg, Phys. Rev. **34**, 65 (1929).

$$\gamma^3 = [32\pi^3 \cdot \mu c/ha^4][d(\nu/c)/dy].$$

This newly determined value of $\gamma = \gamma_1$, gives a new value for $b = b_1$. The procedure is repeated until $\gamma_m = \gamma_{m-1}$. This is the case in Fig. 2. The probable

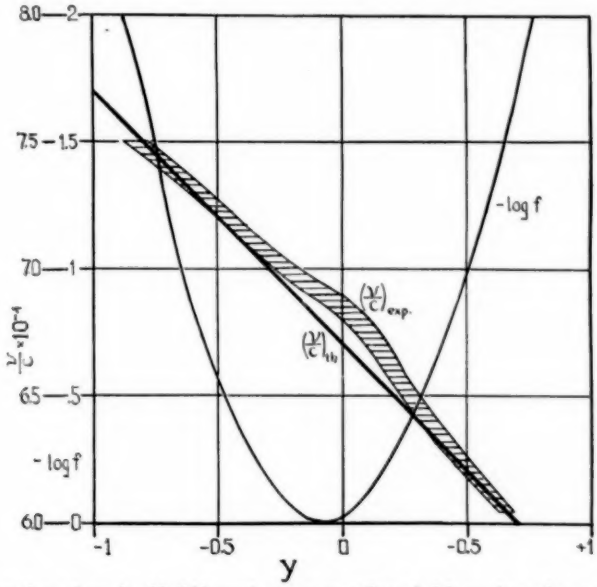

Fig. 2. $-\log f = -\log(\alpha_\nu/(\nu/c))$ and wave number (ν/c) as functions of the parameter $y = 4\rho/\gamma a^4$. The experimental points (L.V. and B.) are plotted as a broad stripe. The black line has been chosen to determine curve A in Fig. 3.

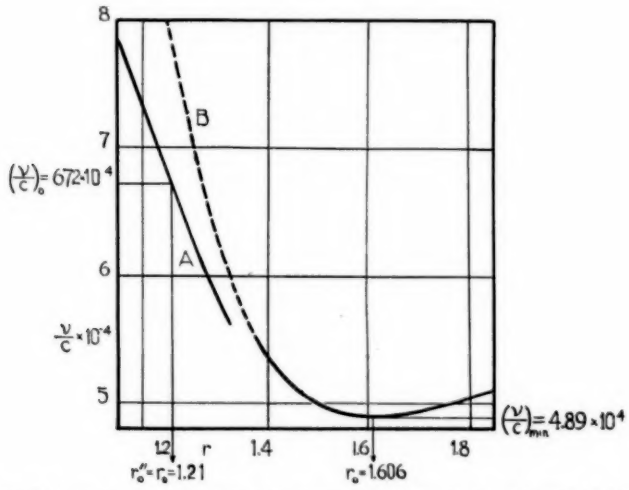

Fig. 3. Potential energy curves for the upper $^3\Sigma$-state of the O_2 molecule. The ordinates are the energy in wave numbers (ν/c), measured from the lowest vibrational level of the normal $^3\Sigma$-state. $r_0'' = r_0$ is the equilibrium separation of the normal $^3\Sigma$-state. (r in 10^{-8} cm^{-1}.)

error in γ is about 2 percent. The value of ν/c for $y = \rho = 0$ determines the height of the potential energy curve over the equilibrium separation r_0''.

The value of γ determines the inclination of the potential energy curve at this point.

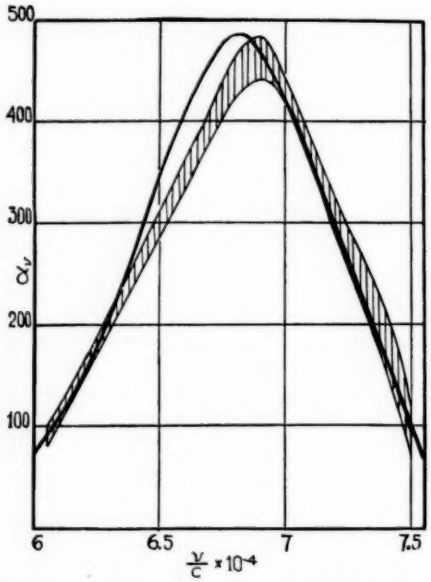

Fig. 4. Absorption coefficient of O_2 as a function of (ν/c). The broad stripe represents the experimental result of L.V. and B., while the black line shows the theoretical absorption coefficient α_ν based upon the potential energy curve A in Fig. 3.

The results are:

$$(\nu/c)_{r=r_0} = (6.72 \pm 0.05) \times 10^4 \text{ cm}^{-1}$$
$$\gamma = (0.51 \pm 0.01) \times 10^{29} \text{ cm}^{-3}$$
$$(d(\nu/c)/dr)_{r=r_0} = (10.8 \pm 0.2)(10^4 \text{ cm}^{-1}/10^{-8} \text{ cm}).$$

Fig. 3 is a comparison between the so defined curve A and the curve calculated by Morse[9] and Stueckelberg,[10] B. One sees that the extrapolation of their calculation (dotted line B in Fig. 3) is too steep. However the curve A seems to point in the right direction. Fig. 4 compares the theoretical absorption coefficient (based upon A) with the experimental values of L.V.a.B. Like in Fig. 2, an area is plotted instead of marking their individual points.

Eq. (13) permits a determination of $M(r_0)$ under the assumption of room temperature ($T = 290°\text{K}$) and with $B_0 = 1.44 \text{ cm}^{-1}$):[6]

$$M(r_0) = (4.77 \times 10^{-10} g^{1/2} \text{ cm}^{3/2} \text{ sec.}^{-1/2}) \times (0.65 \times 10^{-8} \text{ cm}).$$

This is a reasonable result.

Photoelectric Quantum Counters for Visible and Ultraviolet Light. Part I

By GORDON L. LOCHER[1]
The Rice Institute

(Received September 28, 1932)

Extremely sensitive instruments for measuring faint light, from 900A to 7500A, have been made by combining the essential features of photoelectric cells and Geiger-Müller tube counters, so that the photoelectrons ejected by the radiation are individually counted. With some of the tubes described, photocurrents of 0.05 electrons per second can be measured. Photoelectric surfaces of Sn, Cd, Zn, Cu, brass, Ag, Hg, Mg, I_2, and Se, were used for measuring ultraviolet light. Visible-sensitive surfaces were made by coating Cu cathodes with fused NaCN, and with amalgams of Na, K, Cs, Sr, and Na-K, and subsequently directing intense H^+ bombardment against them, in a hydrogen atmosphere. In this manner, thin films of hydrides of the respective metals were formed by reduction. The KH-on-Hg cathodes were the most sensitive to visible light, while the most sensitive one for ultraviolet light was a thin layer of I_2 on Se. Very thin films of about 30 aniline dyes and photographic sensitizers were successively coated on the zinc cathode of a counter. The dye usually shifted the photoelectric threshold toward the ultraviolet, but increased the total sensitivity of the surface. Similar effects were obtained by reversing the direction of field in the counting tube and introducing traces of certain organic liquids into the vicinity of the tungsten wire, which was then the cathode. Thus diethyl-aniline increased the sensitivity by a factor of about 25. Different gases were also tried in the counting tubes; it was found best to use a gas with a high minimum ionization potential, when possible. A counter was used for comparing the total ultraviolet luminosities of several light sources. Thus a particular quartz mercury arc, using about 120 watts, gave 6×10^6 times as much ultraviolet as did a 1000-watt incandescent lamp. Amplifying and recording apparatus is described which is suitable for counting as many as 100 electrons per second, arriving at random times. The paper also discusses criteria for determining the useful electron-counting sensitivity of a counter, the factors limiting its counting speed, an explanation of its mode of operation, and evidence for the existence of other ionic emissions, besides electrons, from counter cathodes. Some possible applications of the counters are mentioned.

I. INTRODUCTION

THE devices described here are combined photoelectric cells and Geiger-Müller tube counters. Photoelectrons liberated from the sensitive surfaces cause small individual discharges between the electrodes, which are amplified and made to operate an impulse recorder or oscillograph. The number of photoelectrons liberated, hence the number of impulses, in unit time, is a measure of the intensity of the incident light.

The main advantage of these counters over other kinds of light detectors lies in their enormous sensitivity for measuring photocurrents. This is shown by comparison of the counters with a Hoffmann electrometer and photoelectric cell. About 1000 electrons per second are required to give a detectable

[1] Later, National Research Fellow, Bartol Research Foundation of The Franklin Institute.

current in the electrometer, even when adjusted to very high sensitivity, whereas some of the counters described here will readily detect a "current" of 0.05 electrons per second, or about 1/20,000 as much. Other desirable features of the counters include simplicity of construction and use, portability while operating, and cheapness of construction. Certain limitations inherent in them will be discussed in a later section of this paper.

In counting individual photoelectrons, occasionally liberated, one seems to approach the limit of sensitivity of a photocurrent measuring device. So the problem of measuring the faintest light becomes one of preparing stable photoelectric surfaces of high quantum efficiency, that have the most suitable spectral distribution of response for the light to be measured.

The work reported here is of a preliminary nature. It includes details of construction of the counters, their general behavior while in use, methods of amplifying and recording impulses, and most especially, methods of preparing numerous photoelectric surfaces that respond to light from the far ultraviolet to the infrared.[2] The writer believes that these counters will find useful application in numerous problems requiring the detection and measurement of faint radiation, and that by their high sensitivity they will make possible the performance of others hitherto very difficult, or impossible. One may especially cite astronomical photometry, spectroscopy, and physical optics, as fields where advantageous application is expected.

B. Rajewski[3] has shown that the usual type of Geiger-Müller[4] tube counters can be modified to respond to ultraviolet light, by adding quartz windows and coating the interior of the metal tubes with cadmium or zinc. He believes one of these to be sensitive enough to detect 12 quanta of 2650A light per sq. cm per second, and further reports the detection of the "mitogenetic rays," supposed by some biologists to be emitted by rapidly dividing plant cells and certain animal tissues. Rajewski's counters were sufficiently large to give a rather high rate of spontaneous counting, in darkness. This is due to radioactivity, cosmic rays, and other spurious causes. By surrounding the counters with a heavy iron shield, the accidental rate was reduced to 20 or 30 impulses per minute.

Rapid spontaneous counting is objectionable for two reasons. In the first place, the accidental count is subject to statistical variation, and in the second, it forms a background on which the true count is superposed, thereby raising the minimum detectable light intensity. In this respect, the use of counters exactly parallels that of vacuum photoelectric cells. Statistical variation in their dark currents becomes troublesome when very feeble light is to be measured; and the superposition of the fluctuating dark current on the true photocurrent diminishes the useful sensitivity of the cell. By the *useful*

[2] The important matter of measuring the quantum efficiencies and sensitivities of particular counters, expressed as the least number of quanta that can be detected in a given time, has not yet been done.

[3] B. Rajewski, Phys. Zeits. **32,** 121 (1931).

[4] H. Geiger and W. Müller, Phys. Zeits. **29,** 839 (1928); Phys. Zeits. **30,** 489 (1929); Phys. Zeits. **30,** 523 (1929).

sensitivity of a cell or counter, one means the best sensitivity for which the results may be *reproduced*, within arbitrarily assigned limits of error, under identical experimental conditions.

The problem in hand is one of measuring light that can be concentrated by lenses and mirrors. This offers a means of reducing the accidental count inherent in large tubes, by using small ones and focusing the light on the photoelectric surfaces. However, the resistance between electrodes must be at least 10^{10} ohms,[5] so a modified form of counter construction is necessary in order to get the required insulation. The use of alkali photoelectric surfaces lowers the resistance and greatly accentuates the difficulty of maintaining good insulation.

The tube described in the next section had a minimum path between electrodes of about 25 cm, over Pyrex glass. Its resistance is estimated at 10^{18} to 10^{16} ohms. The rate of accidental counting, in darkness, depended on the electrodes. Thus the average for cathodes of copper, zinc, cadmium, tin, and mercury was about 1.5 per minute. Similar electrodes bearing alkali metals gave accidental counts ranging from about 3 per second to 6 per minute. Several iodine-coated silver and copper ones showed very high sensitivity to ultraviolet light, with rates as low as 0.7 per minute, in darkness. No shield was used for stopping penetrating radiation; the count due to stray γ-rays and cosmic rays should be 0.5 to 0.9 per minute, with counters of the size used.

II. Description of the Counters

Fig. 1 is a sectional diagram of the counting tube. Essential parts are the axial electrodes E_1 and E_2, the Pyrex tube A, and the quartz window B, which is attached with wax. E_2 is a three-fourths-cylindrical cathode, carrying the photoelectric surface on its concave side. The tube is filled with a gas at 6 to 8 cm pressure. E_2 is maintained at a high negative potential with respect to E_1, so that photoelectrons set free by the impinging light will be drawn to E_1 with sufficient velocity to start "bursts" of ionization by collision. These cause minute current-impulses that are amplified and automatically counted. By means of the ground joint C, the part-cylindrical electrode may be removed for replacement or treatment. The wire electrode is also removable. It is attached to the lead wires L_1, by hooks, and is kept under a slight tension by a small steel spring.

This design has been found very convenient for experimentation with photoelectric surfaces, and for studying the operating characteristics of the tube. The counter used by the writer has been assembled and dismounted some hundreds of times during the course of various tests.

The cylindrical electrodes had an average length of 11 mm, and were about 7 mm in internal diameter. Longitudinal slots about 4.5 mm wide were sawed in them to admit the light. The wire electrodes were usually of polished platinum or tungsten, from 0.038 mm to 0.11 mm in diameter.

[5] Otherwise, fluctuations in the leakage current across the insulators are amplified and recorded as impulses. This spurious count becomes more numerous as the insulator resistance diminishes. The writer found a metal-ebonite G.-M. tube, 1 cm in diameter, to be very unsatisfactory for that reason.

It has been found desirable to use especial care in centering the electrodes, and in making the anode surface smooth. If the wire does not lie nearly along the axis of the cylinder, or if there are major irregularities on the latter, the field may be so distorted as to render much of the photoelectric surface feeble or inoperative. Photoelectrons released with very low velocities in small pits in the metal probably fail to get into the field, and are not counted. It

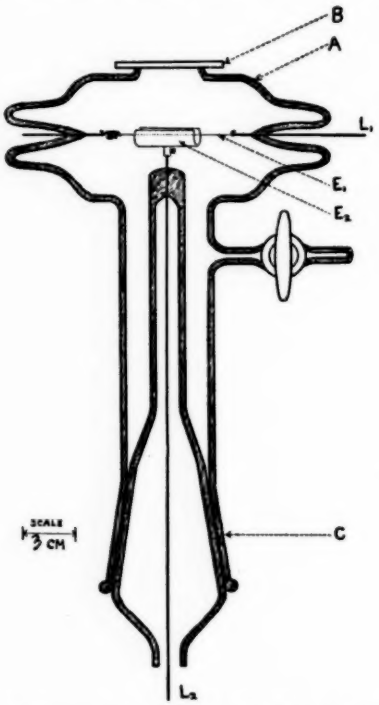

Fig. 1. Cross section of the counting tube. E_1, wire electrode; E_2, cylinder electrode, carrying the photoelectric surface; B, quartz qindow; A, glass body of tube; C, ground joint; L_1 and L_2, leads to amplifier and high-potential source, respectively.

was shown that cathodes differing appreciably from cylindrical form were completely unsatisfactory. Sharp points on the wires are even more objectionable than those on the cylinders, because of the tendency to discharging action. Hence it is good practice to polish the wire with rouge paper before introducing it into the counter. The use of oxide and other coatings on the wires will be discussed in the section dealing with the preparation of electrodes.

III. Amplifiers and Impulse Recorders

Numerous good amplifiers for use with Geiger-Müller counters have been described elsewhere.[6] But the requirements of the present work are rather

[6] For example: J. A. Van den Akker and E. C. Watson, Phys. Rev. **37**, 1631 (1931); B. Rajewski, reference 3; R. Jaeger and J. Kluge, Zeits. für Inst. **52**, 229 (1932); N. A. de Bruyne and H. C. Webster, Cambridge Phil. Soc. Proc. **27**, 113 (1931).

more stringent than for other counters, because the tube electrodes are much nearer together and less ions are produced by collision at each impulse. The impulse current must also be kept sufficiently small that no *light* will be emitted by the discharge. Even when this light is far below the limit of visual sensitivity, its photoelectric action will generally cause extended impulses, instead of sharp ones. It is little more than a fortunate accident that one can get impulses that are strong enough to amplify and record, but too weak to generate light in the counters, especially when alkali metals are present. These remarks apply as well to Geiger-Müller counters for cosmic rays, γ-rays, and x-rays. On the basis of the behavior of photoelectric counters with many different cathodes, filled with different gases, and on comparison of their behavior with that of ordinary tube counters, the writer has become of the opinion that the extension (i.e., "drawling") of impulses observed when the operating potential across the tube is slightly too high, results chiefly from this secondary photoelectric action of the light generated by the discharges themselves.

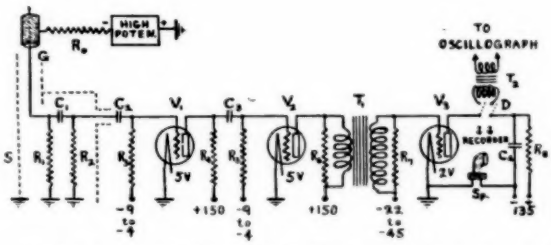

Fig. 2. Amplifying and recording circuit. The resistances, R, are in megohms; capacities, C, are in microfarads.

$R_0 = 1000.$ (xylene)	$R_7 = 2.$ to ∞	V_1, UX 240
$R_1 = 30.$ (xylene)	$R_8 = 0.1$ (variable)	V_2, UX 240
$R_2 = 0.5$	$C_1 = 0.01$* to 0.0005	V_3, W.E. 269-A (thyratron)
$R_3 = 10.$	$C_2 = 0.01$	G, counting tube
$R_4 = 5.$	$C_3 = 0.01$	Sp, loud speaker
$R_5 = 1.$	$C_4 = 1.$	S, grounded shield
$R_6 = 0.5$ to ∞	$T_1 = 1$ to 3	D, d.p.d.t. switch

Another feature of obvious importance is that the amplifier and recorder be capable of accurate and very fast counting when relatively high light intensities are being handled. Several high-gain amplifiers were tried and discarded before a rather satisfactory one was developed. The circuit diagram of this one is shown in Fig. 2. The use of a thyratron as a relay tube is a great convenience; it gives uniform impulses and eliminates the relatively slow-moving mechanical parts of a relay, yet allows enormous gain in amplification. The arrangement for stopping the thyratron discharges is patterned after that of Jaeger and Kluge:[7] the condenser C_4 is charged through the resistance R_8; when an impulse causes an arc to strike in the thyratron, C_4

* The 0.01 mfd condenser used was of rather low resistance, so that R_1C_1 did not represent the true constant for the discharge of C_1. In this case, C_2 was added in order to better isolate the grid of V_1 from the high-potential source.

[7] R. Jaeger and J. Kluge, Zeits. für Inst. **52,** 229 (1932).

discharges through the tube and recording device, after which the arc stops. R_8 is made just large enough to keep the arc from being maintained directly from the battery. Fig. 3 shows some typical impulses recorded on an over-damped string oscillograph. It will be observed that they normally last for about 0.01 second. With oscillographic recording, the thyratron recovers quickly enough to record about 100 random-spaced impulses per second. Considerable gain in the time resolving-power of the apparatus is effected by recording the impulses on an oscillograph so that the wave form of the amplifier output can be examined.

R_0 and R_1 are liquid resistors each consisting of an appropriate mixture of pure xylene and absolute alcohol, sealed in a small glass T-tube provided with platinum electrodes.[8] The resistance is adjusted by altering the proportions of the two liquid components, while filling the tube. The magnitude of

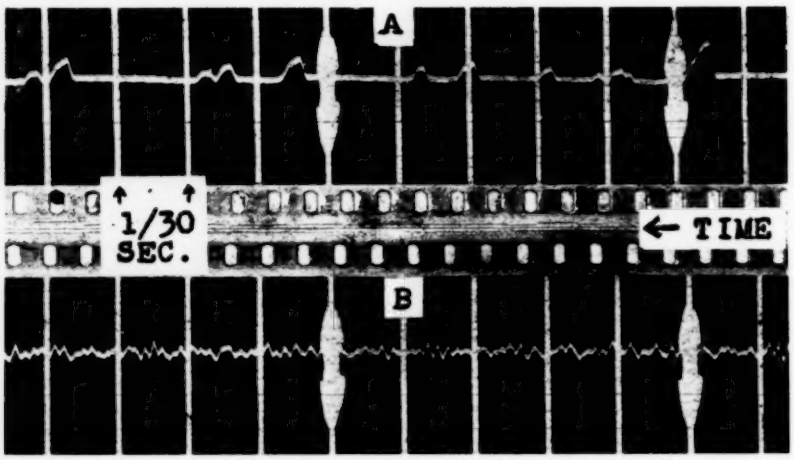

Fig. 3. Oscillograms showing rapid counting: *A*, about 30 per second; *B*, about 225 per second.

the resistance is not critical, but should be constant, for good operation. R_0 limits the current that can flow during each impulse, in order to prevent the discharges from being luminous. The resistance of the counting tube, itself, becomes relatively small while the discharge is taking place, hence it cannot be used to limit the current

A convenient recorder for low-speed impulses has been made by replacing the balance wheel of an Ingersoll watch with an electromagnetic escapement. The energy required to operate the recorder is about 0.03 watt, and its maximum counting speed for regularly spaced impulses is about 40 per second. But for impulses spaced at random, the safe counting rate is only about 10 per

[8] Similar to that of N. Campbell, Phil. Mag. **22,** 301 (1911), and **23,** 668 (1912). Other constant high-resistance units have been described by J. A. Van den Akker, reference 6., H. C. Rentschler and D. E. Henry, Rev. Sci. Inst. **3,** 91 (1932), and by H. L. White and E. A. Van Atta, Rev. Sci. Inst. **3,** 235 (1932). The writer is indebted to Dr. L. M. Mott-Smith for the loan of a shielded xylene resistor and condenser used in the preliminary part of this work.

second. The characteristics of this device seem to be similar to those of a recorder used by Van den Akker[9] for counting x-ray photoelectrons.

Wynn-Williams[10] has recently described an elegant arrangement for counting electric impulses at high rates. This might be used to a great advantage with any kind of Geiger counter, to increase the range of intensity of the phenomenon being measured. Instead of recording every impulse, each second, or fourth, or eighth, etc., is recorded, depending on the number of reducing units put in the circuit. A time resolving-power of about 1/1400 second is reported, so that the circuit should be capable of accurately counting *several hundred random impulses per second.* The limiting factor is the deionization time of the thyratron tubes used, not the inertia of any mechanical system. Corresponding to a count-reducing factor F, there is an uncertainty in the number of impulses, $\pm F/2$. But since F would rarely be made greater than 16, the error thus introduced is negligible, except for short or slow counts.

IV. The Field in the Counter

For supplying the potential across the counters, a high-voltage battery is considered preferable to a rectifier, in all respects except economy. A simple rectifier, similar to that of Van den Akker and Watson,[6] was used in most of the experimental work reported here. It consisted of a 1 mfd condenser charged by a small transformer and kenotron tube; voltage variation was obtained by altering the primary voltage of the transformer. However, a rectifier that draws its energy from a fluctuating source of power is very apt to have slow but troublesome fluctuations in its output potential. There is also some difficulty in accurately adjusting this potential, because the "soakage current" into the condenser makes the voltage drift slowly upward to its maximum value.

The voltage suitable for operating a counter depends on the shape, material, and state of the cathode surface, and on the kind and pressure of the gas in the tube. In the present work, the voltages ranged from 600 to 2000; they were usually 1000 to 1200 volts. The correct value for a given counter may be ascertained by causing faint light or γ-radiation to strike the cathode, while slowly raising the applied voltage until it crosses the threshold value. The threshold is the same for light, x-rays, and radioactive radiations.

It is important to determine and maintain the correct operating potential. The low-voltage edge of the threshold is quite sharp, but above this there is usually a *voltage plateau*, any part of which may be used. Impulses will be feeble or absent on the low-voltage side of the plateau; on the high-voltage side they become extended (mushy), and spontaneous discharges develop with increasing rapidity and finally merge into a steady discharge. The width of the plateau may be 10 to 100 volts; this depends on the gas, and on the counter cathode.

The range just described is one in which the counter *must* be operated,

[9] J. A. Van den Akker, Rev. Sci. Inst. **1,** 672 (1930).
[10] C. E. Wynn-Williams, Proc. Roy. Soc. **A136,** 312 (1932).

if its results are to have any significance. But the characteristics of operation are not constant within this range. In particular, the sensitivity of the counter usually increases as the applied potential increases toward the high-voltage side of the plateau, a gain as high as 100 percent sometimes being observed. The augmented count is believed to be a *bona fide* effect, if the potential is not too near the edge of the range. The explanation of this is not yet clear. Since the increase in field strength never exceeded 10 percent of its initial value, it is impossible to account for any large added sensitivity by merely supposing that the photoelectric work function of the surface was diminished by the increase of field, although this effect undoubtedly takes place to a certain extent in counters.[11] So if the quantum efficiency (ratio of the number of photoelectrons to the number of incident quanta) remains about the same across the voltage plateau, while the sensitivity of the counter increases, it is reasonable to suppose that the efficiency of the tube *for counting the photoelectrons liberated* is improved by the use of a more intense field. Two possible explanations of this appear. The first and more favorable one supposes that under normal conditions, a few of the photoelectrons cross the inter-electrode space without producing enough ionization by collision to give impulses, but that on accelerating them more strongly, a larger fraction will be counted. The second possibility is that higher fields may extend more deeply into the microscopic crevices in the cathode surface, thereby removing and counting photoelectrons that were liberated with almost zero velocity in them. In photoelectric counters we have a problem not met in other counters, or in vacuum photoelectric cells, namely the difficulty of collecting the very slow photoelectrons that are set free by light just shorter than the threshold wave-length; if these electrons are in a weak field, many will be turned back into the metal by collisions with gas molecules. In practice, it seems safest to use a potential slightly higher than the threshold value. The voltage plateau of the best visible-sensitive counters is so narrow that there is little choice, anyhow.

V. Preparation and Characteristics of Electrodes

Photoelectric quantum-counters have characteristics of behavior not less distinctive than those of photoelectric cells. The sensitivity, spectral distribution of response, and wave-length threshold of a counter depend not only on the material of its cathode, but on its previous history, its physical state, the presence of traces of foreign substances, and amount of previous ionic bombardment. The use of outgassed surfaces, or of surfaces in vacuum, is precluded by the principle of operation of the counters. Further, the success of those with alkali metal surfaces, or any other, is contingent upon the maintenance of very high resistance between electrodes.

Cathodes sensitive to ultraviolet light only

Experiments were first done with cathodes of zinc, cadmium, tin, copper, brass, silver, mercury, and magnesium. Under normal conditions, the sensi-

[11] On the basis of effects found by Lawrence and Linford, Ives, Schurmann, and Nottingham (see Hughes and DuBridge, *Photoelectric Phenomena*, p. 110).

tivities and dark-rates of these counters were very constant with time; the photoelectric thresholds, which were about the same that the metals show in ordinary photoelectric cells, were in the ultraviolet, except in the case of magnesium. Silver, mercury, magnesium, and tin electrodes were more sensitive within their ranges of response than were the others. Also, the average rate of spontaneous counting in darkness, or *dark-rate*, for the entire group was about 1.5 per minute, while cathodes of magnesium and very pure silver had dark-rates consistently less than 1 per minute. This fact, and the discovery that the dark-rate of copper could be reduced to a similarly low value by covering the entire electrode with a molecularly-thick coat of iodine, leads to the conclusion that the higher rates of uncoated copper, cadmium, tin, etc., are largely due to the emission of α-particles by the metals themselves.

Following the interesting work of Olpin,[12] concerning the effect of dyes on the photoelectric properties of alkali metals, many tests were made with counters having cadmium and zinc cathodes coated with extremely thin films of aniline dyes and photographic sensitizers.[13] The relation of the sensitivity to the film thickness makes it appear that the photoelectrons were mainly liberated from the metal and drawn through the film. The *sensitivity* of zinc electrodes was markedly increased by the addition of certain thicknesses of dyes, but the photoelectric threshold was always displaced toward the ultraviolet. This displacement is the reverse of that found by Olpin, in alkali photoelectric cells. Furthermore, the thickness and texture of the coating on the cathode seems to have more to do with the increase of sensitivity than did the color or composition of the dye. An explanation tentatively suggested is that the dye merely served as an insulating layer, which allowed the potential to be raised above the normal operating value, with a resulting increase in the sensitivity. Reasons for the rise of sensitivity with voltage have already been discussed. On this theory, one would account for the shift of photoelectric threshold by assuming that the slowest photoelectrons failed to penetrate the film. A similar effect was remarked in the case of thin oxide films on magnesium and copper: the sensitivity increased, but the threshold moved toward the ultraviolet. Fig. 4 shows the response of a slightly oxidized magnesium cathode to light from a carbon arc. Cadmium was found less sensitive to the effects of dyes than was zinc. Much additional work will be required to determine with certainty what the action of dyes on counter electrodes may be. In view of Olpin's results, it would be especially interesting to try dyed alkali metal cathodes.

The total sensitivity of a thin cathode in an air-filled counter was found to decay almost exponentially with time, falling to half its original value in 12 hours. The air was at 6 cm pressure. This decay is due to the formation of a film of oxide of increasing thickness. There was also a decrease in the dark-rate during the same period (28 hr.), but it was by a smaller percentage. How-

[12] A. R. Olpin, Phys. Rev. **36**, 251 (1930).

[13] Including: aesculin, alizarine, aniline black, anthracene, China-blue, Congo-red, cyanin, eosine, fluorescein, litmus, methylaniline violet, orthochromblau, picric acid, pinacyanol, pinaverdol, pinachromviolett, salicylic acid, uranin, and others.

ever, the sensitivity and dark-rate of a clean tin cathode, in nitrogen, were not perceptibly altered by standing $5\frac{1}{2}$ months.

If either electrode is coated with an insulating film of oil, grease or lacquer, the applied voltage can be raised far above the normal maximum, without starting a discharge. But once a discharge is started by the action of light or other radiation, it continues until the potential is removed. The break will then "heal" in an interval that varies from a small fraction of a second, in the case of a light oil, to nearly a minute, for a viscous grease. Under some conditions, the disruptions may begin and stop spontaneously; they then take place rythmically with a frequency that rises with the applied voltage, often to several hundred per second. This action superficially re-

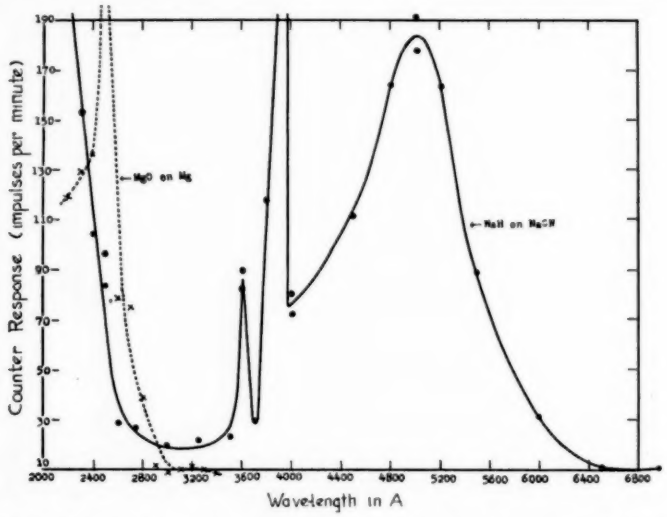

Fig. 4. Response of two counter electrodes to light from a carbon arc.

sembles that of an electrolytic interrupter. Fast rythmic discharges may sometimes take place only when light falls on the cathode. Under such conditions they might be mistaken for normal response; but their regularity shows that this is not the case.

A curious displacement of the photoelectric threshold of a tin electrode was accidentally brought about by strongly bombarding the surface with ionic nitrogen, in a nitrogen atmosphere. The counter showed greatly increased sensitivity and responded to light well into the visible region, for several minutes after treatment of the surface; it then returned to its initial state. This effect could be repeated an indefinitely large number of times. It is likely that the shift is due to the partial dislodgment of a compact gaseous layer from the electrode, in spite of the high pressure of the surrounding gas (7 cm). Another possibility is that a photosensitive but unstable compound is formed. Unfortunately, no other gases have yet been tried for the effect with tin, nor has nitrogen bombardment been tried on cathodes of other metals. The thresholds of silver and copper did not show any appreciable shift after strong and extended bombardment with ionic hydrogen, in a

hydrogen atmosphere. The large *permanent* shift of the threshold toward the red, effected by bombardment of some salts with hydrogen, is the subject of part of the next section.

Alkali metal cathodes

The advantages of alkali metal cathodes, arising from their high sensitivity and response to long wave-lengths, more than compensates for the difficulties met in preparing them. Even if it were possible to move the photoelectric thresholds of other metals into the visible region by means of dyes, it seems certain that the quantum efficiencies of such surfaces would be much inferior to those of alkali metals. The chief obstacle encountered is in finding a good way to introduce the latter into the tube as a deposit on the cathode. If sent in by distillation, the metal tends to spread over the interior surface of the glass. This results in diminished resistance that is fatal to the successful operation of the counter. A possible alternative is to coat the photoelectric material on the demountable cathode, while *outside* the counter, and then seal it into the counting tube. Naturally the air and moisture must be kept away from the surface during all processes, and this is not easy to do. However, two modifications of this second method have been devised and carried out by the writer, with very gratifying results.

The first process *consists in the formation of a hydride of the desired metal on the cathode, by reducing a salt with atomic hydrogen.* For example, a copper cathode, coated with a thick layer of fused sodium cyanide, was introduced into the counter; the tube was then exhausted and filled with dry hydrogen at a pressure of 7 centimeters of mercury. Next, a discharge of 15 to 100 microamperes was passed through the gas for 30 minutes, so that the cyanide was under strong bombardment with hydrogen ions. A reaction such as

$$NaCn+2H^{+}\rightarrow NaH+HCN, \text{ or } 2\ NaCn+2H^{+}\rightarrow NaH+2C+N_2$$

is believed to have taken place on the surface; the sensitivity of the counter was greatly increased, and its photoelectric threshold was permanently shifted from the ultraviolet to about 6400A. Choice of the cyanide for this purpose, in preference to another salt, was made on the basis of its low heat of formation; it seemed likely that such a salt could be most easily reduced. Fig. 4 shows the approximate distribution of the response of this counter to the light from a carbon arc. The curve was made with a quartz monochromator, and is uncorrected for the stray light that gets through the instrument. One may observe that the peak at 5000A does not coincide with any shown by sodium metal in an ordinary photoelectric cell. The question may justly be raised as to whether the response is really from sodium metal. The answer seems affirmative, for the high sensitivity and response to red light appear only after the ionic bombardment, and immediately vanish with the admission of any air into the tube. It is also well known that the spectral distribution of response of thin films depends greatly on the nature of the underlying surface, and on the previous ionic bombardment.[14] The dark-rate of

[14] See: A. L. Hughes and L. A. DuBridge, *Photoelectric Phenomena* (McGraw-Hill Book Co., Inc., 1932).

this counter subsided from 86 impulses per minute, just after preparation, to 2.95 per minute, a few hours later. (The results shown in Fig. 4 were obtained about a day after forming the surface.) The peaks at 3600A and 3900A are due to groups of lines in the spectrum of the arc used. Three other similar surfaces were prepared from sodium cyanide; the kind of surface on which the salt was used was found to be immaterial.

It should be mentioned that during the discharge used for sensitizing the cathode, an irregular film was always deposited on the wire anode. These films can, and must, be removed by electrically heating the wire to a bright glow for a few seconds.

Several attempts were made to produce potassium hydride surfaces from the cyanide by a process like that just described. These met with little success and were abandoned when it was found that excellent surfaces could be prepared from amalgams of the alkali metals.

The second process consists in the *formation of alkali hydrides by bombardment of amalgams with atomic hydrogen*. Two surfaces of this type were prepared with sodium, three with potassium, one with sodium-potassium, and one with caesium. The sodium counters made by this process were several times as sensitive as those previously prepared from the cyanide; but their sensitivity was far exceeded by the potassium ones. The latter were, in fact, the most sensitive counters for visible light that the writer has been able to prepare.

The technique for forming them was much like that with the cyanide. The demountable cathode, of heavy copper, was lightly coated with clean mercury and dipped into the amalgam, which was preserved under xylene.[15] While still coated with a protecting film of xylene, the electrode was sealed into the counting tube, from which the air was immediately swept out with dry hydrogen. Long pumping removed the xylene, after which fresh hydrogen was introduced to the proper pressure. A discharge was then passed between the electrodes, and the coating was evaporated from the wire, as before. The copper acted as an absorbent for excess mercury, which presently disappeared into the cathode. At the same time, the physical appearance of the surface changed: sodium and potassium ones became dull gray, while caesium took on a light golden luster. It is not known whether or not this was accompanied by the expected concentration of the alkali metal on the surface. The question hinges on determining whether the light metal sinks into the copper along with the mercury, or is filtered out at the surface. The final step was to evaporate the film that was incidentally deposited on the wire during the discharge. The counter was then ready for use.[16]

[15] Amalgams were prepared by electrolysis of salt solutions, using mercury cathodes. They were then washed with water and xylene. See: J. W. Mellor, *A Comprehensive Treatise on Inorganic and Theoretical Chemistry*, 4, 1010 (Longmans and Co., London).

[16] While preparing this paper, it has occurred to the writer that the use of mercury is superfluous. The technique suggested is to immerse the counter cathode in clean alkali metal, melted under an inert but volatile liquid, and make the transfer to the counter while a film of the liquid remains as a protective coating.

The photoelectric thresholds of the amalgam counters were found by means of filters to be roughly the same as for the alkali metals in photoelectric cells. Thus for sodium, the threshold was around 6000A, for potassium, 6500A, and for caesium, >7500A.[17] Sodium-potassium mainly showed the response properties of sodium, which predominated in the mixture used. Amalgams of potassium and sodium became granular at fairly high concentrations of the light metals, while the mixed amalgam remained fluid at similar concentrations. The latter was thus easier to apply to the electrode than that of the single metal.

Minimum rates of accidental counting for the several cathodes were as follows: sodium, 4.7 per minute; caesium, 5.8 per minute;[18] potassium, 2.3 *per second*. It is not known what part of the potassium count is due to β-particles from its radioactivity. This might, of course, be approximately calculated by measuring the amount of metal, thickness of film, and coefficient of absorption of the particles by the film. The writer believes that the major part of the count is due to other spurious causes, such as the evaporation of charged molecules, or a chemical change involving the emission of electrons or light. In support of this view, it may be mentioned that various other electrodes that were presumedly devoid of radioactive material showed high rates of accidental counting for short periods after their introduction into the counter, or after strong ionic bombardment. The duration of this high count could sometimes be controlled by the length or manner of treatment of the surface, and usually subsided within a period that varied from a few seconds to several hours after treatment.

Several cathodes coated with ammonium amalgam were also tried in the counter. But the ammonium always decomposed before it could be used, in spite of the fact that the time between its preparation and exposure as a photoelectric surface was less than two minutes.

A strontium amalgam counter was also prepared by a process like that used with the alkali metals. Its response was good for $\lambda < 4600$A, and could be detected at $\lambda \sim 7000$A. The sensitivity to light from an incandescent lamp was estimated to be about one-sixth that of the sodium counters. The sensitivity was neither improved, nor was the spectral distribution altered, by directing a stream of hydrogen ions against the cathode. Several barium amalgam surfaces were also tried, but were not successful. The concentration of barium metal was initially small, so it was probably destroyed by combination before it could be tried in the counter.

Non-metallic cathodes

Thin films of numerous non-metallic substances have been tried on counter electrodes, in addition to the dyes previously mentioned. Both liquids and solids were used; the latter were usually more easily handled and more constant in behavior. A few of the surfaces that seemed especially in-

[17] Found with filters. See: A. L. Hughes and L. A. DuBridge, reference 14, p. 457–9.

[18] The electrodes of the Cs counter were not well centered, so the sensitivity and dark-rate are not comparable with those of other counters.

teresting will be mentioned here. Generally speaking, if the film is exceedingly thin, the photoelectric behavior is that of the underlying surface; if it is thick, the characteristics are those of the material of the film itself; intermediate thicknesses lead to a variety of effects.

Iodine was deposited from solution on cathodes of copper, silver, and selenium. (The size of crystals and thickness of the deposit can be reduced at will by heating the electrode in a flame.) The photoelectric threshold of a molecularly thick deposit was between 2300 and 3000A, in air or hydrogen, which were the only gases used. It was observed that the deposition of a thick film on a particular copper electrode reduced the dark-rate from about 1.5 to 0.9 per minute; also, that the behavior of the counter was the same after bombardment of the iodine with atomic hydrogen, provided that the anode wire was subsequently cleaned by heating. The distinctive feature of the iodine counters was their extremely good sensitivity. For example, the response to light from a flame was about twice as high from iodine-coated copper as from clean copper, in spite of the fact that the latter responds to longer wave-lengths. After strong heating in contact with iodine, a copper electrode became coated with a thin film of light-green material, presumedly an iodide. The dark-rate of the counter then increased to 90 per minute, and remained practically constant even after extended bombardment with atomic hydrogen!

Selenium, deposited as a thick coat on copper, by evaporation, also had a threshold between 2300 and 3000A; its dark-rate was 57 per minute. The threshold was shifted to about 4100A by hydrogen bombardment, but returned to its former value when air was admitted to the tube, about 15 minutes later. The operating potential was also made more critical by the discharge. The reason for the change of threshold is not known, but it seems reasonable to suppose that the hydrogen bombardment produced a surface film of a compound whose photoelectric threshold was nearer the red.

The counter having the highest sensitivity to ultraviolet light of any yet prepared, had a non-metallic cathode. It was made by coating copper with a thick film of selenium, depositing on this a very thin film of iodine, subjecting the composite surface to strong bombardment with atomic hydrogen, and removing the film from the anode wire by heating. The photoelectric threshold was again between 2300 and 3000A, and the dark-rate was about 1 per second. Light from a small constant flame, which increased the count from a good tin cathode by 29 impulses per minute, increased that from the Se-I one by 460 per minute. So the sensitivity of the Se-I was about 15 times that of tin, to the source of light used! A possibility that should not be overlooked in the case of this and similar electrodes, is that *the emission of photoelectrons may merely be an electrical by-product of a photochemical change.* One seems obliged to look for the explanation of the high rates of spontaneous counting, sometimes got from electrodes in the relative absence of light, or of radioactive material, by finding out whether physical or chemical changes are taking place that are accompanied by the ejection of charged particles or the emission of photoelectrically active light.

No substance that was coated on the cathode of the counter, and that could be retained there without disturbing the necessary electrical characteristics of the device, failed to show photoelectric response. Thus barium chloride, deposited from solution, responded in the ultraviolet, but also showed very weak response to wave-lengths as long as 7200A. After bombardment, the sensitivity to the red was somewhat improved. Similar behavior was shown by a film of red cuprous oxide on copper; it showed strong response to the ultraviolet and very weak response to $\lambda \sim 7200$A. The absence of this red-response was found a convenient means of testing the "photoelectric cleanness" of the copper surface.

The wire anodes

The anode wires should be very smooth. For successful operation of any counter, a high symmetrical field must be maintained between electrodes, and this is more disturbed by microscopic irregularities on the anodes than by much larger ones on the cathodes. In other kinds of tube counters, some investigators[3,4] have used oxide-coated tungsten wires, while others[9,19] used bare ones. The oxide serves as a partial insulator which allows the operating potential across the tube to be raised above its normal value. The writer has found that the oxide film is, in general, more troublesome than desirable, because of its tendency to become disrupted in spots; even one such break is fatal to the success of the counter. Moreover, in visible-sensitive counters, and some others, it is necessary to remove other kinds of films from the wires by heating them to incandescence (usually in hydrogen), and this excludes the use of the oxide. Platinum and tungsten wires were found most convenient; they may be heated to high temperatures, and will withstand the corrosive action of bombardment with alkali-metal ions. The size of the wire determines the operating potential,[20] but any small diameter seems to serve equally well.

VI. Tests and Measurements Made

Inverse square law

Reliable measurements of light intensity cannot be made with any device, unless the rates of its response to a given source obey the inverse square law of variation with distance. To test this, a small alcohol lamp that burned at a constant rate was set at 250 and 500 cm from a tin-cathode counter; resulting increases in the rate were respectively 68.4 and 17.4 impulses per minute. The deviation of these results from the inverse square relation, (1.8 percent), is within the limits of statistical error and fluctuation of the lamp Pending tests with a better source, we may conclude that the inverse square law is applicable, at least to a good approximation. Incidentally, the maximum permissible counting rate for any counter and recorder may be taken as that at which the departure from the inverse square relation, due to

[19] H. Kniekamp, Phys. Zeits. **30**, 237 (1929), and L. F. Curtiss, Bur. Stds. Jour. Res. **4**, 601 (1930).

[20] D. Cooksey and M. C. Henderson, Bull. Amer. Phys. Soc., June 9, 1932, give an empirical formula relating field, applied voltage, and radii of the electrodes.

coincidence of successive impulses, becomes as large as the greatest permissible error. This rate is the reciprocal of the time resolving-power and can easily be found by experiment.

Ultraviolet light from different sources

Application of the photoelectric counter to intensity measurements is illustrated in Table I, which gives the relative total response of a tin-cathode counter to ultraviolet light from four sources of widely different intensities. The wave-lengths actuating the device lie approximately between 1950 and 3500A. The dark-rate, 1.7 per minute, was deducted from the rates recorded Values in the last column were reduced to a comparable basis by use of the inverse square law, and are proportional to the ultraviolet luminosities of the several sources. The extreme feebleness of the ultraviolet from all but the quartz mercury lamp is made evident by these data.

TABLE I. *Ultraviolet light intensity from various sources.*

Source	Distance (meters)	Cathode area exposed	Counting rate (No. per minute)	Computed rates for source at 1 meter and electrode area of 1 cm², per min.
Mercury arc[a]	47.0	0.000855 cm²	48.0	120,000,000.
Bunsen flame[b]	4.0	0.63 "	73.9	188.
Alcohol lamp[c]	4.0	0.63 "	18.7	47.5
Electric lamp[d]	4.0	0.63 "	7.5	19.

[a] Cooper-Hewitt quartz lamp; 4 amp., 30 volts, d.c.
[b] Meeker burner; 0.024 cu. ft. methane per minute, mixed with air.
[c] Burned 9.3 g of denatured ethyl alcohol per hour.
[d] 1000-watt projection lamp; 8.8 amp., 115 volts, d.c.

The ultraviolet from the slow oxidation of a small piece of white phosphorus was easily detected; but no "mitogenetic rays" were found from any root-tips or bacteria cultures, nor was any radiation that was capable of operating the counter detected from the slow oxidation of iron or aluminum, or from mechanically distorted crystals or other materials.

Different gases

Air, hydrogen, oxygen, nitrogen, and methane were used successfully in a counter with a tin cathode. For a given pressure, the operating potential was found to be higher for gases with high ionization potentials, than for others. Operation was most successful with the gas of highest ionization potential used, namely nitrogen; the voltage plateau was widest, so that the potential was least critical of adjustment. In this connection, one recalls the very satisfactory use of helium in other tube counters, by Bearden and Haines,[21] who also found the gamma-ray sensitivity of these to be somewhat greater than that of similar air-filled counters. Their observations seem significantly related to the fact that helium has the highest (minimum) ionization potential of any ordinary gas.

[21] J. A. Bearden and C. L. Haines, Bull. Amer. Phys. Soc., April 12, 1932.

The question has been raised: Why does the discharge of a Geiger-Müller counter *stop*, once it has been set going by an ion? The explanation proposed here is this: Before the discharge begins, there is a large field between the counter electrodes; this is sufficient to give the initial ion enough velocity to ionize the gas, hence to start a general discharge in the tube. During the course of the discharge, the voltage across the tube falls below the critical value for the gas used, and no new ions are generated. The discharge then declines and the residual ions are swept out of the field with sufficient quickness that none remain when the full potential has become reestablished across the tube. The fall of voltage during the discharge is Ri, where R is the external resistance, and i is the maximum current that flows through the tube. A possible inference from the work with different gases is that the use of a gas with a high ionization potential is desirable because it assists in quenching the discharges.

Cellophane window

The short wave-length limit of response of photoelectric counters is determined by the material of their windows; the cut-off of the counters used in most of the work described here was about 1950A. In order to get transparency to shorter wave-lengths, the quartz was replaced with a sheet of cellophane, 0.02 mm thick, supported on a thin metal plate that was drilled to half its area with 0.68 mm holes. The limit for this window should be about 900A, but the air between it and the source probably raised the limit to about 1450A.[22] In work requiring the measurement of light as short as 900A, the source might be mounted in a vacuum chamber of which the thin counter window formed one side.

VII. Modified Counters for Other Uses

The success of the photoelectric counters has led to their use for other purposes. Three slightly modified types will be briefly described here. The first is a convenient counter for α-particles, especially intended for measuring the strengths of sources; the second is a counter for detecting and measuring faint x-rays and γ-rays; the third is a reversed-field counter which may be useful for measuring intensities of spectral lines.

Alpha-particle counter

This adaptation was made by replacing the quartz window with one of very thin mica, 1.05 mm in diameter. The mica reduced the range of the α-particles from polonium by 1.73 cm, in air, so that its thickness must have been approximately 0.007 mm. In order to have a low spontaneous count and to avoid response to visible light, an iodine-coated copper cathode was used; its dark-rate, 0.7 per minute, was negligibly small.

Fig. 5, A, and B, illustrates the use of the counter with a polonium source about 0.0086 cm² in area; C was made with a source 2 cm² in area. The polonium was electrolytically deposited on platinum foil; different parts of the deposit were found to be of similar activity. Distances shown on the

[22] A. L. Hughes and L. A. DuBridge, *Photoelectric Phenomena*, p. 458.

curves are subject to a lateral displacement of about 0.5 mm, due to the uncertainty of the initial position of the micrometer frame that carried the source.

Other tests with the α-ray counter led to favorable results. The first showed that the voltage plateau was wider than those of most photoelectric counters, so that small fluctuations of the potential applied to the tube did not alter the count from a constant source. A second test showed that variation of the gas pressure in the counting tube had no detectable effect on the

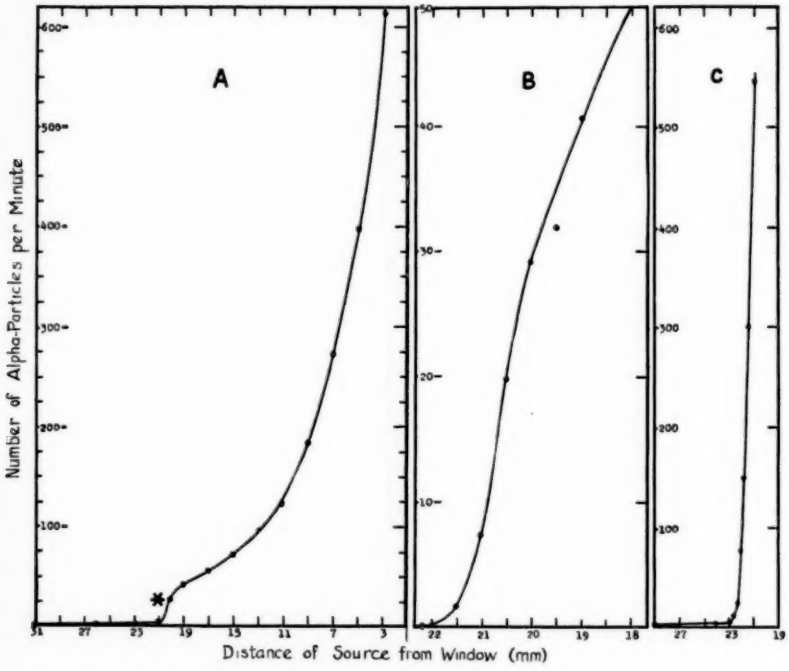

Fig. 5. Curves illustrating use of the α-particle counter with a polonium source: A, count from a plane source of small area; B, starred portion of A, on a larger scale; C, count from a plane source of large area.

range of the α-particles, as determined with the counter. It seems that if the particle gets through the window, it is almost certain to produce enough ions to start an impulse. A third test indicated the order of accuracy to be expected with short observations. Table II contains the data of this test.

TABLE II. *Experiments with alpha-rays.*

Time in minutes	Total number of α-particles	Number per minute	Percent deviation from the mean rate
10	1431	143.1	−0.56
10	1441	144.1	+0.14
10	1450	145.0	+1.10
10	1403	140.3	−2.50
10	1475	147.5	+2.50
10	1436	143.6	−0.21
		Mean: 143.9	

The statistical error of the average count (1.77 percent) is larger than the mean of the absolute values of the observed deviations from the mean rate (1.17 percent).

X-ray and gamma-ray counters

Photoelectric counters may be used for detecting and measuring faint x-rays and γ-rays, without modification of form. A series of experiments, described in a previous note,[23] were done with a tin-cathode counter used in that capacity. The sensitivity of the apparatus was calculated for each arrangement, in terms of the minimum amount of radium, in equilibrium with its decay products, that could be detected by its γ-ray emission.

Shielding against stray radiation is facilitated by the smallness of the electrodes; the small external dimensions of the detector also allow it to be brought close to the source. It is, of course, very desirable to use a cathode with a low dark-rate, such as that used in the α-particle counter. Selection of the material and aperture of the window depends on the purpose for which the counter is to be employed.

Wire-cathode counters

The wire electrode may be used as the photoelectric element of the counter by reversing the direction of the electric field. Some interesting results were obtained with a cathode of tungsten wire, in the presence of vapors of certain organic liquids. These were coated on the cylinder electrode, or thinly on the wire itself. Ethyl chloride, ethyl alcohol, ether, methyl alcohol, and especially nitrobenzene, increased the sensitivity for ultraviolet light by a factor of 1.5 to 3. The effect seems to be due to the presence of *vapor* of the substance in the vicinity of the wire, or on its surface. Sensitizing agents did not appreciably increase the sensitivity of the counter for γ-rays, so their action appears to be a reduction of the photoelectric work function of the surface.

Diethyl-aniline vapor caused an unusually great increase, estimated to be 25 times the original sensitivity! This occurred when the liquid was coated on either electrode, only a trace being required for the purpose. This counter maintained its high sensitivity and low dark-rate for 10 hours; at that time it was dismantled. After treatment, the photoelectric threshold was roughly 3000A, but the matter of a shift due to introduction of the vapor was not examined. It was found that this sensitizer also extended the range of air pressures at which the tube could be operated successfully. The characteristics were about the same at 14 cm as at 0.5 cm, with suitable voltage adjustment.

Water vapor increased the photoelectric sensitivity of the wire nearly as much as diethyl-aniline did. But the water had to be introduced in a much larger quantity, so that it presently spread over the interior of the tube, decreasing the resistance and greatly increasing the rate of spurious counting

These incomplete experiments with reversed fields were among the first tried with photoelectric counters, so that good technique and auxiliary ap-

[23] G. L. Locher, Phys. Rev. **40**, 884 (1932).

paratus were not yet developed. But the results suffice to show that very high sensitivity may be reached with counters having sensitized wire cathodes. Obvious extensions of the work would include the use of thoriated tungsten and oxide-coated wires, and quantitative tests of the sensitizing effects of many other substances, both with these counters and normal photoelectric ones. Organic liquids have not yet been tried on the cathodes of the latter.

Since the wire-cathode counters have active surfaces that are very narrow, they might easily be applied to the measurement of faint spectral lines.

VIII. Discussion

Sensitivity for counting electrons

We may establish certain criteria for determining the useful electron-counting sensitivity of a photoelectric counter, without knowing the magnitude of the quantum efficiency of its photoelectric surface. The total useful sensitivity is taken as the intensity of light that causes the smallest increment in the counting rate that can be detected with certainty. An increment is regarded as "detected with certainty" when it exceeds the statistical error of the count by a pre-determined amount. It is further stipulated that the results be capable of reproduction, within pre-assigned limits of error, under identical experimental conditions.

The useful sensitivity evidently improves with extension of the time of the observation, for the relative statistical error of the count diminishes as the number of electrons recorded increases. It will also be best for a counter with a small dark-rate, for reasons set forth in section I of this paper.

Considerations of the limiting sensitivity are only important when the count is small, either due to shortness of the interval over which the observation is made, or to extreme feebleness of the radiation measured. But since the most important applications of photoelectric counters are apt to be for measurement of faint radiation, it is desirable to consider the factors that limit their sensitivity for counting electrons, in addition to the limitation imposed by the quantum efficiency of the photoelectric surface.

As an illustrative example, consider a typical counter for which the dark-rate is 1.50 ± 0.106 per minute, as determined by a one-hour observation. When exposed to a particular faint source of light for an hour, suppose the total count is 120. Of these impulses, 90 ± 6.36 are due to accidental causes, while 30 ± 3.67 result from the light. Under such conditions, it is evidently possible to detect less than one-half photoelectron per minute, with certainty. But if the same apparatus is run for only 5 minutes, and if the total count is 10, the corresponding distribution would be 7.5 ± 1.84 due to accidental causes, and 2.5 ± 1.06 due to the light. And if we take the minus sign with the latter rate, the increment due to the light is smaller than the statistical fluctuation of the dark-rate, so the light could not be detected with certainty, in 5 minutes. Similarly, if the counter had a dark-rate of 60 ± 0.67 per minute (instead of 1.50 ± 0.106), an increase of 30 ± 3.67 impulses per hour could not be detected by means of a 1-hour observation.

The foregoing discussion applies as well to counters for measuring other feeble ionic emissions, as to photoelectric ones. Moreover, S. Smith[24] has pointed out that very similar conditions obtain in the measurement of very faint light with a photoelectric cell and electrometer, when the dark-current of the cell, (>30 electrons per second) is comparable with the additional current due to the light.

In cases where the light to be measured can be concentrated on the counter cathode, the total useful sensitivity increases as the size of the cathode diminishes. But if the light cannot be conveniently concentrated, an important question arises: Does the useful sensitivity increase with the size of the cathode, and if so, within what limits? To answer this, one must recall that both the accidental count and the number of desirable photoelectrons increase with the area of the electrode, and that there is an upper limit to the speed of counting, imposed by the time required by the counter and recording apparatus to recover from each previous impulse (i.e., by the time resolving-power). The matter can probably be best settled by experiment.

Limitations of photoelectric counters

The following are believed to be the four chief limitations of photoelectric counters, which affect their use for quantitative measurement. The relative significance of each obviously depends on the specific application of the counter.

(a) The maximum intensity of light that can be measured is restricted by the speed at which the photoelectrons can be counted. Pending further developments of impulse recorders, the safe counting speed can hardly exceed 300 or 400 electrons per second; yet photocurrents of such low orders (5×10^{-17} ampere) are measurable only with great difficulty in other types of instrument. Higher intensities can, of course, be measured with the counters by using smaller cathodes, or by diminishing the area exposed, until the rate comes within the permissible limit.

(b) A very constant source of high potential is required. Otherwise, the sensitivity is apt to vary as the potential moves across the voltage plateau. The permissible variation depends on the requirements of the work, and on the width and slope of the plateau of the counter used.

(c) Accurate measurements of very small intensities require extended observations. This characteristic is shared in common with all other devices for measuring phenomena that are subject to statistical fluctuations.

(d) The spectral distribution of response may change as the counter is used. The existence and magnitude of this effect depend on the kind of gas used, the kind of cathode surface, and the intensity of ionic bombardment of the cathode. Gas-filled photoelectric cells sometimes show similar changes.[25]

It is believed that photoelectric counters will not only provide powerful means of measuring faint radiation, but also of studying a variety of photoelectric phenomena, such as the photoelectric properties of non-metals,

[24] S. Smith, manuscript not yet published.

[25] N. R. Campbell and D. Ritchie, *Photoelectric Cells* (Sir Isaac Pitman and Sons, 1929).

gases, and compounds, the feeble electron emission of substances illuminated with light of very long wave-lengths, and the effects of sensitizers on photo-electric surfaces. They should also make possible investigations of ionic and light emissions accompanying physical and chemical changes and biological processes.[26]

The author wishes to thank Dr. Sinclair Smith for his valuable assistance in the early development of the counters, and for making available the facilities of the Mt. Wilson Observatory Laboratories, where the preliminary work was done. Later development was carried out at the Rice Institute, through the kindness of Professor H. A. Wilson, whose council is gratefully acknowledged. Dr. W. F. G. Swann has very kindly read the manuscript of this paper, and has made helpful suggestions concerning its contents.

[26] One form of the apparatus described in this paper was exhibited at the A.A.A.S. meeting, Dec. 28–31, 1931.

Non-Existence of Ion Mobility Spectrum in Air

By ROBERT N. VARNEY
University of California, Berkeley

(Received July 19, 1932)

A modified form of the Rutherford a.c. method of measuring ion speeds, as suggested by Loeb and Bradbury, has been used to investigate the range of speeds with which negative ions in air travel. It differs in that the ions are produced only during a small fraction of the a.c. period, this being accomplished by interrupting the ultraviolet light beam with a rotating shutter. The theoretical curves of $d(i/i_0)/dV$ against V assuming both the presence and the absence of an ion spectrum are given. The experimental curves for ions 0.03 to 0.006 sec. old agree closely with the theoretical curves for a spectrum, but it is shown that on application of a diffusion correction the spectrum in clean dry air reduces to negligible width; the presence of ozone in considerable amounts, however, produces a spectrum extending 10 to 12 percent on each side of the mean mobility.

INTRODUCTION

THE question of whether normal ions in air travel with a unique speed or with speeds spread over a range or spectrum of values has been completely discussed and all experimental evidence to date on both sides has been analyzed in a recent paper by Loeb and Bradbury.[1] They suggested that, if in the Rutherford a.c. method of measuring mobilities a shutter in conjunction with the commutator which produced the square-wave a.c. were used to interrupt periodically the ultraviolet light beam, a higher resolving power might be obtained for the a.c. method. The principle has been used by Fontell[2] and by Bradbury,[3] both, however, using x-ray ionization, and by Hamshere[4] using α-ray ionization. The suggested photoelectric method promised to be an improvement over the first of these because the exact distance travelled by the ions could be more exactly determined; and over the second, because it was hoped that ultraviolet light would produce less active substances in the air than either x-rays or α-rays.

APPARATUS

The apparatus consisted of a metal ionization chamber provided with plane plates, the upper being brass and the lower speculum metal. A quartz window permitted the light from a quartz-mercury arc to fall on the lower plate. The beam of light passed first, however, through a window of the rotating shutter. The air from the room was slowly passed over P_2O_5 and $CaCl_2$, and through a double trap immersed in liquid air.

[1] L. B. Loeb and N. E. Bradbury, Phys. Rev. **38**, 1716 (1931).
[2] N. Fontell, Commen. Physico Mathematicae Soc. Scientiarium Fennica **23**, 7 (1931).
[3] N. E. Bradbury, Phys. Rev. **40**, 508 (1932).
[4] J. L. Hamshere, Proc. Camb. Phil. Soc. **25**, 205 (1929); Proc. Roy. Soc. **A127**, 298 (1930).

The shutter served at the same time as a commutator to provide a square-wave, alternating potential on the lower plate. The shutter, which was variable in size, allowed the speculum plate to be illuminated from the time the negative potential was applied up to any desired time before that at which the potential reversed. Ions thus produced during the negative part of the cycle travelled upward either until they reached the upper plate or until the potential was reversed, when they were drawn back again to the bottom plate. (A slight positive bias insured complete sweeping out of the ions from the field; see Fig. 1).

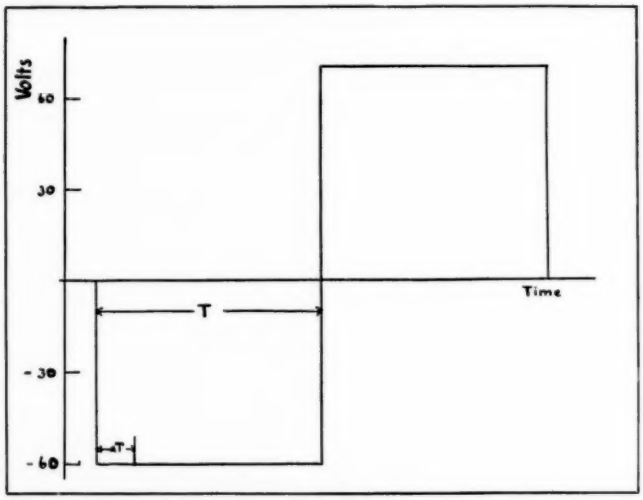

Fig. 1. Diagram showing the characteristics of the square-wave a.c. with the positive bias and the relative magnitudes of T and αT indicated.

Procedure

The following method was used to take and to reduce the results. (1) Electrometer deflections for various voltages applied to the lower plate were taken with the shutter-commutator moving. These deflections are called i. The electrometer could be read to about 0.2 percent of its average deflection, and average reading could be repeated to ± 0.2 percent. The voltmeter could be read to a little better than ± 0.10 volts.

When a smooth curve of i against V was drawn, the curve usually passed directly through all but one or two points. If more than two points deviated noticeably in any one curve, the whole curve was discarded as erratic.

(2) Similar deflections were obtained but with the shutter-commutator stationary, giving the i_0 readings. These gave greater difficulty because of the relatively short time necessary to produce the deflection. A straight line was drawn through the data points and the values of i_0 taken from it. From the work of Bradbury[5] on the photoelectric current in gases, it appears that over ranges of 30 volts or less the use of a straight line is permissible. The probable error on this line was around one-half percent.

[5] N. E. Bradbury, Phys. Rev. **40**, 980 (1932).

(3) The ratio of i to i_0 was then plotted against voltage. Note that i values have not been smoothed. Table I shows a typical set of data. The probable error of points on this curve with respect to the curve lies between ± 0.05 volts and ± 0.02 volts (see Fig. 2).

TABLE I. *Typical set of data for* i/i_0.

V (volts)	i/i_0	V (volts)	i/i_0	V (volts)	i/i_0	V (volts)	i/i_0
150	0.0407	134.5	0.0290	124.84	0.0054	114.9	0.0000
146.75	0.0406	132.2	0.0230	122.8	0.0029	112.9	0.0000
142.75	0.0399	130.5	0.01865	120.8	0.00136		
138.33	0.0363	128.5	0.0128	128.8	0.00039		
136.0	0.0325	126.67	0.00855	116.9	0		

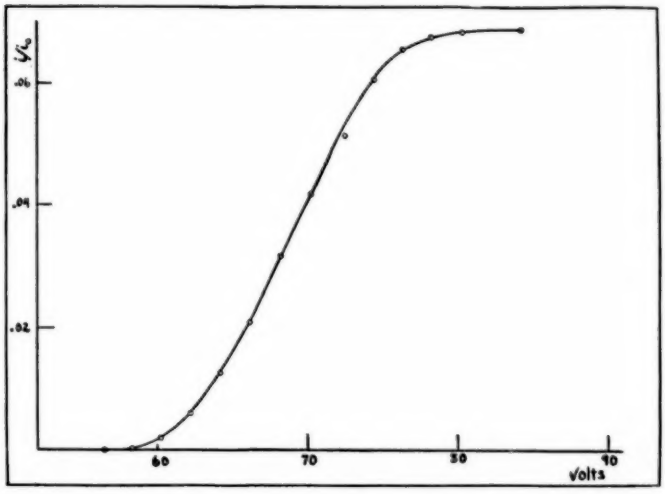

Fig. 2. Experimental curve of i/i_0.

(4) It was desired to plot $d(i/i_0)/dV$ against V, i.e., to plot the derivative curve. It is a well-known fact that integration smooths out while differentiation accentuates discontinuities and irregularities in a curve. In this case, theoretical considerations given below led the writer to believe that the actual discontinuities occurred in the second derivative curve. If so, they would be shown much more sharply in the first derivative curve than in the original curve, a break in the slope appearing in the former case with only an inflexion or hardly noticeable increase in the rate of curvature in the latter case.

Differentiation was performed by taking the slope at various points with a straight edge. An important check was made by placing the straight edge successively through every two adjacent data points and using this for the slope at the mean of the two, i.e., finite differences were used. As a final check, the i/i_0 curve was completely redrawn and redifferentiated in several cases to check against possible personal errors. The deviations were well within the limits claimed for the method.

The probable error in determining the derivative curve is between ± 0.07 volts and ± 0.10 volts. Adding to this the probable errors in reading all instruments, the resulting probable error is between ± 0.15 volts and ± 0.20 volts. The effect of this on the mobilities found is discussed in the conclusion.

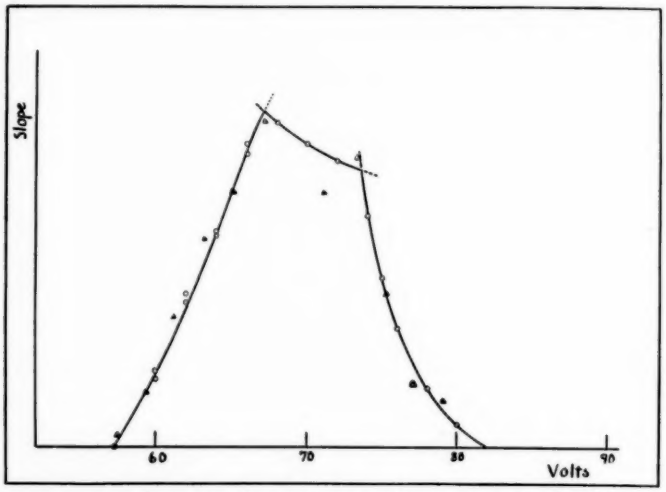

Fig. 3. Curve showing slope of each point of the i/i_0 curve in Fig. 2. This is an experimental result of plotting $d(i/i_0)/dV$ against V and shows the two zeros and the two break points distinctly. The triangles are finite difference points, and the double set of circles come from two different drawings of the i/i_0 curve.

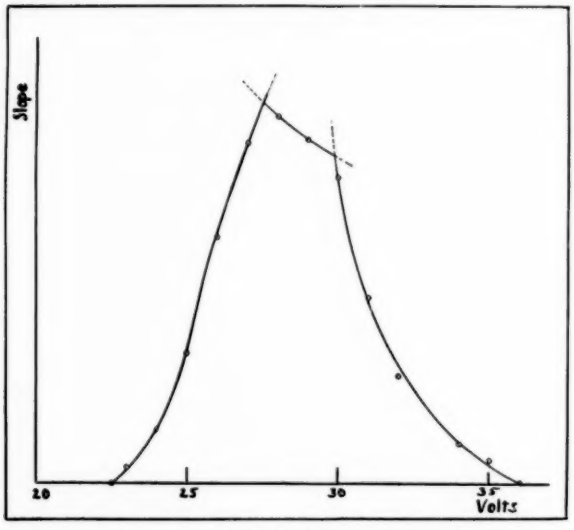

Fig. 4. Another experimental curve of $d(i/i_0)/dV$ against V similar to Fig. 3 but taken with a slower shutter speed.

It is important to notice that while an inflexion point in a curve may only be found by attempting to discover the point at which the curve crosses its tangent, the same point in the first derivative curve may be found as the intersection of two smooth curves, that is, in this case, by the use of five or

more ordinary points instead of a single critical point. Since theory indicates a break point and since experiment gives two curves approaching each other at a sharp angle and showing an apparent point of intersection to an accuracy of ± 0.20 volts at worst, the question of whether or not such a single point actually exists in the data becomes of no interest. Just what its disappearance would mean is unknown, but it certainly would not affect the discussion of the existence or non-existence of an ion mobility spectrum.

Two break points were found in each curve, but only the sharper one, occurring at an inflexion point in the i/i_0 curve, was used (see Figs. 3 and 4).

(5) The determination of the limits of the spectrum from the derivative curves and the corrections for diffiusion are discussed at a later point.

Significance of the Results

Loeb and Bradbury[1] have worked out the essentials of the theory of the method. What happens when the shutter closes and what the derivative curve would be, was not considered by them.

Taking k_1 and k_2 as the highest and lowest mobilities, respectively, in an assumed ion spectrum; V as the field strength; d as the plate separation; T the half period of the a.c.; and αT the length of time the shutter is open; their work gives directly

$$i/i_0 = [1/V(k_1 - k_2)T](Vk_1T - d - d \log (k_1VT/d)) \tag{1}$$

holding over the region $V=d/k_1T$ to $V=d/[k_2T$ and

$$i/i_0 = 1 - [d/V(k_1 - k_2)T] \log (k_1/k_2) \tag{2}$$

holding from $V=d/k_2T$ on indefinitely.

When the shutter is used, it can be shown that Eq. (2) ceases to hold at $V=[d/k_1(T-\alpha T)]$ and that a new equation

$$\frac{i}{i_0} = 1 - \frac{k_1(T - \alpha T)}{(k_1 - k_2)T} + \frac{d}{V(k_1 - k_2)T}\left(1 + \log \frac{Vk_2[T - \alpha T]}{d}\right) \tag{3}$$

holds over the region $V=d/[k_1(T-\alpha T)]$ to $V=d/[k_2(T-\alpha T)]$.

On differentiating Eqs. (1), (2), and (3) with respect to V, the required result is obtained;

$$\frac{d(i/i_0)}{dV} = \frac{d}{V^2(k_1 - k_2)T} \log \frac{k_1VT}{d} \tag{4}$$

$$\frac{d(i/i_0)}{dV} = \frac{d}{V^2(k_1 - k_2)T} \log \frac{k_1}{k_2} \tag{5}$$

$$\frac{d(i/i_0)}{dV} = -\frac{d}{V^2(k_1 - k_2)T} \log \frac{Vk_2(T - \alpha T)}{d}. \tag{6}$$

Eqs. (4), (5), and (6) hold respectively over the same regions as Eqs. (1), (2), and (3). Fig. 5 represents a theoretical curve for a spectrum of negative ions having mobilities between 1.6 and 2.2 cm/sec. per volt/cm, neglecting any effect of diffusion.

The shape of the curves is not of so much interest as the voltages of the zeros and break points. As the shutter begins to open, the lower zero point at a voltage $V_0=d/k_1T$, and the first break point at $V_1=d/k_2T$, are obtained. Similarly, when the shutter closes, the second break point at $V_2=d/k_1(T-\alpha T)$ and the upper zero at $V_3=d/k_2(T-\alpha T)$ appear.

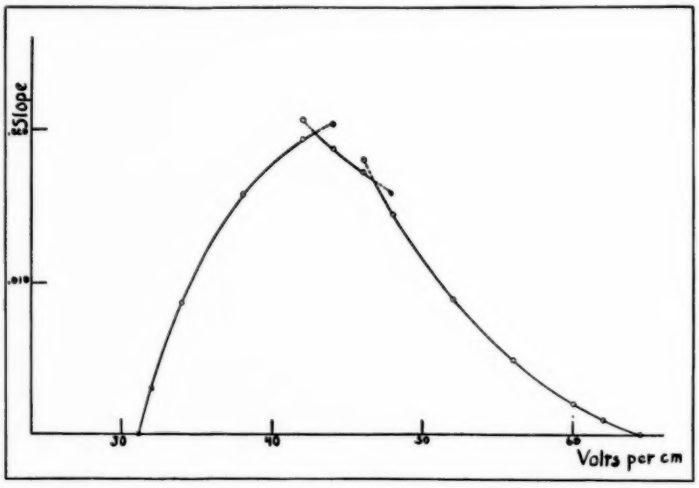

Fig. 5. Graph of the theoretical values of $d(i/i_0)$ with the following assumptions: $k_1=2.2$, $k_2=1.6$, shutter size, $\alpha T=T/3$, $T=0.0292$ sec., no diffusion. This is a graph of Eqs. (4), (5), and (6).

In obtaining Eqs. (1), (2), and (3), it was assumed that the mobilities were spread uniformly over the region bounded by k_1 and k_2. The spread in any case would undoubtedly not be uniform, but this would only change the shape of the curves without altering either the positions of the break points or of the zero points. Furthermore, it would alter the equation of the middle curve only by changing its constant coefficient.

Two things are apparent from the curve: (1) If there is a unique mobility, i.e., *no spectrum at all*, the lower break point will occur at the same voltage as the lower zero, and the upper break point will occur at the same voltage as the upper zero. The curves represented by Eqs. (4) and (6) will then become vertical straight lines, (see Fig. 6). This corresponds to saying that the i/i_0 curve will have no asymptotic feet. (2) At any constant speed the smaller the shutter is made the closer together will the two break points lie. Care must be taken not to make the shutter too small for it is possible to eliminate completely the middle curve, represented by Eq. (5), thus giving only one break point which has no significance with respect to the limits of the mobility spectrum.

One further point of great importance is the diffusion of the ions. The effect of diffusion on the curve will be to yield an apparent mobility spectrum, i.e., asymptotic feet on the i/i_0 curve and therefore a derivative curve like Fig. 5 rather than Fig. 6.

The chance that a molecule will move by diffusion in a time t from its position to any point between two parallel planes dx apart and at a normal distance x away, is given by[6,7]

$$[1/(4\pi Dt)^{1/2}]e^{-x^2/4Dt}dx$$

where D is the coefficient of diffusion and is given by $D=0.0236k$.[8]

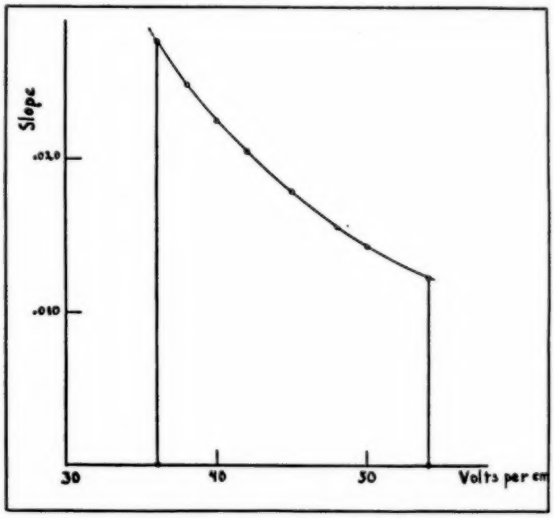

Fig. 6. This curve is represented by the equation $d(i/i_0)/dV=V_0/V^2$, and it is computed on the assumption that there is no mobility spectrum and no diffusion. The other conditions are the same as for Fig. 5.

In order, therefore, to get the number of ions which will diffuse from their non-diffused positions in a band of width αTVk to a distance equal to or greater than the remaining plate distance, the given probability must be integrated with respect to x between the limits $d-Vkt$ and infinity, and with respect to t from $T-\alpha T$ to T. This result must be multiplied by N_0 and divided by the elapsed time αT.

$$N=\frac{N_0}{\alpha T}\int_{T-\alpha T}^{T}\int_{d-Vkt}^{\infty}\frac{1}{(4\pi Dt)^{1/2}}e^{-x^2/4Dt}dxdt.$$

The integrations were performed with the aid of a table of values of the probability integral and by a standard method of approximation (Simpson's rule).

[6] J. Zeleny, Phys. Rev. **34**, 310 (1929).
[7] A. Einstein, Ann. d. Physik **17**, 558 (1905).
[8] L. B. Loeb, *The Kinetic Theory of Gases*, p. 451. McGraw-Hill, N. Y., 1927.

The minimum value of N/N_0, that could be detected by the apparatus was measured, and the value of x, where x is the distance of the upper edge of the undiffused band of ions from the upper plate, was calculated for this N/N_0. In other words, the distance was found to which the minimum detectable number of ions would diffuse. Now ions moved by diffusion as well as by electric forces may be regarded in exactly the same light as ions moving with an extended mobility spectrum. The fastest ions travel a distance $d+x$ while the slowest ions travel a distance $d-x$ under the same voltage. By applying the same method as was used in obtaining the theoretical mobility spectrum curve, it is apparent that under the force of the voltage V_0 the fastest and most diffused ions will travel a distance d, while the undiffused ions of greatest speed will travel a distance $d-x$; likewise, under the voltage V_1, the ions which have been diffusing backward with the greatest speed will have travelled a distance d (forward while the slowest undiffused ions travelled a distance $d+x$.

Therefore, $d-x=V_0k_1T$, and $d+x=V_1k_2T$ where k_1 and k_2 apply as previously defined to the undiffused ions. Thus k_1 and k_2 may be calculated from the voltages of the zeros and the break points (see Figs. 3 and 4).[9]

On applying the diffusion correction the results given in Table II were obtained (results A applying to ions in clean air, and B to ions in old and heavily irradiated air; k_1 and k_2 are in units of cm/sec. per volt/cm).

TABLE II. *Values of highest and lowest mobilities, after correcting for diffusion.*

	k_1	k_2	T	α	k_1-k_2
A	2.22	2.14	0.00580	7/60	0.08
	2.23	2.20	0.00586	7/60	0.03
	2.23	2.13	0.01150	1/6	0.10
	2.22	2.18	0.01150	7/60	0.04
	2.22	2.22	0.0117	7/60	0.00
	2.25	2.20	0.0280	1/6	0.05
	2.27	2.20	0.01148	1/6	0.07
B	2.4	2.0	0.0292	7/30	0.4
	2.4	1.86	0.0292	7/30	0.54

CONCLUSIONS

It is interesting to note that when the air is allowed to remain in the chamber for several sets of readings, a mobility spectrum appears as shown by the results in B above. The spectrum did not appear when air was left in the chamber for several days without exposure to ultraviolet light from the quartz-mercury arc. It was thus shown that ozone and the nitric oxides, which are formed in air in considerable quantity by the light from such an arc, cause a mobility spectrum. The very small residual spectrum that was found in A might be attributed to the inevitable presence of traces of these

[9] A consideration similar to the above applies to the case of the second break point and zero respectively, but these are not used because of the inaccurate knowledge of the exact time at which the shutter closes.

impurities, but it is much more likely due, in large part, to small instrumental irregularities in the measurements.

It is therefore safe to conclude that there was no mobility spectrum in air over the intervals studied, in terms of the magnitude of the spectrum asserted to exist by some writers,[4,10] if the air was relatively clean. An appreciable spectrum did appear after prolonged radiation. The resolving power of the method is excellent and is capable of greater refinement if needed. At the slowest shutter speed, a shift of one volt in the position of one of the critical points shifts the mobility by 0.085 cm/sec. per volt/cm while at the highest speed the mobility is only altered by 0.017 cm/sec. per volt/cm. The probable error in determining the derivative curve is between ± 0.15 volts and ± 0.20 volts, a small figure in consideration of the high resolving power. Whether greater refinement is desirable remains an open question because of the difficulties of accurately correcting for diffusion.

In conclusion, the writer wishes to express his indebtedness to Professor L. B. Loeb under whose direction and continual guidance the experiment was carried out, and to Mr. P. L. Porterfield, who assisted throughout the work. The writer is also grateful to Professor R. T. Birge for his instructions on the method of determining the probable errors and for his critical examination of the work of reduction of the observations.

[10] M. La Porte, Ann. de Physique **8**, 466, 711 (1927).

The Vapor Pressure Constant of Methane

By THEODORE E. STERNE*
Harvard University and The Massachusetts Institute of Technology

(Received September 12, 1932)

§1. It can be shown by statistical quantum mechanics that the vapor pressure constant of a molecule whose principal moments of inertia are all equal to A is

$$i = \log (64\pi^5 k^4 m^{3/2} A^{3/2}/h^6) + \Sigma_r D_r \log (G_r/{}_r\omega_0)$$

at ordinary temperatures; where m is the mass, k is Boltzmann's constant, h is Planck's constant, the D_r's are the gram molecular fractions of the two varieties, and where the G_r's and ${}_r\omega_0$'s are constants.

§2. It is found that G_1 for methane is 5/12, G_2 is 9/12 and G_3 is 2/12.

§3 and §4. It is shown by quantum mechanics that ${}_1\omega_0$ for methane is 5, ${}_2\omega_0$ is 9, and ${}_3\omega_0$ is 2; if the spins of the hydrogen nuclei are taken into consideration but the spin of the carbon nucleus neglected, which is permissible.

§5. With the value $A = 5.17 \times 10^{-40}$ c.g.s. units, it is found that the vapor pressure constant in atmospheres and common logarithms of methane at ordinary temperatures should be -1.94. The experimental result given by Eucken, -1.97 ± 0.05, agrees with this.

INTRODUCTION

IN RECENT papers[1,2,3,4] the author has studied the vapor pressures of diatomic vapors. The work was an extension of that of R. H. Fowler,[5] who first investigated, theoretically, the vapor pressure of hydrogen made up of the two non-combining varieties para-hydrogen and ortho-hydrogen. In a subsequent paper[6] the author investigated the vapor pressure constant of a polyatomic vapor, ammonia. It was shown that the vapor pressure constant i of a molecule such as ammonia, two of the principal moments of inertia of which, A and B, were equal with the third C differing from A and B, should be given by

$$i = \log \frac{64\pi^5 m^{3/2} k^4 A C^{1/2}}{h^6} + \Sigma_r D_r \log \frac{G_r}{{}_r\omega_0}$$

at ordinary temperatures for which the constant part of the specific heat of the vapor at constant pressure was equal to $4R$ per gram molecule. There R was the gas constant; m was the mass of the molecule; k was Boltzmann's constant; h was Planck's constant; the D_r's were the gram molecular fractions of the different sorts r of molecules present (there were two varieties of ammonia molecules); G_r was the numerical factor by which the expres-

* National Research Fellow.
[1] T. E. Sterne, Proc. Roy. Soc. **A130,** 367 (1931).
[2] T. E. Sterne, Proc. Roy. Soc. **A130,** 551 (1931).
[3] T. E. Sterne, Proc. Roy. Soc. **A131,** 339 (1931).
[4] T. E. Sterne, Proc. Roy. Soc. **A133,** 303 (1931).
[5] R. H. Fowler, Proc. Roy. Soc. **A118,** 52 (1928).
[6] T. E. Sterne, Phys. Rev. **39,** 993 (1932).

sion $16(2^{\frac{1}{2}})\pi^{7/2}A\,C^{1/2}k^{3/2}T^{3/2}/h^3$ must be multiplied in order to obtain the rotational partition function R_r for the gas molecule of type r; and ${}_r\omega_0$ was the statistical weight of the lowest quantum state of a molecule of ammonia in the crystalline phase "at the absolute zero."

This theory yielded a value for the vapor pressure constant of ammonia in satisfactory agreement with experiment. It therefore becomes interesting to investigate next the vapor pressures of substances for which all three principal moments of inertia of the polyatomic vapor molecules, A, B and C, are equal to each other. We shall therefore in this paper consider the vapor pressure constant of methane, CH_4. The methane molecule appears to consist of four hydrogen nuclei placed at the vertices of a regular tetrahedron, together with a carbon nucleus at the centroid of the tetrahedron; and the three principal moments of inertia appear to be equal. The Raman spectrum has been studied by Dickinson and others.[7]

§1. The Vapor Pressure of Methane

There should be three varieties of methane molecules, which should retain their separate identities over fairly long periods at ordinary and low temperatures. If we use the notation of the article on ammonia, we say that the first variety is characterized by wave functions which are completely symmetrical $S(4)$ in the spins of the four hydrogen nuclei; the second variety is characterized by wave functions $S(3+1)$ in the spins of the four hydrogen nuclei; and the third variety is characterized by wave functions $S(2+2)$ in the spins of the four hydrogen nuclei. A simpler notation is to follow Dirac's procedure[8] by introducing the observable s, which describes the magnitude of the total proton spin angular momentum, $\frac{1}{2}\Sigma_r\mathfrak{d}_r$ in units of $h/2\pi$, through the formula

$$s^2 - \tfrac{1}{4} = (\tfrac{1}{2}\Sigma_r\mathfrak{d}_r,\ \tfrac{1}{2}\Sigma_t\mathfrak{d}_t)$$

where the scalar product is meant. Then the first variety corresponds to the eigenvalue $s'=5/2$, the second variety to $s'=3/2$, and the third variety to $s'=\frac{1}{2}$. By methods similar to those employed in the article on ammonia,[6] §1, it is easy to show that the vapor pressure constant i of a polyatomic vapor, for which the three principal moments of inertia of the molecules are equal to A, is given by

$$i = \log\,(64\pi^5k^4m^{3/2}A^{3/2}/h^6) + \Sigma_rD_r\log\,(G_r/{}_r\omega_0). \qquad (1.0)$$

Here the symbols have the same meanings as in the INTRODUCTION to this paper. Number G_r is here the factor by which the expression $16(2^{\frac{1}{2}})\pi^{7/2}A^{3/2}k^{3/2}T^{3/2}/h^3$ must be multiplied in order to obtain the rotational partition function R^5 for a gas molecule of the rth sort. The derivation of the Eq. (1.0) above proceeds in the same fashion as the derivation of Eq. (1.92) in the author's paper on ammonia, except that since a number of selector variables has to be used equal to one more than the number of non-combining groups of terms, we are obliged to use four selector variables in the case of methane although

[7] Dickinson, Dillon, and Rasetti, Phys. Rev. **34**, 582 (1929).

[8] Dirac, *Principles of Quantum Mechanics*, first edition, Chap. XI.

three were sufficient in the case of ammonia. A quadruple integral must occur in the case of methane in the equation analogous to the Eq. (1.1) of the article on ammonia. To find the G_r's, we shall have to determine the rotational partition functions R_1, R_2 and R_3 for the three sorts of methane molecules, respectively.

§2. The Rotational Partition Functions of Free Methane Molecules

The rotational energy levels are given by[9]

$$W = (h^2/8\pi^2 A)j(j+1) \tag{2.0}$$

where j can take on positive integral values. There is another quantum number K, which can take on the values 0, 1, 2, 3, $\cdots$, j for each value of j. The weights of the levels are given by Villars and Schultze,[10] and are taken from the work of Elert.[11] The rotational partition functions R_1, R_2 and R_3 for the three sorts of methane molecules, respectively appear to have been calculated correctly by Villars and Schultze, at least insofar as the asymptotic expressions

$$R_1 \sim (5/12)\Omega, \quad R_2 \sim (9/12)\Omega, \quad R_3 \sim (2/12)\Omega \tag{2.1}$$

where

$$\Omega = 16(2^{\frac{1}{2}})\pi^{7/2}A^{3/2}k^{3/2}T^{3/2}/h^3,$$

are concerned. In deriving Eqs. (2.1) we may use methods similar to those used for obtaining the corresponding expressions in the case of ammonia, given in considerable detail in the paper[6] on ammonia.

It appears, therefore, that

$$G_1 = 5/12, G_2 = 9/12, G_3 = 2/12. \tag{2.2}$$

In this paper the spin of the carbon nucleus is neglected, since the vapor pressure constant of methane could not depend upon its value in any case, and since further the spin is zero.

We must now determine the values of ${}_1\omega_0$, ${}_2\omega_0$ and ${}_3\omega_0$.

§3. The Spherical Oscillatory Motion of Methane Molecules in Crystalline Methane

It appears from the considerations advanced by L. Pauling[12] that at very low temperatures, and *a fortiori* at the absolute zero, molecules of methane are not rotating in crystalline methane, but on the contrary are oscillating about orientations of minimum potential energy in the crystal lattice. It will be necessary for us to consider the nature of these motions in some detail in order to be able eventually to evaluate the ${}_r\omega_0$'s for methane.

It is not necessary, however, to solve in detail in this paper the quantum mechanical problem which is involved. Taking into account the geometrical symmetry of the methane molecule, we can generalize at once the results

[9] Dennison, Rev. Mod. Phys. **3**, 280 (1931)
[10] Villars and Schultze, Phys. Rev. **38**, 998 (1931).
[11] Elert, Zeits. f. Physik **51**, 6 (1928).
[12] L. Pauling, Phys. Rev. **36**, 430 (1930).

obtained in the case of the ammonia-type molecule considered in the paper on the vapor pressure of ammonia.[6] We take the origin, O, at the mass center of the molecule; and fixed orthogonal axes OX, OY, OZ such that the orientation of minimum potential energy for the methane molecule corresponds to the presence of the hydrogen nuclei 1, 2, 3, 4 at the points $(0, 0, 6^{\frac{1}{2}}a/2)$, $(-2\cdot 3^{\frac{1}{2}}a/3, 0, -6^{\frac{1}{2}}a/6)$ $(3^{\frac{1}{2}}a/3, -a, -6^{\frac{1}{2}}a/6)$ and $(3^{\frac{1}{2}}a/3, a, 6^{\frac{1}{2}}a/6)$ respectively; the carbon nucleus being of course at O. Let us investigate the forms of the potential and kinetic energies of the molecule, regarded as rigid, for small displacements of the molecule from this orientation of minimum potential energy. As in the case of ammonia, we specify a displacement by the small rotations x, y and z of the molecule about the axes OX, OY and OZ respectively. The Hamiltonian for the methane molecule is similar to the Hamiltonian for the ammonia molecule, but its form is simpler than the latter because of the higher degree of symmetry of the methane molecule. We see therefore as in the case of the ammonia-type molecule that the lowest energy level of the methane-type molecule, when the arrangement of the hydrogen nuclei is that specified above, can be represented by only a single linearly independent wave function describing its spherical oscillatory motion.

In order to find the values of the ${}_r\omega_0$'s, we must now study the symmetry properties of the complete wave functions of the methane molecule, taking into account the spins of the hydrogen nuclei and the various possible distributions of the hydrogen nuclei among the neighborhoods of the four points whose coordinates are specified above.

§4. The Values of ${}_1\omega_0$, ${}_2\omega_0$ and ${}_3\omega_0$

The discussion of the symmetry properties of the spherical oscillatory wave functions of a methane molecule in crystalline methane is somewhat more involved than the discussion of the case of an ammonia molecule in crystalline ammonia, because a methane molecule contains one more hydrogen nucleus than an ammonia molecule. There are 24 possible permutations of the protons in a methane molecule as compared with the 6 which are possible in the case of ammonia. For the sake of simplicity and elegance we shall therefore use the methods described by Dirac[13] in order to consider the symmetry properties of the wave functions of methane. Dirac's procedure can be followed as easily for protons as for electrons, because both protons and electrons have one-half quantum spins. We shall accordingly depart here from the methods which we used for considering ammonia, and in what follows we shall assume that the reader is already familiar with Dirac's theory of the permutation observables.

We must take account of the spins of the hydrogen nuclei and also of the spherical vibrational factors in the wave functions. In dealing with the vibrational factors we must now take account of the different arrangements of the hydrogen nuclei which are possible among the four mean positions, a, b, c and d, say, which we specified in §3. If the vibrational factor in a wave func-

[13] Dirac, *Principles of Quantum Mechanics*, first edition, §66.

tion for the lowest vibrational level with which we are concerned is denoted by f, then $f(1, 2, 3, 4)$ would refer to a state in which nucleus 1 was in the vicinity of position a, 2 in the vicinity of position b, 3 in the vicinity of position c, 4 in the vicinity of position d; with analogous meanings for the other 23 f's which are possible. In accordance with §66 of Dirac's book, let us denote the z-component σ_z of the spin vector $\mathfrak{s}$ of the i'th hydrogen nucleus by σ_i, so that the representative of a state will be $(x_1, x_2, x_3, x_4, \sigma_1, \sigma_2, \sigma_3, \sigma_4|\ )$; the single variable x being written instead of x, y, z and the suffix z being dropped from the σ_z's that occur in representatives. Then in accordance with Dirac's equation (32) it is sufficient to study the permutations P^σ which operate only on the σ's, and this results in a considerable simplification since it allows us to ignore the x's. There are five types of permutations of four particles, namely: the types 4, 3+1, 2+2, 2+1+1 and 1+1+1+1. There are thus five independent commuting observables χ^σ which are constants of the motion:

$$\chi_1^\sigma = (1/6)\Sigma P^\sigma{}_4$$
$$\chi_2^\sigma = (1/8)\Sigma P^\sigma{}_{3+1}$$
$$\chi_3^\sigma = (1/3)\Sigma P^\sigma{}_{2+2}$$
$$\chi_4^\sigma = (1/6)\Sigma P^\sigma{}_{2+1+1}$$
$$\chi_5^\sigma = \Sigma P^\sigma{}_{1+1+1+1} \equiv 1.$$

Here, for instance, $\Sigma P^\sigma{}_{2+2}$ is the sum of all permutations which operate on the spin variables σ, of type 2+2. We shall find it easier to study the χ^σ's than the χ's. There are 15 simultaneous equations like Dirac's Eq. (22) involving the χ^σ's; if we notice that $\chi_5^\sigma \equiv 1$ we have merely the 10 equations

$$(\chi_1^\sigma)^2 = \tfrac{2}{3}\chi_2^\sigma + \tfrac{1}{6}\chi_3^\sigma + \tfrac{1}{6} \qquad (\chi_1^\sigma\chi_3^\sigma) = \tfrac{1}{3}\chi_1^\sigma + \tfrac{2}{3}\chi_4^\sigma$$
$$(\chi_2^\sigma)^2 = \tfrac{1}{2}\chi_2^\sigma + \tfrac{3}{8}\chi_3^\sigma + \tfrac{1}{8} \qquad (\chi_1^\sigma\chi_4^\sigma) = \tfrac{2}{3}\chi_2^\sigma + \tfrac{1}{3}\chi_3^\sigma$$
$$(\chi_3^\sigma)^2 = \tfrac{2}{3}\chi_3^\sigma + \tfrac{1}{3} \qquad (\chi_2^\sigma\chi_3^\sigma) = \chi_2^\sigma$$
$$(\chi_4^\sigma)^2 = \tfrac{2}{3}\chi_2^\sigma + \tfrac{1}{6}\chi_3^\sigma + \tfrac{1}{6} \qquad (\chi_2^\sigma\chi_4^\sigma) = \tfrac{1}{2}\chi_1^\sigma + \tfrac{1}{2}\chi_4^\sigma$$
$$(\chi_1^\sigma\chi_2^\sigma) = \tfrac{1}{2}\chi_1^\sigma + \tfrac{1}{2}\chi_4^\sigma \qquad (\chi_3^\sigma\chi_4^\sigma) = \tfrac{2}{3}\chi_1^\sigma + \tfrac{1}{3}\chi_4^\sigma$$

and when we solve them for the sets of simultaneous eigenvalues $\chi^{\sigma\prime}$ of the observables χ^σ we obtain the values given in Table I, where the sets are denoted by S, α, β, A and γ.

If we introduce the observable s, which we defined in §1, to describe the magnitude of the total spin angular momentum we find by the methods of §66 in Dirac's book that

$$\chi_1^\sigma = [1/192][(4s^2 - 13)^2 + 8(4s^2 - 13) - 48]$$
$$\chi_2^\sigma = (1/16)(4s^2 - 9)$$
$$\chi_3^\sigma = [1/96][(4s^2 - 13)^2 - 48]$$
$$\chi_4^\sigma = (1/24)(4s^2 - 1)$$
$$\chi_5^\sigma = 1.$$

There is therefore one set of numerical values $\chi^{\sigma'}$ for the χ^{σ}'s, and thus one exclusive set of states, for each eigenvalue s' of s. The eigenvalues of s are 5/2, 3/2, and 1/2; we readily find that corresponding to these eigenvalues of s the exclusive sets of states are those which we have denoted by S, β and T respectively. There are no other sets possible; the sets α and A being impossible in the case of a set of four protons. The relationship between s' and the $\chi^{\sigma''}$s is shown in Table I.

TABLE I.

Exclusive sets of states.	S	α	β	A	γ
Eigenvalues s'	5/2	—	3/2	—	1/2
$\chi_1^{\sigma'}$	1	1/3	−1/3	−1	0
$\chi_2^{\sigma'}$	1	0	0	1	−1/2
$\chi_3^{\sigma'}$	1	−1/3	−1/3	1	1
$\chi_4^{\sigma'}$	1	−1/3	1/3	−1	0
$\chi_5^{\sigma'}$	1	1	1	1	1

The three sets, however, may be degenerate; and in fact they are degenerate. Corresponding to any s' there are $2s'$ possible values for the z-component of total spin angular momentum $\Sigma_{r=1}^{4}\sigma_r$ which we may denote by s_z. Thus for the exclusive set of states S, s_z' may be 4, 2, 0,–2 or −4. Similarly for the set β, s_z' may be 2, 0 or −2. For the set γ, s_z' must be 0. Each of the states so defined may itself be degenerate, and some of them are in fact degenerate. These latter degeneracies are essential and cannot be removed by perturbations which are symmetrical between the particles; but we must study them in order to enumerate our representatives correctly and thus obtain our ω_0's.

Let us choose a representation whose fundamental states are the eigenstates of the z-components σ of the spin vectors of the hydrogen nuclei, corresponding to the simultaneous eigenvalues of all four σ's. There will of course be $2^4=16$ fundamental states, since the eigenvalues of the σ's are independent and can each be +1 or −1. We wish to find the number of linearly independent eigenstates corresponding to each choice of simultaneous eigenvalues for s_z and s; that is, we wish to find the number of linearly independent wave functions or representatives capable of representing each of these eigenstates of s_z' and s' in the σ representation. Denoting states by ψ's, we have

$$\psi(s_z', s') = \Sigma\psi(\sigma')(\sigma' \mid s_z', s')$$

and also

$$(s'^2 - \tfrac{1}{4})(\sigma' \mid s_z', s') = \Sigma(\sigma' \mid s^2 - \tfrac{1}{4} \mid \sigma'')(\sigma'' \mid s_z', s'). \qquad (4.1)$$

To calculate the matrix elements $(\sigma' \mid s^2 - \frac{1}{4} \mid \sigma'')$ we use the relation

$$s^2 - \tfrac{1}{4} = 6\chi_4^{\sigma}; \qquad (4.2)$$

to calculate the matrix elements $(\sigma' \mid \chi_4^{\sigma} \mid \sigma'')$ we allow the observable χ_4^{σ} to operate on the various $\psi(\sigma')$'s in turn and we write down the matrix elements by comparison with the equation

$$\chi_4{}^{\sigma}\psi(\sigma'') = \Sigma\psi(\sigma')(\sigma' \mid \chi_4{}^{\sigma} \mid \sigma''). \tag{4.3}$$

If we write down the set of simultaneous Eqs. (4.1) for any set of eigenvalues S_z' and s' and solve it, we shall find thereby a linear relation or linear relations obeyed by the representative $(\sigma' \mid s_z', s')$ and from this we can find the number of linearly independent eigenfunctions $(\sigma' \mid \ )$ which are possible; or in other words, the number of independent $\psi(s_z', s')$'s. The following calculations should make this clear.

Case 1,

$s' = 5/2$, $s_{z'} = 4$. The only $\psi(\sigma')$ which can be concerned is $\psi(1, 1, 1, 1)$ and there is thus only one eigenfunction possible: $(\sigma_1', \sigma_2', \sigma_3', \sigma_4' \mid 4, 5/2)$ is a constant when all the σ''s are 1, and vanishes for all other values of the σ''s.

Case 2,

$s' = 5/2$, $s_z' = 2$. The only fundamental $\psi(\sigma')$'s which can be concerned when $s_z' = 2$ are those which $\Sigma\sigma' = 2$; they are $\psi(1, 1, 1, -1)$, $\psi(1, 1, -1, 1)$, $\psi(1, -1, 1, 1)$ and $\psi(-1, 1, 1, 1)$. We shall denote these states by $\psi(1)$, $\psi(2)$, $\psi(3)$ and $\psi(4)$, respectively, for brevity. We find easily from Eqs. (4.2) and (4.3) that the matrix representing $s^2 - \frac{1}{4}$ is

	1	2	3	4
1	3	1	1	1
2	1	3	1	1
3	1	1	3	1
4	1	1	1	3

. (4.4)

The set of Eqs. (4.1) in this case becomes

$$\begin{aligned}
-3(1 \mid \ ) + (2 \mid \ ) + (3 \mid \ ) + (4 \mid \ ) &= 0 \\
(1 \mid \ ) - 3(2 \mid \ ) + (3 \mid \ ) + (4 \mid \ ) &= 0 \\
(1 \mid \ ) + (2 \mid \ ) - 3(3 \mid \ ) + (4 \mid \ ) &= 0 \\
(1 \mid \ ) + (2 \mid \ ) + (3 \mid \ ) - 3(4 \mid \ ) &= 0
\end{aligned}$$

and hence

$$(1 \mid \ ) = (2 \mid \ ) = (3 \mid \ ) = (4 \mid \ )$$

so that only one linearly independent eigenfunction exists, given by $(r \mid 2,5/2) = \text{const.}$, $r = 1, 2, 3, 4$.

Case 3,

$s' = 5/2$, $s_z' = 0$. The $\psi(\sigma')$'s concerned when $s_z' = 0$ are $\psi(1, 1, -1, -1)$, $\psi(1, -1, 1, -1)$, $\psi(-1, 1, 1, -1)$, $\psi(1, -1, -1, 1)$, $\psi(-1, 1, -1, 1)$ and $\psi(-1, -1, 1, 1)$; denoted by $\psi(1)$, $\psi(2)$, $\psi(3)$, $\psi(4)$, $\psi(5)$ and $\psi(6)$ respectively. The other $\psi(\sigma')$'s can be ignored. The matrix representing $s^2 - 1/4$ is

	1	2	3	4	5	6
1	2	1	1	1	1	0
2	1	2	1	1	0	1
3	1	1	2	0	1	1
4	1	1	0	2	1	1
5	1	0	1	1	2	1
6	0	1	1	1	1	2

(4.5)

and we find after solving the Eqs. (4.1) in this case that $(r\,|0,\,5/2) = \text{const.}$; $r = 1, 2, 3, 4, 5, 6$. This is the only eigenfunction possible.

Cases 4 and 5,

for $s' = 5/2$, $s_z' = -2, -4$ respectively, are similar to cases 1 and 2 and in each case only one eigenfunction exists.

Case 6,

$s' = 3/2$, $s_z' = 2$. When we solve the set of Eqs. (4.1) in this case, using the matrix for $s^2 - 1/4$ given by (4.4), we find that

$$(1\,|\,2,\,3/2) + (2\,|\,2,\,3/2) + (3\,|\,2,\,3/2) + (4\,|\,2,\,3/2) = 0. \qquad (4.6)$$

We can choose three and only three linearly independent eigenfunctions obeying Eq. (4.6). All other possible eigenfunctions obeying (4.6) can be expressed as linear combinations of these three. Thus we might choose the 3 eigenfunctions $(r\,|\;\;)_1$, $(r\,|\;\;)_2$, $(r\,|\;\;)_3$ defined by the following table:

r	1	2	3	4
$(r\,|\;\;)_1$	1	-1	0	0
$(r\,|\;\;)_2$	1	0	-1	0
$(r\,|\;\;)_3$	1	0	0	-1

Any fourth function $(r\,|\;\;)_4$ obeying (4.6) would be in the form

r	1	2	3	4
$(r\,|\;\;)_4$	a	b	c	$-a-b-c$

and we should have

$$(r\,|\;\;)_4 = -b(r\,|\;\;)_1 - c(r\,|\;\;)_2 + (a+b+c)(r\,|\;\;)_3$$

so that it would not be linearly independent.

Case 7,

$s' = 3/2$, $s_z' = 0$. Using the matrix (4.5) we find eventually that $(1\,|\;\;) = -(6\,|\;\;)$; $(2\,|\;\;) = -(5\,|\;\;)$; $(3\,|\;\;) = -(4\,|\;\;)$. There are three and only three linearly independent eigenfunctions.

Case 8,

$s'=3/2$, $s_z'=-2$. This is similar to case 6, and there are three linearly independent eigenfunctions.

Case 9,

$s'=1/2$, $s_z'=0$. Using the matrix (4.5) we find that

$$(1|\ ) = (6|\ );\ (2|\ ) = (5|\ );\ (3|\ ) = (4|\ );\ (1|\ ) + (2|\ ) + (3|\ ) = 0.$$

There are two and only two linearly independent eigenfunctions possible, which might be for instance the functions $(r|\ )_1$ and $(r|\ )_2$ given by

r	1	2	3	4	5	6
$(r\|\ )_1$	1	−1	0	0	−1	1
$(r\|\ )_2$	1	0	−1	−1	0	1

Recapitulating, we can prepare Table II showing the numbers ω_0 of eigenfunctions which are possible in the different cases:

TABLE II.

s'	s_z'	ω_0	Totals
5/2	4	1	5
	2	1	
	0	1	
	−2	1	
	−4	1	
3/2	2	3	9
	0	3	
	−2	3	
1/2	0	2	2

and we see therefore that ${}_1\omega_0=5$; ${}_2\omega_0=9$; ${}_3\omega_0=2$.

§5. THE VAPOR PRESSURE CONSTANT OF METHANE

From the results of §2, we have at once that $D^1=5/16$, $D^2=9/16$, $D_3=2/16$. Hence it follows from the results of the last section and §2 that the last term in Eq. (1.0) is log 1/12. We are now in a position to calculate the vapor pressure constant of methane. Taking the molecular weight with sufficient accuracy to the 16.04 and the moment of inertia A to be[7] 5.17×10^{-40} c.g.s. units, we find that the vapor pressure constant i' at ordinary temperatures, in atmospheres and common logarithms,[14] is $i'=-1.94$. This is in good agreement with the experimental value given by Eucken[15] $i'=-1.97\pm.05$.

The writer wishes to thank the National Research Council for a grant which enabled these investigations to be carried out.

[14] We merely use Eq. (1.0) with common logarithms instead of natural logarithms, and subtract the quantity 6.006 from the right-hand member.

[15] Eucken, Phys. Zeits. **31**, 361 (1930).

On the Origin of the Actinium Series of Radioactive Elements

By A. v. GROSSE
Kent Chemical Laboratory, University of Chicago

(Received September 13, 1932)

Data on the actinium series gathered from carefully selected material have been correlated. It can be definitely concluded from these data that the actinium series is independent and the decay much more rapid than in the uranium-radium series. The significance of this fact for geology (age determinations, heat evolution) is pointed out.

THE experimental material on the actinium series and its theoretical interpretation has been so far extremely conflicting.[1] This is chiefly due to the fact that the determinations of the chemical composition, geologic age, activity ratio of the actinium to the uranium-radium series, the chemical atomic weights of uranium leads and lately the isotopic constitution of these leads have never been determined with the same material for all investigations.

Thanks to the help and cooperation of Mme. Pierre Curie, Mme. Irene Joliot-Curie and Drs. G. Baxter, K. Fajans, O. Hönigschmid, A. C. Lane and H. Schlundt we were able to gather and to investigate a valuable collection of uranium-minerals and preparations from uranium-lead atomic weight determinations.

F. W. Aston had the great kindess to investigate in his mass-spectrograph some lead preparations from these sources, and it is to him that the credit for clearing the problem is due.[2]

We laid special stress on the determination of the so-called "branching ratio" or as we may better call it now "activity ratio." The older determination of O. Hahn and L. Meitner[3] (3 percent), and newer ones of J. Wildish[4] (1.5–5 percent) and E. Gleditsch and co-workers[5] (2.7–3.3 percent) are all based on the separation of protactinium with tantalum and seem to us un-

[1] For older literature see St. Meyer and E. v. Schweidler, *Radioaktivität*, 1927, p. 490. J. Wildish, Jour. Amer. Chem. Soc. **52**, 163 (1930). E. Gleditsch and E. Foyn, Comptes Rendus **194**, 1571 (1932). E. Gleditsch and S. Klementsen, Comptes Rendus **194**, 1731 (1932). G. Kirsch, *Geologie und Radioaktivität*, p. 184, 1928. F. W. Aston, Nature **123**, 313 (1929). Lord Rutherford, Nature **123**, 313 (1929). A. Holmes, Nature **126**, 348 (1930). A. F. Kovarik, Science **72**, 122 (1930). G. B. Baxter and A. D. Bliss, Jour. Amer. Chem. Soc. **52**, 4850 (1930). For summaries on the actinium problem see: M. C. Neuburger, Sammlung chem. and chem.-techn. Vorträge **26**, No. 10/11 (1921). G. Elsen, Zeits. f. anorg. Chem. **180**, 304 (1929). G. Elsen, Chemisch Weekblad **25**, 517 (1928); **28**, 1, 7, 714 (1931). G. Elsen, Rec. des Trav. chim. Plays-Bas **51**, 284 (1932).

[2] F. W. Aston, Nature **129**, 649 (1932).

[3] O. Hahn and L. Meitner, Phys. Zeits. **20**, 529 (1919); Zeits. f. Physik **8**, 202 (1922).

[4] Reference 1.

[5] Reference 1.

reliable since it could be shown through the isolation of element 91[6] that its chemical properties widely differ from those of tantalum,[7] just as those of its neighbors uranium and thorium differ from their lower homologues, tungsten and hafnium.

Our determination of the Pa:UI ratio was carried out, in collaboration with Dr. I. D. Kurbatov, at the Chemical Institute of the Technische Hochschule in Berlin-Charlottenburg.[8]

TABLE I.

		1	2	3	4	5
1	Mineral Geographical origin	Carnotite[a] Colorado, U.S.A.	Kolm[b] Gullhogen, Westergotland, Sweden	Pitchblende[c] Katanga, Belg. Congo, Africa	Pitchblende[d] Morogoro, East Africa	Pitchblende[e] Wilberforce, Canada
3	Chemical analysis U %	19.09	0.43[9]; 0.41	72.26	70.45	53.52[11]; 52.71
	Th %	0	0.0	0.01[10]	ab. 0.2	10.37[11]
	Pb %	trace	0.026[9]	6.68	8.30	9.26[11]
4	Isotopic constitution of Pb Pb 206%			93.3[12]		85.9[12]
	207%			6.7[f]		8.3[g]
	208%			0.0		5.8
	others			0.0		0.0
	Percentage of RaG			93.3[13]		85.9
	AcD			6.7		8.3
	ThD			0.0		5.8[14]
6	Chem. atomic weight of Pb		206.013[15] ±0.008	206.048[16]		206.195[17]
7	Phys. atomic weight of Pb		206.058 ±0.01	206.067[18]		206.20[18]
8	Pb:U ratio	very small	0.061	0.0924	0.1178	0.1730
9	RaG:UI ratio	very small	0.058	0.086	0.1093	0.1486
10	Geological age in years	$<70.10^6$	404.10^6	591.10^6	748.10^6	987.10^6
11	Pa-α activity in mg. U_3O_8 for every 1 g U in the mineral	28.0	27.9	27.8	27.6	28.2
12	Number of disintegrating Pa-atoms for 100 decaying UI-atoms		4.0±0.1, mean value, calculated from row 11			
13	Number of AcD atoms for 100 atoms RaG in U-Pb		4.8±1.8[19]	7.2±0.3		$9.7^{+0.3}_{-1.0}$

[a] Obtained from H. Schlundt; from the same lot used by J. Wildish (reference 4) for which he obtained Pa:UI = 5.16:100.
[b] Obtained from A. C. Lane, from the same general lot used for G. P. Baxter's kolm lead atomic weight determination.
[c] Obtained from Mme. Pierre Curie and Mme. Irene Joliot-Curie.
[d] Obtained from F. Kranz, Bonn, Germany.
[e] Obtained from A. C. Lane and G. P. Baxter, from the same lot used for the Wilberforce lead atomic weight determination.
[f] The lead tetramethyl used by F. W. Aston was prepared from the original $PbCl_2$ used by O. Hönigschmid. According to private information from Dr. Aston the lead from Mme. Curie's sample had an identical isotopic constitution.
[g] The material used by F. W. Aston was prepared from G. P. Baxter's original atomic weight preparation.

[6] A. v. Grosse, Naturwiss. **15,** 766 (1927); Nature **120,** 621 (1927); Ber. d. Deut. Chem. Ges. **61,** 233 (1928).

[7] A. v. Grosse, Jour. Amer. Chem. Soc. **52,** 1742 (1930).

[8] Part of these results were reported at the meeting of the Chicago Section of the Amer. Chem. Society on September 25, 1931; see also G. Elsen, Chem. Weekblad **28,** 714 (1931).

[9] R. C. Wells and R. E. Stevens, Jour. Washington Acad. of Science **21,** 412 (1931).

[10] The Th was separated with UX_1, added as indicator, concentrated and the Th-content determined with W. Noddack's x-ray spectrograph at the Physikalisch-Technische Reichsanstalt, Berlin-Charlottenburg.

[11] R. C. Wells, Jour. Amer. Chem. Soc. **52,** 4852 (1930).

[12] F. W. Aston, Nature **129,** 649 (1932).

[13] Since the mineral contains practically no Th, and therefore no ThD, the absence of Pb^{208} indicates the absence of ordinary lead, the latter containing 49.55 percent Pb^{208} (see Aston, reference 12).

[14] From the Th-content and age we calculate, using Th = 6, $1.10^{-11}a^{-1}$, the percent of ThD = 6, 0 indicating the absence of ordinary lead.

Our method consisted in precipitating the Pa from a strongly acid (HNO_3, HCl) solution of the U-mineral together with added Zr (in the proportion of 20–50 mg ZrO_2, in the form of oxychloride or nitrate, to 1 g U) by an excess of H_3PO_4, and freeing the filtered Pa-ZrP_2O_7 precipitate from adsorbed radioactive impurities (especially Io, Ra, and Po) through the addition and subsequent separation (repeated if necessary) of minute quantities (2–10 mg) of Th, Ba, Bi (and Te), Pb and La salts. The method was tested with radioactively pure Pa preparations in different concentrations and found to separate 98–99 percent of the available Pa in a radioactively pure state. The activity of the Pa preparation was compared with that of pure U_3O_8, both in extremely thin layers, in an ordinary Rutherford α-electroscope and expressed in mg U_3O_8.

The results of all determinations and investigations with our material are correlated in Table I.

These data all support A. Piccard's[20] and especially Lord Rutherford's[21] ideas about the actinium series. The following conclusions can be drawn:

1. The actinium series is independent of the U-Ra series. It is derived from a U-isotope, the actino-uranium (Ac-U), which occurs in all U-minerals in a constant ratio to UI, independent of the geological age, geographic origin, thorium content and uranium concentration. 4.0 atoms Ac-U, or of any other member of the Ac-family, decay for every 100 UI-atoms disintegrating, i.e., the activity ratio of the Ac to the U-Ra series is 4:100. Our determinations completely support the older results of Stefan Meyer, V. F. Hess and G. Kirsch.[22,23,24]

2. AcD, the end product of the actinium series, has an atomic weight of 207 (or more exactly 207.010 ± 0.01), therefore Ac = 227 and Pa = 231.

3. The AcD content of uranium lead (and therefore also its atomic weight) increases with the geological age of the mineral. From the AcD content in U-Pb of minerals of definite age and the activity ratio the half period of Ac-U can be calculated (see formula 2 below); the best value is $T_{(AcU)} = 4.0 \times 10^8$ years, $\lambda_{(AcU)} = 5.5 \times 10^{-17}$ sec.$^{-1}$.

Fig. 1 shows the increase of AcD content in uranium lead with the age of the mineral. The theoretical curve is calculated for $T_{(AcU)} = 4.0 \times 10^8$ years.

The values of AcD content, derived from chemical atomic weight determinations of uranium leads of different ages, including kolm[25] and also oldest pitchblendes, for instance, from Black Hills, South Dakota[26] (at. wt. = 206.07$_1$

[15] G. P. Baxter and A. D. Bliss, Jour. Amer. Chem. Soc. **52,** 4848 (1930).

[16] O. Hönigschmid and L. Birkenbach, Ber. Deut. Chem. Ges. **56,** 1837 (1923).

[17] G. P. Baxter and A. D. Bliss, Jour. Amer. Chem. Soc. **52,** 4851 (1930).

[18] F. W. Aston, reference 12.

[19] Value tentatively calculated from the chem. atomic weight of kolm lead.

[20] A. Piccard, Arch. sciences phys. and natur. **44,** 161 (1917); A. Piccard and E. Stahel, same journal (5) **3,** 541 (1921).

[21] Lord Rutherford, Nature **123,** 313 (1929).

[22] St. Meyer and V. F. Hess, Wiener Ber. (Akad. d. Wiss.) **128,** 909 (1919).

[23] St. Meyer, Wiener Ber. (Akad. d. Wiss.) **129,** 483 (1920).

[24] G. Kirsch, Wiener Ber. (Akad. d. Wiss.) **129,** 309 (1920).

corrected age = about 1300.10^6 years) are, within experimental errors, in agreement with this theoretical curve.

4. The AcU content of the element uranium, independent of source, equals at present 0.4 percent by weight. It was much larger in former geological epochs, i.e., over 4 percent about 1600×10^6 years ago; it will diminish in the future, for instance in about 1600.10^6 years the content will be only 0.03 percent. Similarly the activity and heat evolution due to the actinium series and their importance for geology were much larger in past times, equalling about half the value of the uranium series in the earliest part of the earth's history. (The determination of the AcU/UI or Pa/UI ratio affords a method of measuring the "age of uranium" in meteorites as compared with our uranium on earth.)

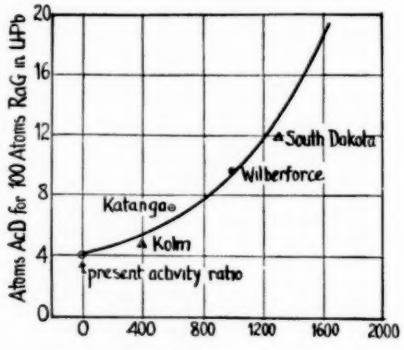

Fig. 1. Theoretical curve for $T(\mathrm{AcU}) = 4.0 \times 10^8$ years. Triangles with dots are calculated from chemical atomic weight determinations.

5. Owing to the more rapid decay of AcU it is necessary to make corrections in geological age calculations.[27]

The exact age (t) is

$$t = 1/\lambda_{(\mathrm{UI})} \cdot \log_e \left(1 + \frac{238\,\mathrm{U} - \mathrm{Pb}}{206\mathrm{UI}(1 + r)}\right) \tag{1}$$

where r is the ratio of AcD to RaG in U-Pb (see Fig. 1) and

$$r = R \cdot \frac{\lambda_{(\mathrm{UI})}\left(e^{\lambda_{(\mathrm{AcU})} t} - 1\right)}{\lambda_{(\mathrm{AcU})}\left(e^{\lambda_{(\mathrm{UI})} t} - 1\right)} \tag{2}$$

when R is the activity ratio of Ac to U-Ra series, i.e., 0.040.

---

[25] Compare G. P. Baxter and A. D. Bliss, Jour. Amer. Chem. Soc. **52,** 4850–51 (1930).

[26] T. W. Richards and L. P. Hall, Jour. Amer. Chem. Soc. **48,** 706 (1926).

[27] A. Holme's objections (Nature **126,** 348 (1930)) to Lord Rutherford's conclusions (Nature **123,** 313 (1929)) are only correct so far as Aston's first value for the AcD content in U–Pb was too high, owing to the so-called "hydride effect," i.e., coincidence of the Pb^{207} line with the Pb^{206} H^1 line. With the help of a nearly pure ThD (94.1 percent Pb^{208}) which we owe to the kindness of Professor K. Fajans (for its source and at wt., see K. Fajans, Sitzungsber. Heidelberg. Akad. d. Wiss. 1918 A, Abh. 3, 0. Hönigschmid, Zeit. f. Elektrochemie **25,** 91 (1919)), Aston was able to measure this effect and correct for it in his subsequent determinations.

Since t occurs also in the correction factor it is easier to calculate the RaG:UI and U-Pb:U ratios for set values of t and derive the age from the Table II ($T_{(AcU)}=4.0\times10^8$ years).

TABLE II.

Age, t (years)	RaG: UI ratio or g RaG for 1g UI	U-Pb: U ratio or g U-Pb for 1g U
0×10^6	0.0000	0.0000
100	0.0139	0.0145
200	0.0280	0.0293
300	0.0423	0.0445
400	0.0569	0.0600
500	0.0718	0.0760
600	0.0868	0.0924
700	0.1022	0.1094
800	0.1177	0.1269
900	0.1335	0.1450
1000	0.1495	0.1638
1100	0.1658	0.1835
1200	0.1824	0.2040
1300	0.1992	0.2258
1400	0.2164	0.2492
1500	0.2337	0.2733

6. 1 g U contains in equilibrium $2.7_3\times10^{-7}$ g Pa, since $T_{(Pa)}=32{,}000$ years.[28] 1 g Ra is associated with 0.8_1 g Pa at the present geological time; in the past it was more common than radium (1600×10^6 years ago about 10 g Pa occured for every g of Ra) and in the future it will become rapidly rarer (in 1600×10^6 years the Pa:Ra-ratio will be only 0.06).

7. The pleochroic haloes discovered by S. Iimori and Y. Yoshimura[29] cannot be due to the Ac-series, since these have always occurred together with the U-Ra-series on earth.

8. The transformation scheme for the actinium series is as follows (atomic weight, period):[30]

$$\begin{array}{lcccccccc} ?\rightarrow & \mathrm{AcU} & \xrightarrow{\alpha} & \mathrm{UY} & \xrightarrow{\beta} & \mathrm{Pa} & \xrightarrow{\alpha} & \mathrm{Ac} & \xrightarrow{\beta} \cdots \mathrm{Ac}D \\ & 235;\ 4.0\times10^8\ \mathrm{yr.} & & 231;\ 24.6\ \mathrm{hr.} & & 231;\ 32{,}000\ \mathrm{yr.} & & 227;\ 13.5\ \mathrm{yr.} & & 207;\ \infty \end{array}$$

The only fact not in harmony with the other data on the actinium series presented here is the presently accepted value for the atomic weight of uranium (238.14, O = 16). The atomic weights of all members of the three series can be calculated with precision, if the atomic weight of their corresponding end product is known, by adding to it, step by step, the well-known masses of particles and energies emitted during each distintegration.

From Aston's recent measurements[31] we have for the physical atomic weight of $Pb^{206}=206.01\pm0.01$ or 205.96 ± 0.02 on the chemical scale, using

[28] A. v. Grosse, Naturwiss. **27**, 505 (1932).

[29] S. Iimori and Y. Yoshimura, Scient. pap. Inst. Tokyo **5**, 11 (1926).

[30] "?" indicates that there still is a possibility for the existence of a second actino-uranium, see also A. v. Grosse, reference 28.

[31] F. W. Aston, Nature **129**, 649 (1932).

R. Mecke's[32] conversion factor (1.00022). From this starting point the calculated values for the following members of the U-Ra-series are:[33]

Radio element	Phys. at. wt., $O^{16}=16$		Chem. at. wt., $O=16$	
RaF (Po)	210.02	±0.02	209.97	±ab. 0.02
Ra-Em	222.05		222.00	
Ra	226.06		226.01	
UI	238.08		238.03	

This atomic weight of UI and Aston's observation[34] that it constitutes at least 97 percent of the element uranium indicate that the value 238.14 for the latter is too high.

The author wishes to express his gratitude to the *Notgemeinschaft der Deutschen Wissenschaft* in Berlin and to Mr. H. J. Halle of New York City for financial support in this investigation.

[32] R. Mecke and W. H. J. Childs, Zeits. f. Physik. **68,** 362 (1931).

[33] Our complete data were published in F. G. Houterman's report—Ergebnisse der exakten Naturwissenschaften, p. 199, 1930.

[34] F. W. Aston, Nature **128,** 725 (1931).

Permeability of Iron at Ultra-Radio Frequencies

By J. Barton Hoag and Haydn Jones
Ryerson Physical Laboratory, University of Chicago

(Received September 12, 1932)

Measurements have been made by the self-inductance method at ultra-radio frequencies of the "initial" magnetic permeability of iron wire by use of the new frequency determination method of Hoag. The following values have been obtained: 30.31, 22.10, 18.69 and 9.65 at frequencies of 469.8, 589.8, 829.8 and 1350 megacycles, respectively, corresponding to wave-lengths of 63.81, 50.83, 36.13 and 22.21 cm. These values of permeability are appreciably lower than those of Arkadiew in this region but show a similar decrease with increase of frequency.

Introduction

THE study of permeability of iron at very high radio frequencies is of great interest in connection with theories of magnetism. Anomalies in the measured values of permeabilities at frequencies from 10^8 to 10^6 cycles per second (3 to 300 meters wave-length) were observed by Kartschagin[1] and by Wwendensky and Theodortschik[2] and discussed by Arkadiew[3] and Page.[4] However, the more recent experiments of Sokolow,[5] Michels,[6] Strutt,[7] Wait,[8] Laville,[9] and Wait, Brickwedde and Hall[10] do not show these peculiarities of the permeability values in this range.

Two fundamental procedures employing the skin-effect equations derived by Maxwell, Heaviside, Rayleigh, Kelvin and others, have been used to determine permeabilities at high frequencies. The first is based upon a measurement of the damping or high-frequency resistance in two parallel (Lecher) wires while the second depends on the measurement of their high-frequency inductance. It is found in all cases that the values of permeability μ_k obtained by the resistance method are greater than those μ_n obtained by the inductance method. The possible accuracy of measurement by the former method is much greater than by the latter. For example, values given by Michels for μ_k in the wave-length range from four to thirteen meters are accurate to 3 percent while μ_n values are in error by 4–13 percent. The present work was undertaken with a view to increasing the accuracy and high frequency range of the inductance method.

[1] W. Kartschagin, Ann. d. Physik **67**, 325 (1922).
[2] B. Wwendensky and K. Theodortschik, Phys. Zeits. **24**, 216 (1923). Ann. d. Physik **68**, 463 (1922).
[3] W. Arkadiew, Zeits. f. Physik **28**, 11 (1921).
[4] L. Page, Phys. Rev. **21**, 456 (1923).
[5] L. Sokolow, Ann. d. Physik **83**, 1136 (1927).
[6] R. Michels, Ann. d. Physik **8**, 877 (1931).
[7] M. J. O. Strutt, Zeits. f. Physik **68**, 632 (1931).
[8] G. R. Wait, Phys. Rev. **29**, 566 (1927).
[9] M. G. Laville, Comptes Rendus **176**, 573–986 (1923).
[10] G. R. Wait, F. G. Brickwedde and E. L. Hall, Phys. Rev. **32**, 967 (1928).

Fig. 1 gives a résumé of typical values of the measured permeabilities of iron in the range from 1 cm to 500 m. The letters refer to the workers listed above and the $H-J$ values are those presented in this paper. The anomalies of Kartschagin (K), Wwendensky and Theodortschik (W and T), suggestive of natural resonance phenomena, are shown, while the constancy of the more recent work of the others (excluding Arkadiew) is apparent. The work of Hagens and Rubens with long heat waves reflected from metallic mirrors, indicated that the value of permeability at these frequencies was unity. It is seen in Fig. 1 that the values obtained by Arkadiew with damped waves, as well as our values with undamped waves, show a gradual transition as the region of heat waves is approached. The intensity of the magnetic fields in all cases is less than 0.5 gauss. Variation with field intensity has not been detected.

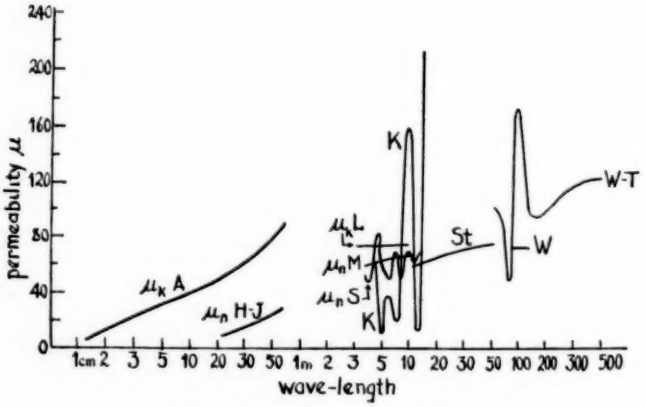

Fig. 1. Permeability of iron at high frequencies.

Theory of μ_n Determination

The J. W. Nicholson[11] form of the equation for the inductance of two parallel wires whose magnetic permeability at high frequencies is μ_n is given by the following equation

$$L = 4 \log_e \frac{d}{r} + \frac{4\mu_n}{x} \cdot \frac{\text{ber } x \cdot \text{ber}' x + \text{bei } x \cdot \text{bei}' x}{(\text{ber}' x)^2 + (\text{bei}' x)^2} \tag{1}$$

where L is the high-frequency inductance per centimeter of the double wire system; d is the separation of the wires in cm; r is the radius of one wire in cm;

$$x = 2r(\pi\omega\mu_n/\rho)^{1/2} \tag{2}$$

in which $\omega = 2\pi \times \text{frequency} = 2\pi V/\lambda$; V is the velocity of waves in the lecher wires; λ is the wave-length in cm; ρ is the specific resistance of one wire; also

$$\text{ber } x = 1 - \frac{x^4}{2^2 4^2} + \frac{x^8}{2^2 4^2 6^2 8^2} - \cdots \tag{3}$$

[11] J. W. Nicholson, Phil. Mag. **17**, 255 (1909).

and

$$\text{bei } x = \frac{x^2}{2^2} - \frac{x^6}{2^2 4^2 6^2} + \frac{x^{10}}{2^2 4^2 6^2 8^2 10^2} - \cdots \tag{4}$$

The primed values (ber′x, bei′x) are the first derivatives with respect to x.

For extremely high frequencies this equation reduces to

$$L = 4 \log_e d/r + [(2\mu_n R \times 10^9)/\omega]^{1/2} = L_a + 2L_i \tag{5}$$

where R = ohms resistance of a one cm length of a single wire, and $L_a (= 4 \log_e d/r)$ is the inductance per cm of the double wire at low frequencies. The second term, which is equal to $2L_i$, represents that part of the inductance which varies with the frequency. This variation is due to the fact that as the frequency increases the currents are more and more confined to the surface of the wire, leaving a larger inner region filled with material of permeability μ_n. This inductance, L_i, is often referred to as the inner self-inductance. Therefore, solving Eq. (5) for the permeability, we obtain

$$\mu_n = \omega(2L_i)^2/(2R \times 10^9). \tag{6}$$

From the usual cable theory, the velocity of propagation of current waves along the parallel wires is given by $V = 1/(LC)^{\frac{1}{2}}$, which, for our case of high frequencies, becomes

$$V = [(L_a + 2L_i)C]^{-1/2}. \tag{7}$$

This velocity is appreciably smaller than the velocity of light c unless L_i is negligible. Further, we have $c = f\lambda_B$ and $V = f\lambda_F$, where f is the frequency of the generator, λ_F is the wave-length in the magnetizable wires and λ_B is the wave-length in non-magnetizable wires. Combining these equations, we obtain

$$2L_i = 2L_a(\lambda_B - \lambda_F)/\lambda_F \tag{8}$$

where $L_a = 4 \log_e d/r$ from Eq. (5). Substituting this value of the inner self-inductance in Eq. (8) gives the following working equation,

$$\mu_n = (1920\pi/R)(\log_e d/r)^2(\lambda_B - \lambda_F)^2/\lambda_B\lambda_F^2 \tag{9}$$

where R is the d.c. resistance in ohms per cm of a single magnetizable wire. It is to be noticed that the accuracy with which μ_n may be determined depends on the precision of the wave-length measurements.

Apparatus

Fig. 2 shows the apparatus used for determining the permeability by the self-inductance or wave-length method. An electron oscillator of the magnetron type was used as a generator of the ultra-radio frequencies. The elements of this vacuum tube consisted of a 4 mil tungsten filament surrounded coaxially by a molybdenum cylinder whose inside diameter was 1 cm. This vacuum tube was placed in a magnetic field so that the filament was parallel to the lines of force. The cylinder was raised to a positive potential of 100–1200 volts. Oscillations were produced by slowly increasing the magnetic field

to a value at which the anode current, indicated by the milliameter (A), suddenly decreased. The frequencies which were produced with this tube ranged from 1.36×10^9 to 0.47×10^9 cycles per second (22 cm–64 cm). These ultra radio frequency oscillations were fed through two 0.01 mfd condensers (c) into a lecher wire system (WW). These wires were 0.318 cm in diameter and 150 cm long and were suspended 1.90 cm apart.

The double short circuiting bridge similar to that described by L. Tonks[12] (B in Fig. 2) consisted of two short-circuiting bars separated by approximately one-fourth of the wave-length in use. This served effectively to reduce the dead-end effect of the portion of the wires to the right of (B).

A small pick-up coil (e) of copper wire was mounted near the coupling condensers as indicated in the figure. Currents induced in this side circuit were rectified by the crystal (d). The a.c. components were by-passed by a small condenser, while the d.c. component served to deflect the galvanometer (G).

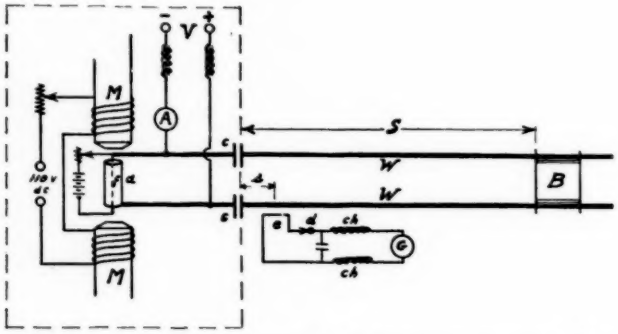

Fig. 2. Circuit used to measure high-frequency permeabilities.

Calculations for this apparatus showed that the impedance of the generator was approximately equal to the characteristic line impedance of the lecher wires.

Measurement of the Wave-Length

The usual cable theory has been applied by Hoag to the present apparatus. This gives the following equation for the galvanometer current i_g in terms of the position S of the bridge (see Fig. 2),

$$i_g = I_g \cos^2 [360(S - s)/\lambda] \tag{10}$$

Fig. 3 shows experimental values for a 64 cm wave. That the equation of this curve is correctly expressed by Eq. (10) may be seen by solving the equation for the bridge position. Thus

$$S = s + (\lambda/360) \cos^{-1} (i_g/I_g)^{1/2}. \tag{11}$$

If we replot the data of Fig. 3 using values of S as ordinates and $\cos^{-1}(i_g/I_g)^{1/2}$ as abscissae, the points fall along the straight line shown in Fig. 4. The y

[12] L. Tonks, Physics **2**, 1 (1932)

intercept gives the value of the distance s, thus eliminating all difficulty in determining the end corrections of the lecher wire system. The slope of the line is equal to $\lambda/360$. In order to obtain the wave-length λ with greater pre-

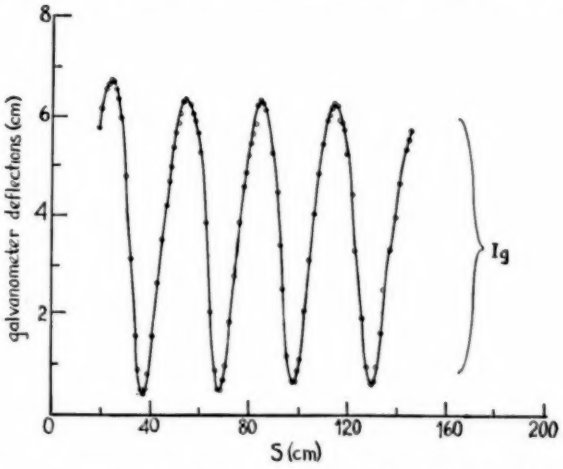

Fig. 3. Galvanometer deflections for various bridge positions.

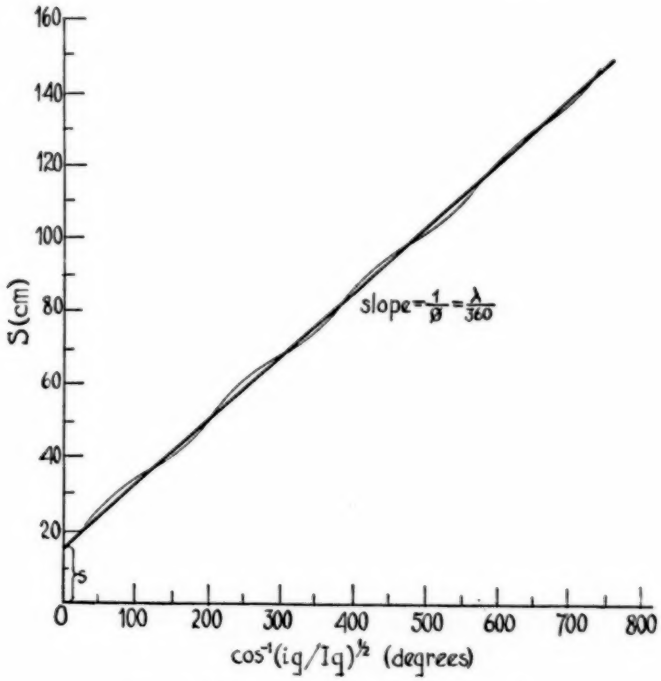

Fig. 4. Measurement of the wave-length.

cision, an average for symmetrical points on the experimental wavy line of Fig. 4 was determined. Wave-lengths measured by this method are accurate to three significant figures throughout the range investigated.

In order to stabilize the frequency and strength of the oscillations, the various currents used to operate the magnetron were continuously maintained at fixed values during the time necessary to obtain the data for both iron and brass lecher wires. In this way, values of λ_F and λ_B for a definitely fixed frequency were obtained. Approximate values of the wave-length were obtained by doubling the distance between successive peaks in Fig. 3.

Results

The wave-lengths measured by this method and the permeabilities calculated from Eq. (9) are given in Table I. The d.c. resistance R was equal to 0.00032 ohms per cm length of a single iron wire. The separation of the lecher

Table I.

Approx λ cm	λ_F cm	λ_B cm	μ_n	f megacycles
64	63.55	63.81	30.31	469.8
51	50.68	50.83	22.10	589.8
36	36.04	36.13	18.69	829.8
22	22.18	22.21	9.65	1350.

wires (d) was 1.90 cm and each wire had a radius r of 0.159 cm. It is to be noted that the μ_n values are appreciably lower than those of Arkadiew. They gradually diminish at shorter wave-lengths, as is to be expected in this transition region.

LETTERS TO THE EDITOR

Prompt publication of brief reports of important discoveries in physics may be secured by addressing them to this department. Closing dates for this department are, for the first issue of the month, the twenty-eighth of the preceding month; for the second issue, the thirteenth of the month. The Board of Editors does not hold itself responsible for the opinions expressed by the correspondents.

Velocities of Ions and Electrons in Pure Gases

In a review on "Electrical Discharges in Gases," K. T. Compton (*Rev. Mod. Phys.* **2,** 123 (1930)) arrives at a general mobility equation which should apply to ions and electrons. No test of the equation was made by comparison with experimental results of the mobilities of positive ions, because at that time no determinations had been made in which the nature of the ions was sufficiently well established.

In a paper read before the New Zealand Institute, I used Compton's equation to calculate the mobilities of certain positive ions moving in pure gases. These mobilities had been experimentally measured with accuracy by Tyndall and Powell (Proc. Roy. Soc. **A134,** 125 (1931) and **136,** 145 (1932); Nature **127,** 592 (1931)). My calculations for the mobility of helium ions in helium showed that Compton's equation yields values several times greater than 21.4 cm/sec. per volt/cm, the value obtained by Tyndall and Powell. Further, for values of X/p ranging from 0.3 to 4.2 volt/cm per mm of mercury, the mobilities calculated from the equation change rapidly, contrary to the experimental values. Hassé's calculations (Phil. Mag. **1,** 139 (1926) and **12,** 554 (1931)) from Langevin's general equation are in much closer agreement with the best experimental values or positive ions in the case of helium and in the other cases I considered, and, in addition, this equation leads to the well-established law connecting mobility and pressure and to the fact that the mobility is independent of the electric field for small to moderate fields.

In obtaining his equation Compton neglects the effect of the attractive forces between ions and molecules. The reasons given for this procedure (R.M.P. **2,** 209 (1930)) justify it in the consideration of electrical discharges through gases, but the simplification is only a rough approximation under the conditions existing during mobility measurements. The expression there quoted for the force between an ion and a neutral molecule is only half the correct form. Assuming that this is a typographical error, there still seems to be a numerical error in Compton's estimates of the effect of attraction, which may have influenced his judgment of the relative unimportance of the attractive forces. These forces depend on the ratio (R) of the energy of dissociation of an elementary cluster to the average kinetic energy of the ions and molecules. From Hassé's calculations I estimated that the effect of the attractive forces for values of R up to 1.6 is greater than indicated by Compton's figures. This emphasizes the vagueness of his conclusion that "the ion free path is not appreciably diminished by the fact of its charge unless the mutual kinetic energy is of the order of the cluster dissociation energy, or less." The mobility of the ions will be much reduced by the attractive forces when the cluster dissociation energy is considerable compared with the average kinetic energy of a molecule. This is the condition that clusters of charged and uncharged molecules should be formed. Although Tyndall and Powell found no evidence of ionic clusters in their work on pure helium, even in this case the effect of the attractive forces is to reduce the calculated mobility by about 50 percent. It is not possible yet to make a much closer approximation to the forces between ions and molecules in close proximity than the inverse fifth power law of attraction.

There appears to be no adequate reason to extend the concept of mobility to the case of electrons where the velocity in the direction of the electric field (W) is not in general pro-

portional to the field strength (X) (*vide* V. A. Bailey, Phil. Mag. **46**, 213 (1923)). Compton's equation for the mobility of electrons can be considered as an equation for the velocity of electrons under standard conditions of temperature and pressure (W_0), and it appears to be as accurate as any equation yet proposed which neglects the large variations of mean free path with velocity of agitation. In my paper I suggested a method whereby the agreement between velocities predicted from Compton's equation and the best experimental results could be improved in the case of typical gases like oxygen, nitrogen and helium. The suggestion was to adopt Townsend's expression for the average fractional energy loss at an encounter between an electron and a molecule, i.e., $f=2.46\ W^2/C^2$, where C is the velocity of agitation of the electrons, instead of assuming that the collisions are like those between perfectly elastic spheres, in which case $f=2.66\ m/M$ approximately, where M is the mass of the molecule. For the purpose of rapid calculation I wrote Compton's equation for electrons (R.M.P. **2**, 234 (1930)) in the form

$$W_0=41{,}600(p\lambda X)^{1/2}\times f^{1/4} \qquad (1)$$

where it is assumed that the drift velocities have been measured at 15°C and p mm pressure. λ is the mean free path of the electron at 0°C and 1 mm pressure and has been assumed equal to the usual kinetic theory value. The results in the case of oxygen are shown in Fig. 1. Curve I shows the experimental velocities obtained by Brose (Phil. Mag. **1**, 536 (1925)), which are believed to be the best available for the range of X/p considered. Curve II shows the values calculated from Compton's equation, and Curve III shows the values calculated from Eq. (1)

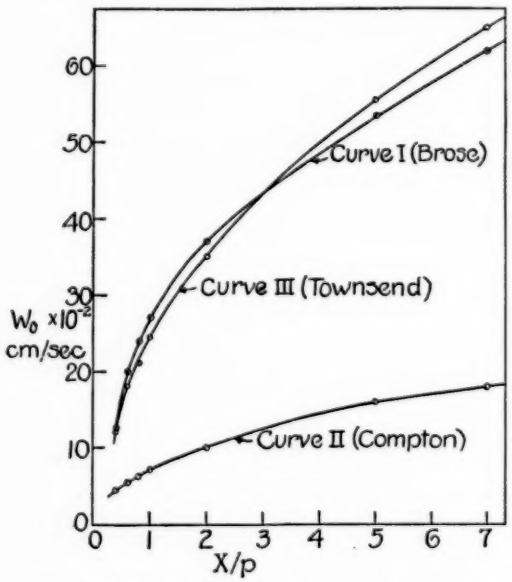

Fig. 1. Drift velocities of electrons in oxygen.

by using Townsend's expression for f and Brose's values for W and C. The improved agreement with the experimental value in this gas by using the method suggested is much more marked than in the case of monatomic gases, where for small values of X/p the collisions are nearly elastic. The agreement thus obtained in the cases of the gases considered is as close as can be expected from any theory which neglects the variation of mean free path of the electrons with their velocity of agitation.

C. M. Focken

Department of Physics,
Otago University,
Dunedin, New Zealand.

October 1, 1932.

Variation of the Structure of Scattered Lines with the Frequency of the Primary Light

In a communication by one of us on a new type of modified radiation[1] mention was made of experiments in which the variation in structure of scattered lines with the variation of the frequency of the primary light was examined. These experiments gave some interesting results which have not yet been published.

The modification of wave-length when the radiation 4047A of the mercury arc was used as the primary light has been studied by means of an echelon grating and compared with that of 4358A. In order to obtain greater accuracy the experiments were carried out with benzene under scattering angle $\theta=135°$. a considerable difference in the displacements of the modified lines. We have undertaken therefore similar experiments with another primary line under another scattering angle.

The yellow radiation 5791A of the mercury arc was chosen as the primary light. The scattering was examined in benzene under the angle $\theta=90°$. In consequence of the smaller sensitivity of the photographic plates in the yellow region of spectrum and the decrease of the intensity of scattered light (according to Rayleigh's law) a very long exposure (80 hours) was required.

The results of the measurements for the yellow line 5791A and those for the blue line

TABLE I.

λ A	$\Delta\lambda$ (obs.) A	$\Delta\lambda$ (calc.) A	$\frac{\Delta\lambda\,(4358)}{\Delta\lambda\,(4047)}$ (obs.)	$\frac{\Delta\lambda\,(4358)}{\Delta\lambda\,(4047)}$ (calc.) $=\frac{4358\cdot n(4358)}{4047\cdot n(4047)}$
4358	0.063	0.050	1.13	1.07
4047	0.056	0.047		

The displacement of the lines modified by elastic heat waves ought to vary with the primary wave-length according to the equation

$$\Delta\lambda=\pm 2\lambda_0 n(v/c)\sin(\theta/2) \qquad (1)$$

where λ_0 is the primary wave-length, v is the velocity of sound in the medium, n is the refractive index of the medium, c is the velocity of light in vacuum and θ is the scattering angle.

The observed and calculated values of $\Delta\lambda$ for 4358A and 4047A as well as their ratios, observed and calculated, are given in Table I.

These results confirm the existence of the 4358A obtained earlier by one of us[1] are compared in Table II. The observed values agree with the calculated ones satisfactorily within the experimental errors.

The variation of $\Delta\lambda$ with the wave-length of the primary light according to the Eq. (1) (as well as with the scattering angle and velocity of sound in the medium)[1] proves again that the observed modification of the wave-length is produced by elastic heat oscillations in the scattering medium and is not the Raman effect due to the frequencies of the rotation spectrum of molecules of liquids.

TABLE II.

λ A	λ] (obs.) A	$\Delta\lambda$ (calc.) A	$\frac{\Delta\lambda\,(5791)}{\Delta\lambda\,(4358)}$ (obs.)	$\frac{\Delta\lambda\,(5791)}{\Delta\lambda\,(4358)}$ (calc.) $=\frac{5791\cdot n(5791)}{4358\cdot n(4358)}$
5791	0.055	0.047	1.17	1.31
4358	0.047	0.036		

connection between $\Delta\lambda$ and λ_0 given by Eq. (2).

The difference between the wave-lengths of the lines 4358A and 4047A is not great enough to produce in the experiments just described

E. GROSS
J. KHVOSTIKOV

Optical Institute,
Leningrad,
October 5, 1932.

[1] E. Gross, Nature **126**, 201 (1930).

Electron Lenses

We wish to amend a statement which appears over our names in an abstract in the Physical Review for August 1, 1931.[1] It is there stated, as a result of calculation, that the distorted electrostatic field about a circular hole in a charged conducting plate (a vacuum tube electrode) has for electrons, or other charged particles, the properties of a spherical lens of focal length $f=2V/(G_2-G_1)$, where V represents the kinetic energy of the particles in equivalent volts, and (G_2-G_1) represents the difference between the potential gradients on the emergence and incidence sides of the plate. The part of this statement which requires amendment is the formula for the focal length, which should read: $f=4V/(G_2-G_1)$.

The original formula, with 2 as the numerical factor, is correct for the other case mentioned in the abstract, that of a rectangular slit. The field about such a slit acts as a cylindrical lens; it was with lenses of this type only that tests had been made at the time the abstract was written. More recently we have made observations on the lens action of the fields about circular holes, and have obtained results in agreement with the corrected formula given above. We hope to have a report of these investigations ready for publication within the next few months.

C. J. DAVISSON
C. J. CALBICK
Bell Telephone Laboratories,
New York City,
October 13, 1932.

[1] Davisson and Calbick, Phys. Rev. (2) **38**, 585 (1931).

On the Secondary Emission from Collectors in Neon Discharge

There are known some deviations from Langmuir's theory for currents to a collector in a neon discharge.[1] In order to investigate the causes of such deviations a number of experiments was carried out by us in 1931–32. The experiments were made with cylindrical tubes of different diameters from 3 to 5 cm (pressure $p=1-2$ mm) with movable collectors of various geometrical shapes. These tubes were made with heated as well as with cold cathodes. The collectors were made of iron, nickel and molybdenum. Before filling the tubes neon was purified in the usual way. The discharge tube could be illuminated by an outside neon source. This illumination caused a corresponding change of the collector current.

When collector potentials approached the anode potential the volt-ampere curves obtained with probe electrode placed in the positive column differ somewhat from those given by Found and Langmuir.[2]

The shifting of the movable collector across the tube permitted the study of the secondary emission from the probe electrode on the axis of the discharge and also its changes when the collector approached the wall of the tube. Close to the wall the shape of the collector's characteristic in the ion part approached the shape of ordinary curves (e.g., mercury vapor) in absence of secondary emission from the collector. Again when the electrode was placed on the axis of the positive column or beyond it at high negative potentials the curves had a shape analogous to that given by Found and Langmuir. It is known that a considerable increase of the ion current can be explained by the ionization in the sheath by electrons escaping from the probe electrode. It should be noted that the conditions in some of our measurements were such that only a slight part of the positive column radiation could pass the anode and reach the collector behind it. In other cases in order to study the influence of the radiation on the secondary emission, special tubes with a "transparent" anode (grid-anode) were used. With the increase of illumination intensity, from the emission tube the corresponding decrease of ion current to the collector in the discharge tube was observed. At probe electrode potentials near the space potential the collector current depends only slightly on the intensity of illumination. Ion currents to the collector placed near the wall do not depend on the magnitude of the discharge current up to certain limits. Thus the changes of the collector current due to illumination also do not depend on the discharge current. When the

[1] W. Uyterhoeven, Proc. Nat. Acad. Sci. **15**, 32 (1929).

[2] C. G. Found and I. Langmuir, Phys. Rev. **39**, 237 (1932), (Fig. 9.)

same collector was shifted towards the axis of the tube not only the collector current changed with the change of the discharge current but the influence of illumination from the outside source as well. Metastable atoms in a neon discharge may firstly, ionize the impurities (volume effect) and secondly, liberate electrons from surfaces (surface effect). The collector current at high negative potentials according to Found and Langmuir depends on the sheath conditions. We believe that our experiments lead to the conclusion that the secondary emission is mainly influenced by the metastable atoms.

Pike's[3] calculations which have led him to the conclusion that the efficiency of metastable atoms is small compared with the photoeffect of the radiation hardly may be applied in our and other authors' experimental conditions. Pike bases his calculations on Penning's curves[4] for spark potential referring to high neon pressures (18–20 mm). It is well known however that the changes in the emission from the cold cathode affect the spark potential only at low pressures. At high pressures the volume effect plays the main role.[5] This explains the small value got by Pike for the efficiency of metastable atoms in liberating the electrons from the collector. Measurements with a plane collector placed beyond the column which could be oriented perpendicular and parallel with the axis of the tube showed that for the perpendicular position of the electrode the ion currents were somewhat greater than for the parallel one. Kenty[6] assumes that this increase of the current is one of the evidences of the direct photoeffect from the collector. But in our experiments this difference in the current existed even when the main discharge was switched off. Thus in our experiments the cause of this effect was not the radiation diffusing from the positive column, but the change of the configuration of the gap between the collector and the anode. In the discharge tube with a transparent anode and a collector placed at the axis of the tube beyond the anode and directly affected by radiation from the positive column the ion currents to the collector decreased sharply when a glass wall was approached by the collector from the side opposite to radiation. When the collector was screened from the positive column with various screens the ion current decreased. But this decrease was almost independent of the optical properties of the screens. All these experiments point out the existence of a surface effect under the action of metastable atoms and a comparatively small direct influence of the photoeffect on the secondary emission.

G. SPIWAK
E. REICHRUDEL
Research Physical Institute of
the Moskow State University.
October 14, 1932.

[3] E. W. Pike, Phys. Rev. **40,** 314 (1932).
[4] F. M. Penning, Zeits. f. Physik **46,** 335 (1928); **57,** 723 (1929), (Fig. 4).
[5] L. I. Neuman, Proc. Nat. Acad. Sci. **15,** 259 (1929), (Fig. 3).
[6] C. Kenty, Phys. Rev. **38,** 377 (1931).

A Filter for the Study of the Raman Effect

To excite Raman spectra[1] by means of the 4358 mercury line, it is current practice to eliminate the 4047 groups by means of a quinine sulphate solution. Since this solution turns brown upon prolonged exposure, recourse is had to the use of a preliminary filter of pale Noviol glass which absorbs the 3650 line as well as lines of shorter wave-lengths—and which, hence, prolongs the useful life of the quinine solution.

Recently, in developing a series of filters transmitting, respectively, only the ultraviolet, the visible, and the infrared, it was found that a solution of sodium nitrite $NaNO_2$ has a short wave-length transmission limit at about 4050. The behavior of a saturated solution of sodium nitrite in a cell 12 mm thick is shown in the accompanying photographs. Actual measurements, carried out with a quartz monochromator and a Weston

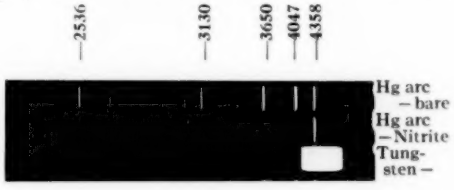

Fig. 1.

Photronic Cell show that while the transmission of the nitrite filter for the 4358 line is

[1] R. W. Wood, Phys. Rev. **38,** 2168 (1931).

65 percent, the transmission for the 4047 line is less than 1 percent. The transmission of the Noviol glass was 56 percent for the 4358 line. This indicated that the sodium nitrite solution would be at least as effective as the quinine sulphate-Noviol combination and possess, in addition, the advantage of permanence. Prolonged exposures to the intense radiation of a quartz mercury arc have failed to show any noticeable effects upon the transmission of the nitrite solution.

A freshly prepared solution of sodium nitrite in water shows turbidity which is not removed by filtering. If the solution be allowed to stand for several days, the suspended matter settles out and leaves the solution quite clear. For most cases a saturated solution in a 12 mm layer will suffice. For use in Wood's system of filters, it is suggested that 2 parts of water be added to 1 part of the saturated nitrite solution and that the mixture be used to fill the glass tube of 3.6 cm internal diameter.

Actual Raman spectrograms taken by Professor Wood showed that the necessary time of exposure with the nitrite filter was no greater than that required by the quinine-Noviol filter and that the nitrite filter did not change its color.

A. H. PFUND

The Johns Hopkins University,
October 22, 1932.

Note on Perturbation Theory of Molecules Formed from Two 2*p* Atoms

The various methods which can be used to estimate (either quantitatively or qualitatively) the energy levels of diatomic molecules do not always give concordant results for the ordering of the levels. Professor Van Vleck has suggested that a comparison of these methods might yield information of some value; this note gives the results of such a comparison in a particular instance. The case chosen is that of a molecule formed from two similar atoms, each containing a single $2p$ electron (plus perhaps non-bonding closed inner shells). We shall neglect the "hybridization" of the $2s$, $2p$ levels; for, though important in hydrogenic atoms because of degeneracy, it is usually less important in heavier atoms. The various schemes of calculation include the following:

1. The Heitler-London perturbation method, inclusive of the electron repulsion term, e^2/r_{12}, in the potential energy. This has been done, to the first order approximation, by Barlett;[1] his results, corrected as suggested in a later paper,[2] are shown in Fig. 1. This is the method leading to the concept of "electron pairs."

2. The Heitler-London perturbation method, exclusive of the electron repulsion term. The results, readily calculated from Bartlett's tables, are indicated in Fig. 2.

3. The "two-center" or "molecular orbital" method, also exclusive of detailed electronic interaction. This is the method used extensively in the "Aufbauprinzip" of Hund and Mulliken. It consists essentially of adding the attractive energies of the separate electrons, each calculated as for the one-electron two-center problem, to the repulsive energy of the nuclei. It will be necessary for us to distinguish the two following ways of applying (3):

(3a) First order perturbation theory, neglecting electronic repulsion, with unperturbed wave functions of the type $[a_i(1)\pm b_i(1)]\times[a_j(2)\pm b_j(2)]$. The choice of sign for each electron's orbital determines whether it is *gerade* or *ungerade*. (Notation: $a_i(1)$ refers to the wave function of electron 1 on nucleus a in the state $m_l=i$, etc.) This method, like (1) and (2), has the disadvantage that it is applicable only for large internuclear distances. It has been worked out by Lennard-Jones;[3] the results for our two-electron case are given in Fig. 3.

(3b) Semi-empirical methods of Hund[4] and Mulliken,[5] which are guided by correlation of the configurations and levels of known molecules with those of the united atoms and

[1] J. H. Bartlett, Jr., Phys. Rev. **37,** 507 (1931).

[2] W. H. Furry and J. H. Bartlett, Jr., Phys. Rev. **39,** 211 (1932).

[3] J. E. Lennard-Jones, Trans. Faraday Soc. **25,** 668 (1929). As a check, the same results have been found with the aid of Bartlett's tables.

[4] F. Hund, Zeits. f. Physik **73,** 577 (1932).

[5] R. S. Mulliken, Rev. Mod. Phys. **4,** 1 (1932); particularly Fig. 43, which is here taken as a standard by which to judge the accuracy of the perturbation methods.

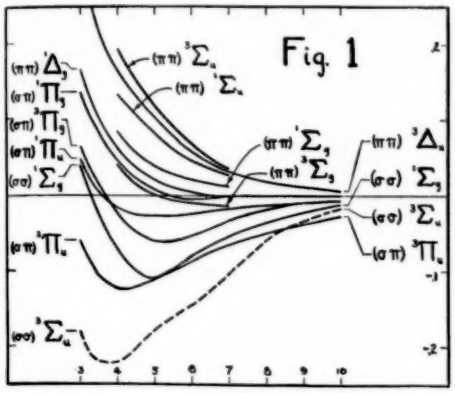

Fig. 1. The Heitler-London method including electron repulsion.

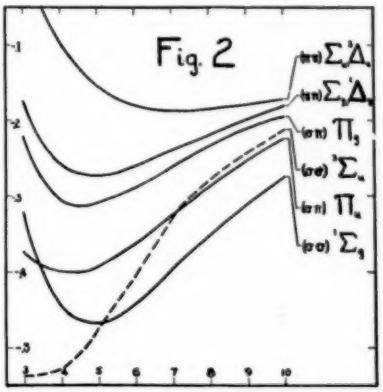

Fig. 2. The Heitler-London method neglecting electron repulsion.

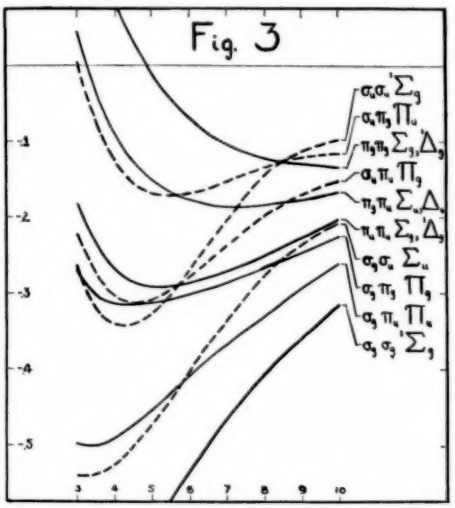

Fig. 3. The two-center method neglecting electron repulsion.

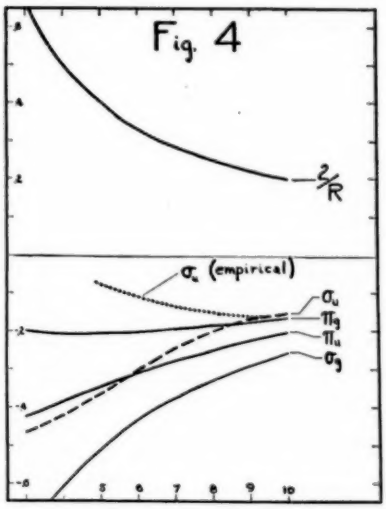

Fig. 4. The two-center method for but one electron.

All these curves have as abscissa the nuclear separation in units of a_0, as ordinate the energy in units of Rh. The parentheses about the small Greek letters of Figs. 1 and 2 indicate merely that σ or π wave functions were used, not that the electrons were individually distinguished as σ or π (as is the case in Figs. 3 and 4). When a singlet and a triplet level coincide, the superscript is omitted.

All the figures are drawn for the special case of unit nuclear charge. Fig. 3 was constructed from Fig. 4 by simple addition of the $2/R$ curve and the individual curves for the two electrons. One may draw the corresponding curves for the case of any nuclear charge Z and any number of $2p$ electrons if one considers the abscissa of Fig. 4 to be ZR and makes the following changes in scale of the ordinate: For the $2/R$ curve (which now becomes $2/ZR$), multiply the ordinates by Z^3; for the remaining curves, multiply the ordinates by Z^2. Addition of these modified curves gives the complete energy, as before. These statements regarding the powers of Z to be inserted are consequences of the fact that the electron energy in the field of the nuclei is of the form $Z^2f(ZR)$, while the mutual potential of the nuclei is, of course, Z^3/ZR.

thereby give at least the correct ordering of energy levels. The results by this method, for the one-electron two-center problem, are roughly the same as those by (3a), shown in Fig. 4, save that the dashed σ_u curve should be replaced by the dotted one. (This discrepancy is the reason for dashing this and other curves affected by it.) The σ_g curve should also be somewhat higher for the smaller values of R.

A study of these figures yields the following information:

(a) Figs. 1 and 2 show that the electronic repulsion term raises the triplet levels less than the singlet ones. This is due to the fact that the triplet wave functions are antisymmetric in their orbital part and therefore become zero whenever both electrons occupy the same position, which is just where $1/r_{12}$ becomes infinite. (The same effect is well known in atomic spectra.)

(b) Methods (2) and (3a) differ only in their choice of unperturbed wave functions. (3a) includes "polar" terms, like a_i (1) a_j (2), which allow the possibility of both electrons being on the same nucleus at once and which keep the u or g property of the individual electronic orbitals; this method should be the better one when inter-electronic action is neglected. (2) excludes polar terms and thus keeps an electron on each nucleus at the cost of spoiling the symmetry properties of the individual electronic orbitals; this method may be preferable whenever the inclusion of electron repulsion tends to prevent the two electrons from accumulating on the same nucleus. The best wave function would probably be a linear combination of that of (2) and that of (3a), as Mulliken[6] has emphasized in the case of 1*s* electrons. The two *ungerade* states made up of equivalent electron configurations, $\sigma_u\sigma_g\Sigma_u$ and $\pi_u\pi_g\Sigma_u$, Δ_u, are the same in both sets of curves. This, as pointed out by Hund,[7] is due to the fact that the polar terms for such equivalent states cancel when one "antisymmetricizes" the product wave function of (3a) to form the triplet wave function, so that the final functions are the same in either method.

(c) The disagreement between methods (3a) and (3b) shown in Fig. 4 tells us that, for $R<8$, the first order perturbation theory (3a) will give not even qualitatively correct results for states involving a σ_u electron—the dashed curves of Fig. 3. This indicates that probably no perturbation calculation for such values of R is reliable. The increase in the discrepancy, as R becomes less than 8, is accompanied by the change in sign of certain integrals in the expression for the energy. This change of sign would, if taken too naïvely, indicate a weakness in the criterion that the amount of "overlapping" of wave functions is a measure of bonding power; for it was upon assumptions as to the definite sign and magnitude of such integrals that the criterion was first built up. Here, after the change in sign, the overlapping would seem a drawback, rather than an asset, to bonding power. However, the criterion still agrees with the empirical results (3b), even for small R. Furthermore, as Professor Mulliken has kindly pointed out, the question is of little practical significance; for in actual molecules ZR (the analogue to R in hydrogen—see caption to figures) is seldom less than 8.

(d) Neglecting electronic interaction, method (3) has the $\sigma_g\sigma_g{}^1\Sigma_g$ state lowest; including that interaction, it might instead place in that position the lowest triplet state, $\sigma_g\pi_u{}^3\Pi_u$. Either of these possibilities, however, disagrees with method (1)'s choice of $(\sigma\sigma)^3\Sigma_u$ as the most stable state. Observations (b) and (c) combine to explain this discrepancy. According to (b), the $\sigma_g\sigma_u\Sigma_u$ state is one of those for which both the Heitler-London and the two-center perturbation methods yield the same results; according to (c), it is one of those states for which the two-center perturbation method gives definitely wrong results. Therefore the Heitler-London method also gives incorrect results for this state; that is why its curve is dashed in Figs. 1 and 2 as well as in Fig. 3.

J. R. STEHN

Department of Physics,
University of Wisconsin,
October 26, 1932.

[6] R. S. Mulliken, Phys. Rev. **41**, 65–71 (1932).

[7] F. Hund, Zeits. f. Physik **73**, 11 (1931).

Law of Force between Two He Atoms

During the last few years a number of papers[1] have appeared dealing with the energy of interaction of two He atoms as they are brought closer and closer together. The purpose of the present Letter is to point out that the law of force obtained by the most recent quantum theoretical considerations agrees surprisingly well with that found by Lennard-Jones[2] from classical considerations on the viscosity and equation of state of helium gas. Classically it is found that for fairly large internuclear distances a force of attraction prevails, but that at distance of 2.5 angstroms or less, a very strong repulsive force dominates the situation. These two types of force receive their interpretation in the quantum theory as electrostatic polar attraction, and repulsion due mostly to electron exchange. The polar attraction has been calculated by Slater and Kirkwood[1] taking account only of the dipole-dipole interaction. This calculation was

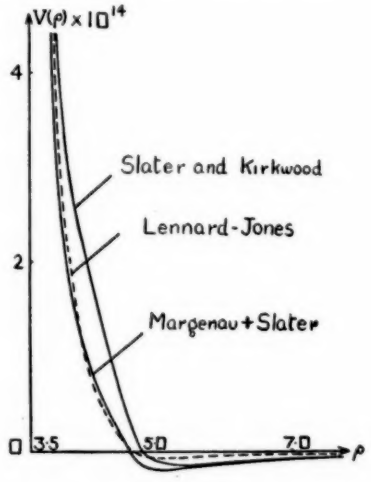

Fig. 1.

improved by Margenau,[1] who introduced the correction for the dipole-quadrupole and quadrupole-quadrupole interactions. The modification engendered by these other terms is considerable. The force of repulsion, or valence force, is known from the work of Slater.[1] Combining the results of Margenau and Slater, the mutual potential energy of two He atoms, distance ρ apart, is

$$V(\rho)=[7.7e^{-2.43\rho}-0.68(1+7.9/\rho^2+30/\rho^4)/\rho^6]\times 10^{-10}\text{ ergs},$$

ρ being measured in terms of a_0, the radius of the first Bohr orbit for H. If the terms in $1/\rho^8$ and $1/\rho^{10}$ are omitted, the energy of interaction as calculated by Slater and Kirkwood is obtained.

Lennard-Jones[2] has found that in order to fit the experimental data on the variation of viscosity of He with temperature and on the equation of state

$$V(\rho)=1.78\times 10^{-6}/\rho^{12}-6.21\times 10^{-13}/\rho^4 \text{ ergs}.$$

The figure shows the variation of $V(\rho)$ with ρ for the three laws. It is surprising how closely the curves follow each other. The agreement is not good at large internuclear distances and it is in this region that the quantum theoretical calculations are most accurate, and are therefore to be preferred. At smaller internuclear separations, however, the reverse situation may very well apply, since the influence of the higher poles increases very rapidly as ρ decreases and these have been taken into account only approximately. Moreover, in this region the valence term may not be accurate although it is probably fairly near the truth.

There have been several attempts to estimate the second virial coefficient of He. Although it is not difficult to make approximate calculations which agree well with the experimental values, an exact theoretical treatment is lacking. The method used up to the present is a semi-classical one in which classical statistics are assumed for the translational energies of the atoms but for the internal motions quantum statistics are employed. Calculations along these lines have given good agreement with experiment as far as the second virial coefficient is concerned. One can use a similar procedure to obtain the coefficient of viscosity. For this calculation the weak attractive field of He is not of much importance. Since the quantum theoretical law of force agrees well with that of Lennard-Jones at those values of ρ where $V(\rho)$ is about equal to the mean thermal energy of the molecules, it must also give a good value for the viscosity. The detailed calculations are rather laborious and it hardly seems worth while to make them until the law of interaction is known with greater accuracy.

W. G. Penney

Department of Physics,
University of Wisconsin,
November 1, 1932.

[1] J. C. Slater, Phys. Rev. **32**, 349 (1928); J. C. Slater and J. G. Kirkwood *ibid.* **37**, 682 (1931); H. Margenau, *ibid.* **38**, 747 (1931).

[2] J. E. Jones, Proc. Roy. Soc. **107**, 157 (1925).

PROCEEDINGS OF THE NEW ENGLAND SECTION OF THE AMERICAN PHYSICAL SOCIETY

Organization of the Section

The New England Section has been organized with the approval of the Council of the American Physical Society, and is under the general supervision of this Council.

Only members or fellows of the American Physical Society are eligible for membership in the section.

The officers of the section are a chairman, vice-chairman, secretary-treasurer, and a program committee, consisting of these three officers and two other elected members.

There will be two meetings of the section a year, one about the middle of October and the other about the end of January. The programs of these meetings will include, not only the usual ten-minute papers, but also invited papers on subjects of interest to physicists in general.

Minutes of the Amherst Meeting, October 8, 1932

The first regular meeting of the New England Section was held in Amherst, Massachusetts, on Saturday, October 8, 1932. The presiding officers were Professor E. C. Kemble, chairman of the section, and Professor Louise S. McDowell. All sessions were held in the Fayerweather Physics Laboratory, Amherst College.

About 80 were present at the morning sessions and about 120 at the afternoon sessions.

The morning session was devoted in part to the reading of contributed papers, and in part to a business meeting.

At the business meeting the organization committee, consisting of Professors E. C. Kemble, S. R. Williams, Louise S. McDowell, G. F. Hull, and P. M. Morse, made its report, outlining the steps which had been taken in organizing the section.

The constitution of the section, which had been approved by the Council of the American Physical Society at its meeting in Washington, April 28, 1932, was adopted by the section.

The secretary of the organization committee reported that 101 members had joined and paid their yearly dues.

The election of officers for the section for the calendar year 1933, then took place. The officers elected were:

Professor E. C. Kemble, Chairman
Professor S. R. Williams, Vice-Chairman
Professor P. M. Morse, Secretary-Treasurer
Professors Louise S. McDowell and G. F. Hull,
members of the Program Committee

Professor W. G. Cady of Wesleyan University kindly invited the section to meet at Middletown, Conn., for its October 1933 meeting. This invitation was later accepted by the program committee.

A vote of thanks was extended to the members of the Physics Department at Amherst for their efforts, which had made the meeting such a success.

The session had its luncheon at the Morrow Cafeteria, Amherst College.

The afternoon session was devoted to invited papers. The first two constituted a colloquium on "Magnetism" and were on *Mechanical Hardness as Measured by Magnetostrictive Effects* by Professor S. R. Williams of Amherst College, and on *Recent Developments in the Theory of Magnetism* by Professor J. C. Slater of Massachusetts Institute of Technology. The third invited paper was a lecture and demonstration of *High-Frequency Sound Effects* given by Professor G. W. Pierce of Harvard University.

The program of the section consisted of 12 papers, the abstracts for which are given below. An author index will be found at the end.

PHILIP M. MORSE, *Secretary-Treasurer*

ABSTRACTS

1. Anomalous rotational temperature of mercury hydride. FOSTER F. RIEKE, *Harvard University.*—Gaviola and Wood obtained the spectrum of mercury hydride by sensitized fluorescence, using the mercury resonance line for excitation. The observations were made that with the mixture hydrogen, nitrogen, and mercury the intensity distribution showed predominance of high rotational quanta, while with water vapor plus mercury, low quanta. An attempt has been made to explain the former observation by a sequence of elementary processes involving the persistance of abnormal rotation through thousands of collisions.The author has obtained the rotational temperature of a band emitted by the mercury plus water mixture; even this has proved to be anomalously high (a few thousand degrees) and cannot be explained by the hypothesis mentioned. It seems to be more compatible with a theory of the transfer of rotational energy in which estimates of probabilities of transfer are based on the laws of impact.

2. Temperature variation of viscosity and of the piezoelectric constant of quartz. K. S. VAN DYKE, *Wesleyan University.*—From measurements of the decrement of the longitudinal vibrations of a quartz resonator at various external circuit loads the decrement under short circuit is found by extrapolation. This decrement measures the inherent viscous losses in the quartz itself when the damping effects of suspension, silver-plated electrodes and surrounding gas have been eliminated. Decrement determinations at different temperatures (same resonator, 67.5 k.c. mode, and method as in Phys. Rev. **40,** 1026 (1932)) show the value of viscosity of quartz (defined as the ratio of logarithmic decrement to Young's modulus) to increase from 0.7×10^{-17} at $-80°$C to 2.4×10^{-17} at 40°C, the increase being about twice as rapid at the upper temperature as at the lower. At room temperatures the variation is of the order of one percent per degree centigrade. The piezoelectric constant of quartz (11) also obtained from these decrement determinations decreases from 5.57×10^{4} absolute e.s.u. at $-80°$C to 5.27×10^{4} at 40°C. This variation is also more rapid for the higher temperatures, being ten times as large at 40° as at $-80°$. At room temperature the variation is about one-tenth of one percent per degree centigrade.

3. The effect of pressure on the electrical resistance of fifteen metals down to liquid oxygen temperatures. P. W. BRIDGMAN, *Harvard University.*—Measurements made 15 years ago on the pressure coefficient of a number of metals between 0° and 100°C have been extended to $-78°$ (solid CO_2) and $-183°$ (liquid oxygen). In order to avoid freezing of the transmitting medium pressure must be transmitted with gaseous helium. This introduces a number of difficulties of technique, which have been so far overcome that routine measurements have

been made to 7000 kg/cm² at −183°. Over this range no very striking results have been found. Resistance decreases nearly linearly with pressure, perhaps even more nearly linearly than at room temperatures. There is in almost all cases a numerical increase in the coefficient at low temperatures, but the increase is usually not large, the largest effect being a doubling of the coefficient of Al, and there is no simple correlation with other properties of the metal.

4. Momentum transfer to cathode surfaces by impacting positive ions in a helium arc. K. T. COMPTON AND E. S. LAMAR, *Massachusetts Institute of Technology.*—The momentum transfer to an auxiliary cathode has been studied in the positive column of a low voltage helium arc. The auxiliary cathode was a flat molybdenum plate insulated on one side by glass and suspended in such a way that its deflection gave a measure of the pressure against it. The measured pressure on the cathode is believed to be due to two phenomena. The first is the recoil of those ions which retain some of their kinetic energy after neutralization. The second is a radiometer effect due to the heating of the cathode by positive ion bombardment. On the basis of these assumptions it was possible to calculate from the experimental data an accommodation coefficient for helium positive ions and the fraction of the measured current carried by electrons. Although the accuracy of the experiment is not high, the values of the accommodation coefficient, ranging from 0.37 to 0.53, are in qualitative agreement with those obtained by Compton and Van Voorhees. The fraction of the current carried by electrons, ranging from 0.54 to 0.62, agrees fairly well with the results of Harrington.

5. Electron diffraction by a silver film on a gold crystal. H. E. FARNSWORTH, *Brown University.*—A thin film of silver (not visible) was deposited on the (100) face of a gold crystal by evaporation in a vacuum. The silver formed in a lattice structure having the same orientation as that of the underlying gold crystal. The diffraction beams obtained for the thin silver film have the same characteristic fine structure, which varies with the angle of incidence, as that previously found for a more massive silver crystal, (Phys. Rev. **40,** 684 (1932)), except that the relative intensities of the components of one of the lowest voltage beams for the silver film are reversed. As previously observed (Phys. Rev. **40,** 1049 (1932)) the fine structure of the diffraction beams for a gold crystal differs from that of the corresponding beams of a silver crystal. Deviations from the plane grating formula for normal incidence are the same for the beams from the thin film as for those from a more massive silver crystal. These results substantiate the previous evidence (Phys. Rev. **40,** 684 and 1049 (1932)) that the fine structure characteristics are at least partly determined by the nature of the atoms composing the crystal rather than by the lattice itself.

6. The continuous electron affinity spectrum of hydrogen. C. K. JEN, *Harvard University.*—A wave-mechanical calculation has been made of the intensity distribution in the continuous emission spectrum due to the capture of electrons by normal hydrogen atoms and in the corresponding absorption spectrum due to the dissociation of negative hydrogen ions. Approximate wave functions for the continuous range of upper energy levels have been combined with the discrete state wave function for H^- given by Hylleraas to give the matrix elements for the desired transitions. The computed results for the emission (assuming uniform distribution of electrons against velocity) or absorption spectrum show that the emitted or absorbed intensity starts with a small value from the edge, determined by the theoretical value of electron affinity, and steadily increases toward the short wave-length side. Due to the low intensity at the edge, the experimental determination of the electron affinity by means of its spectrum becomes quite difficult. If this simple picture holds approximately for the more complicated halogen atoms, the diffusion of the continuous spectrum limit may partially account for the repeated experimental failure to find the electron affinity spectrum of these elements.

7. The effect of exchange on elastic cross sections. PHILIP M. MORSE AND W. P. ALLIS, *Massachusetts Institute of Technology.*—An exact solution has been obtained for the separable type of wave functions for elastic scattering from hydrogen- and helium-like atoms, by using a simplified form of potential field and of atomic electron wave function. Exchange has a considerable effect on the angle distribution of the antisymmetric type function (which is re-

sponsible for all of the cross section for helium-like and for three quarters of that for hydrogen-like atoms). The alteration is greatest for light atoms and for low velocities. The effect on the symmetric wave function is small. The usual approximation methods are shown to be unsatisfactory for light atoms and low velocities.

8. Differential analyzer solution for the wave functions of the *K*-shell. S. CALDWELL, *Massachusetts Institute of Technology.*—With the differential analyzer (see Bush, Jour. Franklin Inst. **212,** 447–488 (1931)), for the solution of the wave equation of helium-like atoms it is possible to consolidate the steps of the Hartree method and to secure self-consistent solutions directly from the machine. Procedures have been established to obtain solutions which also satisfy the requirements of finiteness and normality. The work with the machine has been completed for atoms of atomic numbers $Z=2$ to $Z=8$, inclusive, and also for $Z=32$. Energy values are obtained, and analytic approximations to the wave functions can be gotten.

9. On the possibility of deriving work from statistical fluctuations. V. GUILLEMIN, JR., *Massachusetts Institute of Technology.*—It has been repeatedly suggested that the statistical fluctuations occurring within a system in equilibrium might be used, through the intelligent intervention of an animate being, to obtain useful work from the heat energy of a reservoir at the lowest available temperature. Maxwell put forth such a suggestion quite seriously (the Maxwell demon). His justification is of a very general nature, namely, that all classical laws are independent of the absolute scale of the system. Therefore, a system which obviously works on a large scale will also work on the scale of molecular dimensions. Perhaps the most profound difference between classical and modern (relativity, quantum) laws is that the latter are *not* independent of absolute scale. Making no assumption about the process of perception other than that it requires the existence at the demon, of a vector quantity which is a function of the coordinates of the molecule to be perceived, it can be shown that the energy which must necessarily be dissipated into heat every time the trapdoor is opened or closed is much greater than the energy of the captured molecule. Similar results are obtained for the case of Brownian particles and for fluctuations in general.

10. Mechanical hardness as measured by magnetostrictive effects. S. R. WILLIAMS, *Amherst College.*

11. Recent developments in the theory of magnetism. J. C. SLATER, *Massachusetts Institute of Technology.*

12. Some applications of high-frequency sound effects. G. W. PIERCE, *Harvard University.*

AUTHOR INDEX TO ABSTRACTS OF THE AMHERST MEETING OF THE NEW ENGLAND SECTION

Allis, W. P.—see Morse
Bridgman, P. W.—No. 3
Caldwell, S.—No. 8
Compton, K. T. and E. S. Lamar—No. 4
Farnsworth, H. E.—No. 5
Guillemin, V., Jr.—No. 9
Jen, C. K.—No. 6
Lamar, E. S.—see Compton
Morse, Philip M. and W. P. Allis—No. 7
Pierce, G. W.—No. 12
Rieke, Foster. F.—No. 1
Slater, J. C.—No. 11
Van Dyke, K. S.—No. 2
Williams, S. R.—No. 2

CURRENT LITERATURE OF PHYSICS

Extracts from the Tables of Contents of Some of our Contemporaries

PROCEEDINGS OF THE ROYAL SOCIETY

SERIES A. VOL. 138, NO. A834 — OCTOBER 1, 1932

Modes of Vibration of Quartz Piezoelectric Plates as Revealed by an Interferometer. By the late **W. D. Dye** 1
Theory of Electric Charge. By **Sir Arthur Eddington** 17
Viscosity of a Fluid Containing Small Drops of Another Fluid. By **G. I. Taylor** 41
On the Theory of Errors and Least Squares. By **H. Jeffreys** 48
Contributions to the Mathematical Theory of Epidemics. II.—The Problem of Endemicity. By **W. O. Kermack and A. G. McKendrick** 55
Absorption Spectrum of Nitrous-Oxide and the Heat of Dissociation of Nitrogen. By **A. K. Dutta** 84
Mechanism of the Initiation and Propagation of Detonation in Solid Explosives. By **W. Taylor and A. Weale** 92
Mobility of Alkali Ions in Gases. By **C. F. Powell and L. Brata** 117
Distribution of Suspended Particles under Gravity. By **C. M. McDowell and F. L. Usher** 133
Interferometric Measurements in the Spectrum of Krypton. By **C. V. Jackson** 147
Dipole Moments and Molecular Structure. Part III.—The Oxychlorides of Sulphur. By **J. W. Smith** 154
Swelling of Charcoal. Part II.—Some Factors Controlling the Expansion Caused by Water, Benzene and Pyridine Vapours. By **D. H. Bangham, N. Fakhoury and A. F. Mohamed** 162
Theory of Uncoupling and Formulae for the Stark Effect in H_2. By **J. K. L. MacDonald** 183
Polarity of Thunderclouds. By **E. C. Halliday** 205
Inelastic Electron Scattering in Gases.—I. By **C. B. O. Mohr and F. H. Nicoll** 229
Further Experiments on Superconductivity with Alternating Currents of High Frequency. By **J. C. McLennan, A. C. Burton, A. Pitt and J. O. Wilhelm** 245

PHILOSOPHICAL MAGAZINE

VOL. 14, NO. 92 — OCTOBER, 1932

Viscosity of Strong Electrolyte Solutions according to Electrostatic Theory. By **H. Falkenhagen and E. L. Vernon** 537
Central Deflexion of a Square Plate with Clamped Edges and Subject to a Uniform Pressure over One Face. By **K. R. Gunjikar and V. C. Majmudar** 565
Theory of Heat Conduction and Convection from Tall Hot Vertical Cylinders and High Walls at Uniform Temperature. By **W. S. Kimball and W. J. King** 570
On Atoms of Action, Electricity and Light. By **Sir Ambrose Fleming** 591
On Magnetic Effects in Iron Crystals. By **A. G. Hill** 599
Numerical Values of Atomic Constants and X-Ray Terms. By **H. R. Robinson** 605
Geometrical Method of Determining the Crystal Axes of Single Crystal Wires. By **Bruce Chalmers** 612
On the Spontaneous Generation of Oscillation in Low-Pressure Discharges. By **S. K. Mitra and Premtosh Syam** 616
Mehler-Dirichlet Integral and Some Other Legendre Function Formulae. By **T. M. MacRobert** 632
Incidence of Lattice Distortion and Orientation in Cold-Rolled Metals. By **W. A. Wood** 656
B. A. Standards of Resistance, 1865–1932. By **Sir R. T. Glazebrook and L. Hartshorn** .. 666
Temperature Variation of the Frequency of Piezoelectric Oscillations of Quartz. By **R. E. Gibbs and V. N. Thatte** 682

On the Volume of the Meniscus at the Surface of a Liquid. By **Alfred W. Porter** 694
Hot Wire and Spark Shadowgraphs of the Airflow through an Air-Screw. By **H. C. H. Townend** 700
Cold Electric Arc in Vacuum. By **F. H. Newman** 712
Spectroscopic Investigation of Some Metal Electrodes in Vacuum Arcs. By **F. H. Newman** 718

NATURE

VOL. 130, NO. 3285 OCTOBER 15, 1932

Short Reviews:

Recent Researches on Cosmic Rays 570

Letters to the Editor:

Diamagnetism of Molecules. By **D. P. Ray-Chandhuri** 579
Nuclear Structure. By **E. Gwynne Jones** 580
Absorption of Sound by Porous Materials. By **Viktor Kühl and Erwin Meyer** 580
Efficiency of Geiger Counter and Absorption of Cosmic Rays. By **J. C. Jacobsen** 581
Spectrum of Cosmic Radiation. By **Arthur W. Conway** 581

ZEITSCHRIFT FÜR PHYSIK

VOL. 78, NOS. 5 AND 6 OCTOBER 4, 1932

Asymptotic Integration of the Differential Equation of the Thomas-Fermi Atom. By **A. Sommerfeld** 283
On the Behavior of the Stark Effect with Sudden Field Changes. By **H. Rausch von Traubenberg, R. Gebauer and E. Schrödinger** 309
Electron Microscope. By **M. Knoll and E. Ruska** 318
Investigation of the Emission Distribution from a Hot Cathode with the Magnetic Electron Microscope. By **M. Knoll, F. Houtermans and W. Schulze** 340
Influence of the Foreign Substance on the Cohesion Limits and the Electron Ultramicroscopic Structure of Synthetic Rocksalt Crystals. III. The Addition of Some Heavy Metal Chlorides. By **Walter Metag** 363
Influence of the Foreign Substance on the Cohesion Limits and the Electron Ultramicroscopic Structure of Synthetic Rocksalt Crystals. IV. Density Determinations of Pure Salt Crystals and the Rocksalt with the Heavy Metals Added. By **Johannes Köhler** 375
On the Plastic Extension of α-Iron Crystals. By **W. Fahrenhorst and E. Schmid** 383
Multiple Scattering of α-Particles in Thin Metal Foils. By **Georg Maurer** 395
Light Yield in Helium, Mercury and the Nitrogen Spectrum by Electron Collision Excitation. By **Otto Thieme** 412

DIE NATURWISSENSCHAFTEN

VOL. 20, NO. 41 OCTOBER 7, 1932

Short Original Communications:

Differentiation between Neutrons and γ-Rays. By **H. Becker and W. Bothe** 757
Crystal Photoeffect in Clear Zincblend. By **H. Dember** 758
Selective Focusing of X-Rays. By **Tryggve Johansson** 758
Spectra and Binding Forces of Inner Electrons of Molecules. By **H. Beutler** 759

DIE NATURWISSENSCHAFTEN

VOL. 20, NO. 42 OCTOBER 14, 1932

Short Original Contributions:

Photochemical Separation of the Isotopes. By **Werner Kuhn and Hans Martin** 772

PROCEEDINGS OF THE NATIONAL ACADEMY OF SCIENCE

VOL. 18, NO. 10 OCTOBER, 1932

(No articles of interest to physicists)

THE REVIEW OF SCIENTIFIC INSTRUMENTS

VOL. 3, No. 11 NOVEMBER, 1932

Use of the Wilson Cloud Chamber for Measuring the Range of Alpha-Particles from Weak Sources. By **F. N. D. Kurie** 655

Reflection Densitometer for Photographic Papers. By **C. W. Kendall** 668

Joule Magnetostrictive Effect in a Group of Cobalt-Iron Alloys. By **S. R. Williams** 675

Heat Loss from Dewar Flasks. By **Kenneth S. and Robert H. Cole** 684

Modifications of the Resistance Thermometer Bridge (Mueller Bridge) and of the Commutator Selector for Use with it. By **Marion Eppley** 687